Probabilistic Label Trees for Extreme Multi-label Classification

Kalina Jasinska-Kobus[*1], Marek Wydmuch[†1], Krzysztof Dembczyński[‡1,2], Mikhail Kuznetsov[§2], and Róbert Busa-Fekete[¶3]

[1]Institute of Computing Science, Poznan University of Technology, Poland
[2]Yahoo! Research, New York, USA
[3]Google Research, New York, USA

Abstract

Extreme multi-label classification (XMLC) is a learning task of tagging instances with a small subset of relevant labels chosen from an extremely large pool of possible labels. Problems of this scale can be efficiently handled by organizing labels as a tree, like in hierarchical softmax used for multi-class problems. In this paper, we thoroughly investigate probabilistic label trees (PLTs) which can be treated as a generalization of hierarchical softmax for multi-label problems. We first introduce the PLT model and discuss training and inference procedures and their computational costs. Next, we prove the consistency of PLTs for a wide spectrum of performance metrics. To this end, we upperbound their regret by a function of surrogate-loss regrets of node classifiers. Furthermore, we consider a problem of training PLTs in a fully online setting, without any prior knowledge of training instances, their features, or labels. In this case, both node classifiers and the tree structure are trained online. We prove a specific equivalence between the fully online algorithm and an algorithm with a tree structure given in advance. Finally, we discuss several implementations of PLTs and introduce a new one, NAPKINXC, which we empirically evaluate and compare with state-of-the-art algorithms.

---

[*]kjasinska@cs.put.poznan.pl

[†]mwydmuch@cs.put.poznan.pl

[‡]kdembczynski@cs.put.poznan.pl

[§]kuznetsov@verizonmedia.com

[¶]busarobi@google.com

1 Introduction

In modern machine learning applications, the output space can be enormous containing millions of labels. Some notable examples of such problems are image and video annotation for multimedia search [Deng et al., 2011], tagging of text documents [Dekel and Shamir, 2010], online advertising [Beygelzimer et al., 2009a, Agrawal et al., 2013], recommendation of bid words for online ads [Prabhu and Varma, 2014], video recommendation [Weston et al., 2013], or prediction of the next word in a sentence [Mikolov et al., 2013]. The number of labels in all these applications is extremely large. Therefore, problems of this kind are often referred to as *extreme classification.* To give a more detailed example let us consider the task of tagging Wikipedia articles. In this case, each article is an instance, words appearing in the text of articles can be considered as features, and categories to which articles are assigned as labels. By creating a data set from the current content of Wikipedia, we very easily end up with an enormous problem with millions of examples and features, but also with more than one million labels, because that many categories are used in Wikipedia today.

The extreme classification problems have posed new computational and statistical challenges. A naive solution is to train an independent model (for example, a linear classifier) for each label individually. Such an approach, usually referred to as 1-vs-all, has time and space complexity linear in the number of labels. This is, unfortunately, too costly in many practical applications. Hence there is a need for more advanced solutions characterized by both good predictive performance and sublinear complexity. To tackle extreme classification problems efficiently, one can organize labels as a tree in which each label corresponds to one and only one path from the root to a leaf. A prominent example of such *label tree* model is hierarchical softmax (HSM) [Morin and Bengio, 2005], often used with neural networks to speed up computations in multi-class problems. For example, it is commonly applied in natural language processing [Mikolov et al., 2013]. Interestingly, similar algorithms have been introduced independently in many different research fields. In statistics, they are known as nested dichotomies [Fox, 1997], in multi-class regression as conditional probability trees (CPTs) [Beygelzimer et al., 2009b], and in pattern recognition as multi-stage classifiers [Kurzynski, 1988].

In this paper, we thoroughly investigate *probabilistic label trees* (PLTs) which can be treated as a generalization of the above approaches to multi-label problems. In a nutshell, PLTs use a label tree to factorize conditional label probabilities. Classification of a test example relies on a sequence of decisions made by node classifiers, leading the test example from the root to the leaves of the tree. Since PLTs are designed for multi-label classification, each internal node classifier decides whether or not to continue the path by moving to the child nodes. This is different from typical left/right decisions made in tree-based classifiers. Moreover, a leaf node classifier needs to make a final decision regarding the prediction of a label associated with this leaf. PLTs use a class probability estimator in each node of the tree, such that an estimate of the conditional probability of a label associated with a leaf is given by the product of the probability estimates on the path from the root to that leaf. This requires specific conditioning in the tree nodes which leads to small and independent learning problems. For efficient prediction one needs to follow a proper tree search policy.

Let us also emphasize that extreme classification problems are characterized by many additional issues not present in standard learning problems. For example, for many labels only a small number of training examples is usually available. This leads to the problem of long-tail labels and, ultimately, to zero-shot learning, where there are no training examples for some labels in the training

set. Furthermore, training data might be of low quality as no one could go through all labels to verify whether they have been correctly assigned even to a single training example. The training information is therefore usually obtained from implicit feedback and we often deal with the so-called counterfactual learning. In this paper, however, we do not touch all these challenging and actual problems, but focus on computational issues and statistical properties of PLTs.

1.1 Main contribution

This article summarizes and extends our previous work on probabilistic label trees published in [Jasinska et al., 2016, Wydmuch et al., 2018, Busa-Fekete et al., 2019, Jasinska-Kobus et al., 2020]. In the following points, we describe our main contribution and its relation to existing work.

1.1.1 The PLT model

The PLT model has been introduced in [Jasinska et al., 2016]. It uses the chain rule along the paths in the tree to factorize conditional probabilities of labels. In this way, the model reduces the original multi-label problem to a number of binary classification (estimation) problems. From this point of view, it follows the learning reductions framework [Beygelzimer et al., 2016]. As mentioned above, similar label tree approaches have already been used for solving multi-class problems. Also for multi-label problems under the subset 0/1 loss a method, called probabilistic classifier chains, has been introduced [Dembczyński et al., 2010]. It can be interpreted as a specific label tree, but with paths corresponding to subsets of labels. So, the size of the tree is exponential in the number of labels. Therefore, the PLT model is different. It can be treated as a proper generalization of HSM, CPTs, or nested dichotomies to multi-label estimation of conditional probabilities of single labels. Since the first article [Jasinska et al., 2016] the PLT model has been used in many other algorithms such as PARABEL [Prabhu et al., 2018], BONSAI TREE [Khandagale et al., 2019], EXTREMETEXT [Wydmuch et al., 2018], and ATTENTIONXML [You et al., 2019].

There also exist other label tree approaches which mainly differ from PLTs and other methods mentioned above in that they do not use the probabilistic framework. The most similar to PLTs is HOMER introduced by Tsoumakas et al. [2008]. Tournament-based or filter trees have been considered in [Beygelzimer et al., 2009b] and [Li and Lin, 2014] to solve respectively multi-class and multi-label problems. Another example is label embedding trees introduced in [Bengio et al., 2010]. None of these methods, however, has been thoroughly tested in the extreme classification setting, but initial studies suggest that they neither scale to problems of this scale nor perform competitively to PLTs.

To define the PLT model we can follow one of two different frameworks. The first one is based on the standard concept of a tree. The second one uses the prefix codes, similarly as in [Morin and Bengio, 2005], as each path in the tree indicating a label can be seen as a code. We use the first framework. We discuss the general training schema that can be used for both batch and online learning. Since internal node probabilities are conditioned on parent nodes, PLTs need to properly assign training examples to nodes. We show an efficient procedure for this assignment which follows a bottom-up strategy. For prediction, we consider two tree search procedures. The first one stops exploring a tree whenever the probability of reaching a given node is less than a given threshold. The second one uses a priority queue in order to find labels with the highest estimates of conditional label probabilities.

Busa-Fekete et al. [2019] discuss in depth the computational complexity of PLTs. The training

complexity of node classifiers, as well as the prediction complexity, obviously depends on the tree structure. They prove that building an optimal tree structure in terms of computational cost is an NP-hard problem. Here, we include some of their results, which show that training of node classifiers (with a tree structure given in advance) can be done in logarithmic time under additional assumptions concerning the tree structure and the maximum number of labels per training instance. Moreover, with additional assumptions on estimates of label probabilities also the prediction time is logarithmic in the number of labels. This result is not trivial as a prediction method needs to use a tree search algorithm which, in the worse case, explores the entire tree leading to linear complexity.

1.1.2 Consistency and regret bounds

Our main theoretical results concern the consistency of PLTs for a wide spectrum of performance metrics. We show this by following the learning reductions framework [Beygelzimer et al., 2016]. We upper bound the regret of a PLT by a function of surrogate regrets of node classifiers. We first prove bounds for the L_1 estimation error of label conditional probabilities. These results are the building blocks for all other results, as optimal predictions for many performance metrics can be determined through conditional probabilities of labels [Dembczyński et al., 2010, Kotlowski and Dembczyński, 2016, Koyejo et al., 2015, Wydmuch et al., 2018]. A part of these results has been first published in [Wydmuch et al., 2018]. They follow similar results obtained by [Beygelzimer et al., 2009a] for multi-class problems, however, our proofs seem to be simpler and the bounds tighter as they weight errors of tree nodes by a probability mass of examples assigned to these nodes. We also consider a wider spectrum of surrogate loss functions minimized in tree nodes, namely a class of strongly proper composite losses [Agarwal, 2014], which includes squared error loss, squared hinge loss, logistic loss, or exponential loss.

Next, we show the regret bounds for generalized performance metrics of the linear-fractional form. This class of functions contains among others Hamming loss, micro and macro F-measure. The optimal prediction for metrics from this class relies on thresholding conditional probabilities of labels. For some metrics, this threshold has a simple form independent of a concrete data distribution (for example, it is 0.5 for Hamming loss), or it requires some easy-to-estimate quantities such as priors of labels. Unfortunately, for metrics such as F-measures, an additional step of threshold tuning on a validation set is required. The bounds for PLTs are based on results obtained by [Kotłowski and Dembczyński, 2017] for the 1-vs-All approach. The analysis can also be seen as a theoretical extension of the results published in [Jasinska et al., 2016], where we have discussed algorithmic challenges of the macro F-measure optimization in XMLC.

The last metric considered is precision@k. The regret bounds presented here extend the results published before in [Wydmuch et al., 2018]. We first prove the Bayes optimal prediction for precision@k to be a set of k labels with the highest conditional probabilities. Next, by using the definition of the regret and the bound for the L_1 estimation error we obtain conditional and unconditional bounds for precision@k. This result combined with the priority-queue-based inference shows that PLTs are well-tailored for this metric.

We also study the relation of PLTs to HSM. We show that the former are indeed a proper generalization of the latter to multi-label problems. Namely, for multi-class distribution PLTs reduce to the HSM model. Moreover, we show that a specific heuristic, often used in the deep network community to adapt HSM to multi-label classification, is not consistent in terms of L_1 estimation error and precision@k. This heuristic, used for example in FASTTEXT [Joulin et al., 2017] and LEARNED TREE [Jernite et al., 2017], randomly picks one of labels from a multi-label

training example and treats the example as a multi-class one. Interestingly, this specific reduction to multi-class classification is consistent for recall@k as shown in [Menon et al., 2019].

1.1.3 Online probabilistic label trees

We also consider a challenging problem of training PLTs in a fully online setting, without any prior knowledge about the number of training instances, their features, and labels. In this case, not only node classifiers but also the tree structure is trained online. This framework is similar to the one of CPTs for multi-class problems [Beygelzimer et al., 2009a]. To formalize this setting, we define two properties that a fully online algorithm should satisfy. The first one is a specific equivalence condition between the fully online algorithm and an incremental algorithm operating on a tree structure given in advance. The second one concerns the relative complexity of the fully online algorithm. We prove that a general algorithmic framework we introduce satisfies both properties. Here, we use a simple tree building policy which constructs a complete binary tree. Recently, we have experimented with a more sophisticated method [Jasinska-Kobus et al., 2020] leading to better results.

1.1.4 napkinXC and comparison to the state-of-the-art

Beside our theoretical findings, we discuss several existing implementations of the general PLT scheme, such as XMLC-PLT [Jasinska et al., 2016], PLT-vw, PARABEL [Prabhu et al., 2018], BONSAI TREE [Khandagale et al., 2019], EXTREMETEXT [Wydmuch et al., 2018], and ATTENTIONXML [You et al., 2019]. We compare them from the perspective of feature and model representation, batch and incremental learning, prediction algorithms, or tree structure choice. We also introduce a new library, referred to as NAPKINXC, which can be easily adapted to different settings thanks to its modular design. Finally, in a wide empirical study we thoroughly analyze different instances of PLTs and relate their results to other state-of-the-art algorithms such as FASTXML [Prabhu and Varma, 2014], PFASTREXML [Jain et al., 2016] DISMEC [Babbar and Schölkopf, 2017], and PDDSPARSE [Yen et al., 2017]. The first two algorithms are decision tree approaches adapted to the XMLC setting. Their main difference to label trees is that they split the feature space, not the set of labels. The last two algorithms are efficient variants of the 1-vs-ALL approach, which are known to obtain the top empirical performance. Our experiments indicate that PLTs are very competitive reaching the best precision@1 on majority of benchmark data sets, being at the same time even thousand times faster in training and prediction than the 1-vs-ALL approaches.

1.2 Organization of the paper

In Section 2 we formally state the XMLC problem. Section 3 defines the PLT model and discusses training and prediction procedures, as well their computational complexities. Section 4 contains the theoretical analysis of PLTs, which includes regret bounds and relation to HSM. In Section 5 we discuss online probabilistic label trees. Section 6 provides an in-depth discussion on the implementation choices of the PLT model. The experimental results are presented in Section 7. The last section concludes the paper.

2   Problem statement

Let $\mathcal{X}$ denote an instance space, and let $\mathcal{L} = [m]$ be a finite set of m class labels. We assume that an instance $\boldsymbol{x} \in \mathcal{X}$ is associated with a subset of labels $\mathcal{L}_{\boldsymbol{x}} \subseteq \mathcal{L}$ (the subset can be empty); this subset is often called the set of *relevant* or *positive* labels, while the complement $\mathcal{L} \backslash \mathcal{L}_{\boldsymbol{x}}$ is considered as *irrelevant* or *negative* for $\boldsymbol{x}$. We identify the set $\mathcal{L}_{\boldsymbol{x}}$ of relevant labels with the binary vector $\boldsymbol{y} = (y_1, y_2, \ldots, y_m)$, in which $y_j = 1 \Leftrightarrow j \in \mathcal{L}_{\boldsymbol{x}}$. By $\mathcal{Y} = \{0,1\}^m$ we denote the set of all possible label vectors. We assume that observations $(\boldsymbol{x}, \boldsymbol{y})$ are generated independently and identically according to a probability distribution $\mathbf{P}(\boldsymbol{x}, \boldsymbol{y})$ defined on $\mathcal{X} \times \mathcal{Y}$. Notice that the above definition concerns not only multi-label classification, but also multi-class (when $\|\boldsymbol{y}\|_1 = 1$) and k-sparse multi-label (when $\|\boldsymbol{y}\|_1 \leq k$) problems as special cases. In case of extreme multi-label classification (XMLC) we assume m to be a large number (for example $\geq 10^5$), and k to be much smaller than m, $k \ll m$.[1]

The problem of extreme multi-label classification can be defined as finding a *classifier* $\boldsymbol{h}(\boldsymbol{x}) = (h_1(\boldsymbol{x}), h_2(\boldsymbol{x}), \ldots, h_m(\boldsymbol{x}))$, from a function class $\mathcal{H}^m : \mathcal{X} \to \mathbb{R}^m$, that minimizes the *expected loss* or *risk*:

$$R_\ell(\boldsymbol{h}) = \mathbb{E}_{(\boldsymbol{x}, \boldsymbol{y}) \sim \mathbf{P}(\boldsymbol{x}, \boldsymbol{y})}(\ell(\boldsymbol{y}, \boldsymbol{h}(\boldsymbol{x}))) ,$$

where $\ell(\boldsymbol{y}, \hat{\boldsymbol{y}})$ is the (*task*) *loss*. The optimal classifier, the so-called *Bayes classifier*, for a given loss function ℓ is:

$$\boldsymbol{h}_\ell^* = \arg\min_{\boldsymbol{h}} R_\ell(\boldsymbol{h}) .$$

The *regret* of a classifier $\boldsymbol{h}$ with respect to ℓ is defined as:

$$\mathrm{reg}_\ell(\boldsymbol{h}) = R_\ell(\boldsymbol{h}) - R_\ell(\boldsymbol{h}_\ell^*) = R_\ell(\boldsymbol{h}) - R_\ell^* .$$

The regret quantifies the suboptimality of $\boldsymbol{h}$ compared to the optimal classifier $\boldsymbol{h}_\ell^*$. The goal could be then defined as finding $\boldsymbol{h}$ with a small regret, ideally equal to zero.

We are interested in multi-label classifiers that estimate conditional probabilities of labels, $\eta_j = \mathbf{P}(y_j = 1 | \boldsymbol{x})$, $j \in \mathcal{L}$, as accurately as possible, that is, with possibly small L_1-estimation error,

$$|\eta_j(\boldsymbol{x}) - \hat{\eta}_j(\boldsymbol{x})| , \tag{1}$$

where $\hat{\eta}_j(\boldsymbol{x})$ is an estimate of $\eta_j(\boldsymbol{x})$. This statement of the problem is justified by the fact that optimal predictions for many performance measures used in multi-label classification, such as the Hamming loss, precision@k, and the micro- and macro F-measure, are determined through the conditional probabilities of labels [Dembczyński et al., 2010, Kotlowski and Dembczyński, 2016, Koyejo et al., 2015]. In Section 4 we derive statistical guarantees for PLTs, in a form of regret bounds, for a wide spectrum of losses including those mentioned above. Here, we only mention that to obtain estimates $\hat{\eta}_j(\boldsymbol{x})$ one can use the label-wise logistic loss, sometimes referred to as binary cross-entropy:

$$\ell_{\log}(\boldsymbol{y}, \boldsymbol{h}(\boldsymbol{x})) = \sum_{j=1}^m \ell_{\log}(y_j, h_j(\boldsymbol{x})) = \sum_{j=1}^m (y_j \log(h_j(\boldsymbol{x})) + (1 - y_j) \log(1 - h_j(\boldsymbol{x}))) .$$

---

[1] We use $[n]$ to denote the set of integers from 1 to n, and $\|\boldsymbol{x}\|_1$ to denote the L_1 norm of x.

The expected label-wise logistic loss for a single $\boldsymbol{x}$ (the so-called *conditional risk*) is:

$$\mathbb{E}_{\boldsymbol{y}}\ell_{\log}(\boldsymbol{y}, \boldsymbol{h}(\boldsymbol{x})) = \sum_{j=1}^{m} \mathbb{E}_{\boldsymbol{y}}\ell_{\log}(y_j, h_j(\boldsymbol{x})) = \sum_{j=1}^{m} R_{\log}(h_j(\boldsymbol{x}) \,|\, \boldsymbol{x})\,.$$

This is a sum of conditional risks of binary problems under the logistic loss. Therefore, it is easy to show that the pointwise optimal prediction for the j-th label is given by:

$$h_j^*(\boldsymbol{x}) = \arg\min_h R_{\log}(h_j(\boldsymbol{x}) \,|\, \boldsymbol{x}) = \eta_j(\boldsymbol{x})\,.$$

The above loss function corresponds to the vanilla 1-VS-ALL approach. Unfortunately, it is too costly in the extreme setting as training and prediction is linear in the number of labels. In the following sections, we discuss an alternative approach based on label trees, which estimates the marginal probabilities with a competitive accuracy, but in a much more efficient way.

3   Probabilistic label trees (PLTs)

Probabilistic label trees (PLTs) follow a label-tree approach to efficiently estimate the marginal probabilities of labels. They reduce the original problem to a set of binary estimation problems organized in the form of a rooted, leaf-labeled tree with m leaves. We denote a single tree by T, a root node by r_T, and the set of leaves by L_T. The leaf $l_j \in L_T$ corresponds to the label $j \in \mathcal{L}$. The set of leaves of a (sub)tree rooted in an inner node v is denoted by L_v. The set of labels corresponding to leaf nodes in L_v is denoted by $\mathcal{L}_v$. The parent node of v is denoted by $\mathrm{pa}(v)$, and the set of child nodes by $\mathrm{Ch}(v)$. A pre-leaf is a parent node whose all children are leaves. The path from node v to the root is denoted by $\mathrm{Path}(v)$. The length of the path, that is, the number of nodes on the path, is denoted by len_v. The set of all nodes is denoted by V_T. The degree of a node $v \in V_T$, being the number of its children, is denoted by $\deg_v = |\mathrm{Ch}(v)|$. An example of a label tree is given in Figure 1.
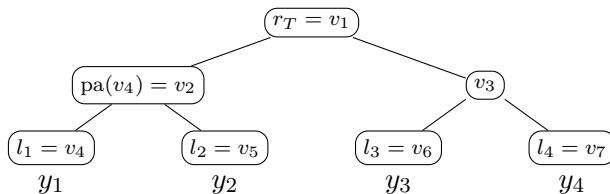

Figure 1: An example of a label tree T with labels $\mathcal{L} = \{y_1, y_2, y_3, y_4\}$ assigned to the leaf nodes.

The assignment of labels to tree leaves corresponds to encoding them by a prefix code, as any such code can be given in the form of a tree. Under the coding, each label y_j is uniquely represented by a code word $\boldsymbol{c}_j = (1, c_{j1}, \ldots, c_{jd})$ corresponding to a path from the root to leaf l_j. Obviously, the length of the code equals the length of the path, that is, $|\boldsymbol{c}_j| = d + 1 = \mathrm{len}_{l_j}$. The zero position of the code allows one to indicate a situation in which there is no label assigned to an instance. Therefore, each label code starts with 1. For $c_{ji} \in \{0, 1\}$, the code and the label tree are binary. In general, the code alphabet can contain more than two symbols. Furthermore, c_{ji}s can take values from different sets of symbols depending on the prefix of the code word. In other

words, the code can result in nodes of a different arity, like in [Grave et al., 2017] and [Prabhu et al., 2018]. Notice that any node v in the tree can be uniquely identified by the partial code word $\boldsymbol{c}_v = (1, c_{v1}, \ldots, c_{vd_v})$. An example of the coding is visualized in Figure 2. This coding perspective has been used in the original paper introducing the HSM model [Morin and Bengio, 2005], as well as in some later articles [Dembczyński et al., 2016]. In the following, however, we mainly use the tree notation introduced in the paragraph before.
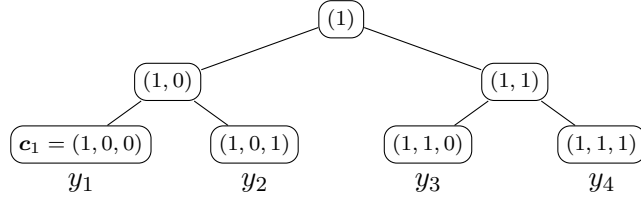

Figure 2: Example of assignment of codes to nodes and labels $\mathcal{L} = \{y_1, y_2, y_3, y_4\}$.

A PLT uses tree T to factorize the conditional probabilities of labels, $\eta_j(\boldsymbol{x}) = \mathbf{P}(y_j = 1|\boldsymbol{x})$, for all $j \in \mathcal{L}$. To this end let us define for every $\boldsymbol{y}$ a corresponding vector $\boldsymbol{z}$ of length $|V_T|$,[2] whose coordinates, indexed by $v \in V_T$, are given by:

$$z_v = [\![\textstyle\sum_{j \in \mathcal{L}_v} y_j \geq 1]\!], \quad \text{or equivalently by } z_v = \bigvee_{j \in \mathcal{L}_v} y_j. \tag{2}$$

In other words, the element z_v of $\boldsymbol{z}$, corresponding to the node $v \in V_T$, is set to one iff $\boldsymbol{y}$ contains at least one label in $\mathcal{L}_v$. With the above definition, it holds based on the chain rule that for any node $v \in V_T$:

$$\eta_v(\boldsymbol{x}) = \mathbf{P}(z_v = 1 \,|\, \boldsymbol{x}) = \prod_{v' \in \mathrm{Path}(v)} \eta(\boldsymbol{x}, v'), \tag{3}$$

where $\eta(\boldsymbol{x}, v) = \mathbf{P}(z_v = 1 | z_{\mathrm{pa}(v)} = 1, \boldsymbol{x})$ for non-root nodes, and $\eta(\boldsymbol{x}, v) = \mathbf{P}(z_v = 1 \,|\, \boldsymbol{x})$ for the root. Notice that for leaf nodes we get the conditional probabilities of labels, that is,

$$\eta_{l_j}(\boldsymbol{x}) = \eta_j(\boldsymbol{x}), \quad \text{for } l_j \in L_T. \tag{4}$$

Remark that (3) can also be stated as recursion:

$$\eta_v(\boldsymbol{x}) = \eta(\boldsymbol{x}, v)\eta_{\mathrm{pa}(v)}(\boldsymbol{x}), \tag{5}$$

with the base case $\eta_{r_T}(\boldsymbol{x}) = \eta(\boldsymbol{x}, r_T) = \mathbf{P}(z_{r_T} = 1 \,|\, \boldsymbol{x})$.

As we deal here with multi-label distributions, the relation between probabilities of a parent node and its children is not obvious. The following result characterizes this relation precisely.

Proposition 1. *For any T, $\mathbf{P}(\boldsymbol{y}|\boldsymbol{x})$, and internal node $v \in V_T \setminus L_T$ we have that:*

$$\sum_{v' \in \mathrm{Ch}(v)} \eta(\boldsymbol{x}, v') \geq 1. \tag{6}$$

Moreover, the probability $\eta_v(\boldsymbol{x})$ satisfies:

$$\max\left\{\eta_{v'}(\boldsymbol{x}) : v' \in \mathrm{Ch}(v)\right\} \leq \eta_v(\boldsymbol{x}) \leq \min\left\{1, \textstyle\sum_{v' \in \mathrm{Ch}(v)} \eta_{v'}(\boldsymbol{x})\right\}. \tag{7}$$

---

[2]Note that $\boldsymbol{z}$ depends on T, but T will always be obvious from the context.

Proof. We first prove the first inequality. From the definition of tree T and z_v we have that if $z_v = 1$, then there exists at least one $v' \in \mathrm{Ch}(v)$ for which $z_{v'} = 1$. This gives that $\sum_{v' \in \mathrm{Ch}(v)} z_{v'} \geq 1$, if $z_v = 1$. By taking expectation and recalling that $\eta(\boldsymbol{x}, v') = \mathbf{P}(z_{v'} = 1 | z_v = 1, \boldsymbol{x})$, for $v' \in \mathrm{Ch}(v)$, we get:

$$\sum_{v' \in \mathrm{Ch}(v)} \eta(\boldsymbol{x}, v') \geq 1 \,.$$

To prove (7) we use the above result and (5). Obviously $\eta(\boldsymbol{x}, v) \in [0, 1]$, for any $v \in V_T$, therefore $\eta_{v'}(\boldsymbol{x}) \leq \eta_v(\boldsymbol{x})$ for every $v' \in \mathrm{Ch}(v)$. Moreover, from (5) we have that

$$\eta(\boldsymbol{x}, v') = \eta'_v(\boldsymbol{x}) / \eta_v(\boldsymbol{x}) \,,$$

for every $v' \in \mathrm{Ch}(v)$. Substituting this to (6) gives $\eta_v(\boldsymbol{x}) \leq \sum_{v' \in \mathrm{Ch}(v)} \eta_{v'}(\boldsymbol{x})$. Since we obviously have $\eta_v(\boldsymbol{x}) \leq 1$, we get the final result. $\qquad\square$

3.1 Training

Let $\mathcal{D} = \{(\boldsymbol{x}_i, \boldsymbol{y}_i)\}_{i=1}^n$ be a training set consisting of n tuples consisting of a feature vector $\boldsymbol{x}_i \in \mathcal{X}$ and a label vector $\boldsymbol{y}_i \in \mathcal{Y}$. Depending on the context we also use the set notation for label vectors, that is, $\boldsymbol{y}_i \equiv \mathcal{L}_{\boldsymbol{x}_i}$. From factorization (3) we see that we need to train classifiers estimating $\eta(\boldsymbol{x}, v)$, for $v \in V_T$. We use a function class $\mathcal{H}^1_{\mathrm{prob}} : \mathcal{X} \mapsto [0, 1]$ which contains probabilistic classifiers of choice, for example, logistic regression. We assign a classifier from $\mathcal{H}^1_{\mathrm{prob}}$ to each node of the tree T. We index this set of classifiers by elements of V_T as $H = \{\hat{\eta}(v) \in \mathcal{H}^1_{\mathrm{prob}} : v \in V_T\}$. We denote by $\hat{\eta}(\boldsymbol{x}, v)$ the prediction made by $\hat{\eta}(v)$ for some $\boldsymbol{x}$, which is the estimate of $\eta(\boldsymbol{x}, v)$. The training algorithm for a PLT is given in Algorithm 1. For simplicity we discuss here a batch procedure, but an online counterpart can be easily obtained based on it (see Section 5).

To train probabilistic classifiers $\hat{\eta}(v)$, $v \in V_T$, we need to properly filter training examples as given in (3). The TRAIN procedure first initializes the sets of training example in all nodes of T. Then, for each training example it identifies the set of *positive* and *negative nodes*, that is, the nodes for which the training example is treated respectively as positive or negative. The ASSIGNTONODES method, given in Algorithm 2, initializes the positive nodes to the empty set and the negative nodes to the root node (to deal with $\boldsymbol{y}$ of all zeros). Next, it traverses the tree from the leaves, corresponding to the labels of the training example, to the root adding the visited nodes to the set of positive nodes. It also removes each visited node from the set of negative nodes, if it has been added to this set before. All children of the visited node, which are not in the set of positive nodes, are then added to the set of negative nodes. If the parent node of the visited node has already been added to positive nodes, the traversal of this path stops. Using the result of the ASSIGNTONODES method the algorithm distributes the training example to the corresponding nodes. Finally, a probabilistic classifier $\hat{\eta}(v)$ is trained in each node v using algorithm A of choice. Notice that training of each node classifier can be performed simultaneously as an independent task. The output of the algorithm is a set of probabilistic classifiers H.

Algorithm 1 PLT.TRAIN$(T, A, \mathcal{D})$

1: $H = \emptyset$ ▷ Initialize a set of node probabilistic classifiers
2: **for** each node $v \in V_T$ **do**   ▷ For each node in the tree
3:      $\mathcal{D}(v) = \emptyset$ ▷ Initialize its set of training example in $\mathcal{D}$
4: **for** $i = 1 \to n$ **do**   ▷ For each training example
5:      $(P, N) = \text{ASSIGNTONODES}(T, \boldsymbol{x}_i, \mathcal{L}_{\boldsymbol{x}_i})$ ▷ Compute its positive and negative nodes
6:      **for** $v \in P$ **do**   ▷ For all positive nodes
7:          $\mathcal{D}(v) = \mathcal{D}(v) \cup \{(\boldsymbol{x}_i, z_v = 1)\}$ ▷ Add the modified example to the training set of node t
8:      **for** $v \in N$ **do**   ▷ For each negative node
9:          $\mathcal{D}(v) = \mathcal{D}(v) \cup \{(\boldsymbol{x}_i, z_v = 0)\}$ ▷ Add the modified example to the training set of node t
10: **for** each node $v \in T$ **do**   ▷ For all nodes in the tree
11:      $\hat{\eta}(v) = A(\mathcal{D}(v))$, $H = H \cup \{\hat{\eta}(v)\}$ ▷ Train a node classifier with algorithm A
12: **return** H ▷ Return the set of node probabilistic classifiers

---

Algorithm 2 PLT.ASSIGNTONODES$(T, \boldsymbol{x}, \mathcal{L}_{\boldsymbol{x}})$

1: $P = \emptyset$, $N = \{r_T\}$ ▷ Initialize sets of positive and negative nodes
2: **for** $j \in \mathcal{L}_{\boldsymbol{x}}$ **do**   ▷ For all labels of the training example
3:      $v = \ell_j$ ▷ Set v to a leaf corresponding to label j
4:      **while** v not null **and** $v \notin P$ **do**   ▷ On a path to the root or the first positive node (excluded)
5:          $P = P \cup \{v\}$ ▷ Assign a node to positive nodes
6:          $N = N \setminus \{v\}$ ▷ Remove the node from negative nodes if added there before
7:          **for** $v' \in \text{Ch}(v)$ **do**   ▷ For all its children
8:              **if** $v' \notin P$ **then**   ▷ If a child is not a positive node
9:                  $N = N \cup \{v'\}$ ▷ Assign it to negative nodes
10:      $v = \text{pa}(v)$ ▷ Move up along the path
11: **return** (P, N) ▷ Return a set of positive and negative nodes for the training example

---

3.2 Prediction

For test example $\boldsymbol{x}$, the estimate of the marginal probability of label j can be readily computed as a product of probability estimates on the path from the root to leaf $l_j \in L_T$:

$$\hat{\eta}_j(\boldsymbol{x}) = \prod_{v \in \text{Path}(l_j)} \hat{\eta}(\boldsymbol{x}, v) \,, \tag{8}$$

where we assume $\hat{\eta}(\boldsymbol{x}, v) \in [0, 1]$. Obviously, the recursive dependency (5) also holds for the estimates. We have, for any $v \in V_T$, that:

$$\hat{\eta}_v(\boldsymbol{x}) = \hat{\eta}(\boldsymbol{x}, v)\hat{\eta}_{\text{pa}(v)}(\boldsymbol{x}) \,, \tag{9}$$

with the base case $\hat{\eta}_{r_T}(\boldsymbol{x}) = \hat{\eta}(\boldsymbol{x}, r_T)$. However, the estimates may not satisfy property (6) given in Proposition 1. Namely, it may not hold, for $v \in V_T$, that:

$$\sum_{v' \in \text{Ch}(v)} \hat{\eta}(\boldsymbol{x}, v') \geq 1 \,,$$

since the node classifiers are trained independently from each other. The remedy relies on an additional normalization step during prediction, which may take the following form, for each child node $v' \in \text{Ch}(v)$:

$$\hat{\eta}(\boldsymbol{x}, v') \;\leftarrow\; \frac{\hat{\eta}(\boldsymbol{x}, v')}{\sum_{v'' \in \text{Ch}(v)} \hat{\eta}(\boldsymbol{x}, v'')}\,, \quad \text{if} \sum_{v'' \in \text{Ch}(v)} \hat{\eta}(\boldsymbol{x}, v'') < 1\,. \tag{10}$$

Nevertheless, this normalization is not always necessary. The theoretical results presented in Section 4 hold without it. Also empirically an algorithm without normalization performs similarly, being often slightly better. However, the complexity analysis of the prediction algorithms, presented later, requires this normalization.

The estimation of the label probabilities is only a part of the solution as we usually need a prediction algorithm that delivers a set of labels being as similar as possible to the actual one with respect to some application-specific loss function. Below we introduce two such algorithms based on tree search. Let us first consider a prediction algorithm which finds, for a test example $\boldsymbol{x}$, all labels such that:

$$\hat{\eta}_j(\boldsymbol{x}) \geq \tau_j\,, \quad j \in \mathcal{L}\,,$$

where $\tau_j \in [0, 1]$ are label-specific thresholds. The threshold-based predictions are inline with the theoretical analysis given in the next section, as for many performance metrics they lead to optimal decisions. Here, we present the algorithmic solution assuming that the particular values of τ_j, for all $j \in \mathcal{L}$, have been provided. Consider the tree search procedure presented in Algorithm 3. It starts with the root node and traverses the tree by visiting the nodes $v \in V_T$ for which $\hat{\eta}_{pa(v)}(\boldsymbol{x}) \geq \tau_v$, where $\tau_v = \min\{\tau_j : l_j \in L_v\}$. It uses a simple stack $\mathcal{Q}$ to guide the search. Obviously, the final prediction consists of labels corresponding to the visited leaves for which $\hat{\eta}_{\ell_j}(\boldsymbol{x}) \geq \tau_j$.

Algorithm 3 PLT.PREDICTWITHTHRESHOLDS$(T, H, \boldsymbol{\tau}, \boldsymbol{x})$

1: $\hat{\boldsymbol{y}} = \boldsymbol{0}$, $\mathcal{Q} = \emptyset$ ▷ Initialize prediction vector to all zeros and a stack
2: $\mathcal{Q}.\text{add}((r_T, \hat{\eta}(\boldsymbol{x}, r_T)))$ ▷ Add the tree root with the corresponding estimate of probability
3: **while** $\mathcal{Q} \neq \emptyset$ **do**   ▷ In the loop
4:      $(v, \hat{\eta}_v(\boldsymbol{x})) = \mathcal{Q}.\text{pop}()$ ▷ Pop an element from the stack
5:      **if** $\hat{\eta}_v(\boldsymbol{x}) \geq \tau_v$ **then**   ▷ If the probability estimate is greater or equal τ_v
6:          **if** v is a leaf **then**   ▷ If the node is a leaf
7:              $\hat{y}_v = 1$ ▷ Set the corresponding label in the prediction vector
8:          **else**   ▷ If the node is an internal node
9:              **for** $v' \in \text{Ch}(v)$ **do**   ▷ For all child nodes
10:                  $\hat{\eta}_{v'}(\boldsymbol{x}) = \hat{\eta}_v(\boldsymbol{x}) \times \hat{\eta}(\boldsymbol{x}, v')$ ▷ Compute $\hat{\eta}_{v'}(\boldsymbol{x})$ using $\hat{\eta}(v') \in H$
11:                  $\mathcal{Q}.\text{add}((v', \hat{\eta}_{v'}(\boldsymbol{x})))$ ▷ Add the node and the computed probability estimate
12: **return** $\hat{\boldsymbol{y}}$ ▷ Return the prediction vector

---

The next algorithm finds the top k labels with the highest $\hat{\eta}_j(\boldsymbol{x})$, $j \in \mathcal{L}$. Consider a variant of uniform-cost search [Russell and Norvig, 2009] presented in Algorithm 4. It uses, in turn, a priority queue $\mathcal{Q}$ to guide the search. In each iteration a node with the highest $\hat{\eta}_v(\boldsymbol{x})$ is popped from the queue. If the node is not a leaf, then its each child node v' is added to the priority queue with its $\hat{\eta}_{v'}(\boldsymbol{x})$. Otherwise, a label corresponding to the visited leaf is added to the prediction. If the number of predicted labels is equal k, then the procedure returns prediction $\hat{\boldsymbol{y}}$. Clearly, the priority queue guarantees that k labels with the highest $\hat{\eta}_j(\boldsymbol{x})$, $j \in \mathcal{L}$, are predicted.

Algorithm 4 PLT.PREDICTTOPLABELS($T, H, k, \boldsymbol{x}$)

1: $\hat{\boldsymbol{y}} = \boldsymbol{0}, \mathcal{Q} = \emptyset,$ ▷ Initialize prediction vector to all zeros and a priority queue
2: $k' = 0$ ▷ Initialize counter of predicted labels
3: $\mathcal{Q}.\text{add}((r_T, \hat{\eta}(\boldsymbol{x}, r_T)))$ ▷ Add the tree root with the corresponding estimate of probability
4: **while** $k' < k$ **do**   ▷ While the number of predicted labels is less than k
5:     $(v, \hat{\eta}_v(\boldsymbol{x})) = \mathcal{Q}.\text{pop}()$ ▷ Pop the top element from the queue
6:     **if** v is a leaf **then**   ▷ If the node is a leaf
7:         $\hat{y}_v = 1$ ▷ Set the corresponding label in the prediction vector
8:         $k' = k' + 1$ ▷ Increment the counter
9:     **else**   ▷ If the node is an internal node
10:         **for** $v' \in \text{Ch}(v)$ **do**   ▷ For all its child nodes
11:             $\hat{\eta}_{v'}(\boldsymbol{x}) = \hat{\eta}_v(\boldsymbol{x}) \times \hat{\eta}(\boldsymbol{x}, v')$ ▷ Compute $\hat{\eta}_{v'}(\boldsymbol{x})$ using $\hat{\eta}(v') \in H$
12:             $\mathcal{Q}.\text{add}((v', \hat{\eta}_{v'}(\boldsymbol{x})))$ ▷ Add the node and the computed probability estimate
13: **return** $\hat{\boldsymbol{y}}$ ▷ Return the prediction vector

Both algorithms presented above in the worst case can visit all nodes of the tree. However, in many practical applications they work in time logarithmic in the number of labels m. In the following subsection, we briefly discuss some basic results related to the computational complexity of PLT algorithms.

3.3 Computational complexity of PLTs

Following [Busa-Fekete et al., 2019], we define the training complexity of PLTs in terms of the number of nodes in which a training example $(\boldsymbol{x}, \boldsymbol{y})$ is used. From the definition of the tree and the PLT model (3), we have that each training example is used in the root, to estimate $\mathbf{P}(z_{r_T} = 1 | \boldsymbol{x})$, and in each node v for which $z_{\text{pa}(v)} = 1$, to estimate $\mathbf{P}(z_v = 1 | z_{\text{pa}(v)} = 1, \boldsymbol{x})$. Therefore, the training cost for a single observation $(\boldsymbol{x}, \boldsymbol{y})$ can be given as:

$$c(T, \boldsymbol{y}) = 1 + \sum_{v \in V_T \backslash r_T} z_{\text{pa}(v)} \,. \tag{11}$$

This definition agrees with the time complexity of the ASSIGNTONODES procedure, which is $O(c(T, \boldsymbol{y}))$ if the set operations are performed in $O(1)$ time. From the perspective of the training complexity of node classifiers, the above definition of cost is only justified for learning algorithms that scale linearly in the number of training examples. There exists, however, plenty of such algorithms with a prominent example of stochastic gradient descent.

The next proposition determines the upper bound for the cost $c(T, \boldsymbol{y})$.

Proposition 2. *For any tree T and vector $\boldsymbol{y}$ it holds that:*

$$c(T, \boldsymbol{y}) \leq 1 + \|\boldsymbol{y}\|_1 \cdot \text{depth}_T \cdot \text{deg}_T \,,$$

where $\text{depth}_T = \max_{v \in L_T} \text{len}_v - 1$ is the depth of the tree, and $\text{deg}_T = \max_{v \in V_T} \text{deg}_v$ is the highest degree of a node in T.

This result has been originally published in [Busa-Fekete et al., 2019]. For completeness, we present the proof in the Appendix. The immediate consequence of this result is the following remark which states that the training complexity of PLTs can scale logarithmically in the number of labels.

Remark 1. *Consider k-sparse multi-label classification (for which, $\|\boldsymbol{y}\|_1 \leq k$). For a balanced tree of constant $\deg_T = \lambda \ (\geq 2)$ and $\text{depth}_T = \log_\lambda m$, the training cost is $c(T, \boldsymbol{y}) = O(k \log m)$.*

Interestingly, the problem of finding the optimal tree structure in terms of the training cost is NP-hard, as proven in [Busa-Fekete et al., 2019]. However, the balanced trees achieve a logarithmic approximation of the optimal tree in the number of labels.

For the prediction cost, we use a similar definition. We define it as the number of calls to node classifiers for a single observation $\boldsymbol{x}$. Let us first consider Algorithm 3 with a threshold vector $\boldsymbol{\tau}$. Its prediction cost is clearly given by:

$$c_\tau(T, \boldsymbol{x}) = 1 + \sum_{v \in V_T \backslash r_T} [\![\hat{\eta}_{pa(v)}(\boldsymbol{x}) \geq \tau_v]\!] = 1 + \sum_{v \in V_T} [\![\hat{\eta}_v(\boldsymbol{x}) \geq \tau_v]\!] \cdot \deg_v .$$

Analogously to Proposition 2, we determine the upper bound for the prediction cost. To this end, let us upper bound $\sum_{j=1}^m \hat{\eta}_j(\boldsymbol{x})$ by a constant $\hat{P}$. Moreover, we assume that $\hat{\eta}_v(\boldsymbol{x})$ are properly normalized to satisfy the same requirements as true probabilities expressed in Proposition 1. For simplicity, we set all τ_v, $v \in V_T$, to τ. Then, we can prove the following result.

Theorem 1. *For Algorithm 3 with all thresholds τ_v, $v \in V_T$, set to τ and any $\boldsymbol{x} \in \mathcal{X}$, we have that:*

$$c_\tau(T, \boldsymbol{x}) \leq 1 + \lfloor \hat{P}/\tau \rfloor \cdot \text{depth}_T \cdot \deg_T , \tag{12}$$

where $\hat{P}$ is a constant upperbounding $\sum_{j=1}^m \hat{\eta}_j(\boldsymbol{x})$, $\text{depth}_T = \max_{v \in L_T} \text{len}_v - 1$, and $\deg_T = \max_{v \in V_T} \deg_v$.

We present the proof of this result in Appendix A. Similarly as in the case of the training cost, we can conclude the logarithmic cost in the number of labels.

Remark 2. *For a tree of constant $\deg_T = \lambda (\geq 2)$ and $\text{depth}_T = \log_\lambda m$, the cost of Algorithm 3 is $O(\log m)$.*

The above result can also be related to the sum of true conditional label probabilities, $\sum_{j=1}^m \eta_j(\boldsymbol{x})$. In this case one needs to take into account the L_1-estimation error of $\eta_j(\boldsymbol{x})$. In the next section, we discuss the upper bound of the L_1-estimation error that can be incorporated into the above result. A theorem of this form has been published before in [Busa-Fekete et al., 2019].

The analysis of Algorithm 4 which predicts the top k labels is more involved. Its prediction cost defined as before is upperbounded by $c_{\tau_k}(T, \boldsymbol{x})$, where τ_k is equal to $\hat{\eta}_j(\boldsymbol{x})$ being the k-th highest estimate of conditional label probabilities. However, this algorithm uses a priority queue which operations require $O(\log m)$ time. Therefore, each call of a node classifier is not associated with $O(1)$ cost. Nevertheless, in practical scenarios the maintenance of the priority queue is almost negligible as only in the worst case scenario its size approaches m.

Finally, let us shortly discuss the space complexity. The space needed for storing the final model can also be expressed in terms of the number of nodes. As the number of nodes of a label tree is upperbounded by $2m - 1$, that is, the maximum number of nodes of the tree with m leaves, the space complexity is $O(m)$. During training or prediction there are no other structures with a higher space demand. Nevertheless, different design choices impact the space requirements of PLTs. We discuss some of them in Section 6.

4 Statistical analysis of PLTs

In this section, we thoroughly analyze the PLT model in terms of its statistical properties. The main results concern the regret bounds for several performance measures commonly used in XMLC. We first upperbound the L_1 estimation error of marginal probabilities of labels, $|\eta_j(\boldsymbol{x}) - \hat{\eta}_j(\boldsymbol{x})|$, by the L_1 error of the node classifiers, $|\eta(\boldsymbol{x}, v) - \hat{\eta}(\boldsymbol{x}, v)|$. We then generalize this result to a wide class of strongly proper composite losses [Agarwal, 2014] to make a direct connection between the marginal probability estimates and a learning algorithm used in the tree nodes. We then analyze a wide class of generalized performance metrics. Instances of such metrics are Hamming loss, being a canonical loss function for multi-label classification, the AM metric which weights labels by their priors, or the macro and micro F_β-measures. Next, we present the regret analysis for precision@k which is the most popular metric used in XMLC. Finally, we discuss the relation of PLTs to hierarchical softmax.

4.1 L_1 estimation error

We start with a bound that express the quality of probability estimates $\hat{\eta}_v(\boldsymbol{x})$, $v \in V_T$. The lemma and corollary below generalize a similar result obtained for multi-class classification in [Beygelzimer et al., 2009b].

Lemma 1. *For any tree T and distribution $\mathbf{P}(\boldsymbol{y}|\boldsymbol{x})$ the following holds for each $v \in V_T$:*

$$|\eta_v(\boldsymbol{x}) - \hat{\eta}_v(\boldsymbol{x})| \leq \sum_{v' \in \text{Path}(v)} \eta_{\text{pa}(v')}(\boldsymbol{x}) \left|\eta(\boldsymbol{x}, v') - \hat{\eta}(\boldsymbol{x}, v')\right|, \tag{13}$$

where we assume $\hat{\eta}(\boldsymbol{x}, v) \in [0, 1]$, for each $v \in V_T$, and $\eta_{\text{pa}(r_T)}(\boldsymbol{x}) = 1$, for the root node r_T.

From this lemma we immediately get guarantees for estimates of the marginal probabilities, for each label $j \in \mathcal{L}$ corresponding to leaf node l_j.

Corollary 1. *For any tree T and distribution $\mathbf{P}(\boldsymbol{y}|\boldsymbol{x})$, the following holds for each label $j \in \mathcal{L}$:*

$$|\eta_j(\boldsymbol{x}) - \hat{\eta}_j(\boldsymbol{x})| \leq \sum_{v \in \text{Path}(l_j)} \eta_{\text{pa}(v)}(\boldsymbol{x}) |\eta(\boldsymbol{x}, v) - \hat{\eta}(\boldsymbol{x}, v)|, \tag{14}$$

where we assume $\eta_{\text{pa}(r_T)}(\boldsymbol{x}) = 1$ for the root node r_T.

It is worth to notice that the above bounds are tighter than the one in [Beygelzimer et al., 2009b], since the L_1 estimation error of the node classifiers is additionally multiplied by the probability of the parent node $\eta_{\text{pa}(v')}(\boldsymbol{x})$. Our results are also obtained using different arguments. Because of that, we present the entire proof below in the main text.

Proof. Recall the recursive factorization of probability $\eta_v(\boldsymbol{x})$ given in (5):

$$\eta_v(\boldsymbol{x}) = \eta(\boldsymbol{x}, v)\eta_{\text{pa}(v)}(\boldsymbol{x}).$$

As the same recursive relation holds for $\hat{\eta}_v(\boldsymbol{x})$, see (9), we have that

$$|\eta_v(\boldsymbol{x}) - \hat{\eta}_v(\boldsymbol{x})| = \left|\eta(\boldsymbol{x}, v)\eta_{\text{pa}(v)}(\boldsymbol{x}) - \hat{\eta}(\boldsymbol{x}, v)\hat{\eta}_{\text{pa}(v)}(\boldsymbol{x})\right|.$$

By adding and subtracting $\hat{\eta}(\boldsymbol{x}, v)\eta_{\mathrm{pa}(v)}(\boldsymbol{x})$, using the triangle inequality $|a + b| \leq |a| + |b|$ and the assumption that $\hat{\eta}(\boldsymbol{x}, v) \in [0, 1]$, we obtain:

$$
\begin{aligned}
|\eta_v(\boldsymbol{x}) - \hat{\eta}_v(\boldsymbol{x})| &= \left|\eta(\boldsymbol{x}, v)\eta_{\mathrm{pa}(v)}(\boldsymbol{x}) - \hat{\eta}(\boldsymbol{x}, v)\eta_{\mathrm{pa}(v)}(\boldsymbol{x}) + \hat{\eta}(\boldsymbol{x}, v)\eta_{\mathrm{pa}(v)}(\boldsymbol{x}) - \hat{\eta}(\boldsymbol{x}, v)\hat{\eta}_{\mathrm{pa}(v)}(\boldsymbol{x})\right| \\
&\leq \left|\eta(\boldsymbol{x}, v)\eta_{\mathrm{pa}(v)}(\boldsymbol{x}) - \hat{\eta}(\boldsymbol{x}, v)\eta_{\mathrm{pa}(v)}(\boldsymbol{x})\right| + \left|\hat{\eta}(\boldsymbol{x}, v)\eta_{\mathrm{pa}(v)}(\boldsymbol{x}) - \hat{\eta}(\boldsymbol{x}, v)\hat{\eta}_{\mathrm{pa}(v)}(\boldsymbol{x})\right| \\
&\leq \eta_{\mathrm{pa}(v)}(\boldsymbol{x})\left|\eta(\boldsymbol{x}, v) - \hat{\eta}(\boldsymbol{x}, v)\right| + \hat{\eta}(\boldsymbol{x}, v)\left|\eta_{\mathrm{pa}(v)}(\boldsymbol{x}) - \hat{\eta}_{\mathrm{pa}(v)}(\boldsymbol{x})\right| \\
&\leq \eta_{\mathrm{pa}(v)}(\boldsymbol{x})\left|\eta(\boldsymbol{x}, v) - \hat{\eta}(\boldsymbol{x}, v)\right| + \left|\eta_{\mathrm{pa}(v)}(\boldsymbol{x}) - \hat{\eta}_{\mathrm{pa}(v)}(\boldsymbol{x})\right|
\end{aligned}
$$

Since the rightmost term corresponds to the L_1 error of the parent of v, we use recursion to get the result of Lemma 1:

$$
|\eta_v(\boldsymbol{x}) - \hat{\eta}_v(\boldsymbol{x})| \leq \sum_{v' \in \mathrm{Path}(v)} \eta_{\mathrm{pa}(v')}(\boldsymbol{x})\left|\eta(\boldsymbol{x}, v') - \hat{\eta}(\boldsymbol{x}, v')\right| ,
$$

where for the root node $\eta_{\mathrm{pa}(r_T)}(\boldsymbol{x}) = 1$. As the above holds for any $v \in V$, the result also applies to marginal probabilities of labels as stated in Corollary 1. $\qquad\square$

The above results are conditioned on $\boldsymbol{x}$ and concern a single node $v \in V$. The next theorem gives the understanding of the average performance over all labels and the entire distribution $\mathbf{P}(\boldsymbol{x})$. We present the result in a general form of a weighted average as this form we use later to prove bounds for the generalized performance metrics.

Theorem 2. *For any tree T, distribution $\mathbf{P}(\boldsymbol{x}, \boldsymbol{y})$, and weights $W_j \in R$, $j \in \{1, \ldots, m\}$, the following holds:*

$$
\frac{1}{m}\sum_{j=1}^{m} W_j \mathbb{E}_{\boldsymbol{x} \sim \mathbf{P}(\boldsymbol{x})}\left[|\eta_j(\boldsymbol{x}) - \hat{\eta}_j(\boldsymbol{x})|\right] \leq
$$

$$
\frac{1}{m}\sum_{v \in V} \mathbf{P}(z_{\mathrm{pa}(v)} = 1)\mathbb{E}_{\boldsymbol{x} \sim \mathbf{P}(\boldsymbol{x}|z_{\mathrm{pa}(v)}=1)}\left[|\eta(\boldsymbol{x}, v') - \hat{\eta}(\boldsymbol{x}, v')|\right] \sum_{j \in L_v} W_j , \qquad (15)
$$

where for the root node $\mathbf{P}(z_{\mathrm{pa}(r_T)} = 1) = 1$. For $W_j = 1$, $j \in \{1, \ldots, m\}$, we have:

$$
\frac{1}{m}\sum_{j=1}^{m} \mathbb{E}_{\boldsymbol{x} \sim \mathbf{P}(\boldsymbol{x})}\left[|\eta_j(\boldsymbol{x}) - \hat{\eta}_j(\boldsymbol{x})|\right] \leq
$$

$$
\frac{1}{m}\sum_{v \in V} \mathbf{P}(z_{\mathrm{pa}(v)} = 1)\mathbb{E}_{\boldsymbol{x} \sim \mathbf{P}(\boldsymbol{x}|z_{\mathrm{pa}(v)}=1)}\left[|\hat{\eta}(\boldsymbol{x}, v') - \hat{\eta}(\boldsymbol{x}, v')|\right] |L_v| .
$$

The result states that the weighted expected L_1 estimation error averaged over all labels can be bounded by a weighted sum of expected L_1 errors of node classifiers divided by the number of labels. A weight associated with node v is a product of the probability mass of a parent node and the number of leave nodes in a subtree rooted in v. This means that a node closer to the root has a higher impact on the overall performance. This agrees with the intuition as such nodes impact estimates of more labels. We omit the proof of this theorem here as it is quite technical. It is presented with additional auxiliary results in Appendix B.

4.2 Strongly proper composite losses

So far the results concern the probability estimates without any direct link to a learning algorithm. In this subsection, we relate the quality of probability estimates to the error measured in terms of a loss function which can be minimized during the training of a node classifier. We first recall the concept of strongly proper composite losses [Agarwal, 2014] for binary classification. Examples of such losses are commonly used functions such as logistic loss, squared loss, squared hinge loss, and exponential loss. Notice that the standard hinge loss does not belong to this class of losses. Finally, we show an extension of Theorem 2 in which the right-hand side is expressed in terms of a strongly proper composite loss.

The strongly proper composite losses are of a special interest in the problem of class probability estimation with two outcomes, $y \in \{-1, 1\}$. Let pairs $(\boldsymbol{x}, y)$ be generated i.i.d. according to $\mathbf{P}(\boldsymbol{x}, y)$. We denote $\mathbf{P}(y = 1 \,|\, \boldsymbol{x})$ by $\eta(\boldsymbol{x})$ and its estimate by $\hat{\eta}(\boldsymbol{x}) \in [0, 1]$. Let us first define a class probability estimation (CPE) loss as a function $\ell : \{-1, 1\} \times [0, 1] \mapsto \mathbb{R}_+$. Its conditional risk is given by

$$R_\ell(\hat{\eta} \,|\, \boldsymbol{x}) = \eta(\boldsymbol{x})\ell(1, \hat{\eta}(\boldsymbol{x})) + (1 - \eta(\boldsymbol{x}))\ell(-1, \hat{\eta}(\boldsymbol{x})).$$

A CPE loss is proper if for any $\eta(\boldsymbol{x}) \in [0, 1]$, $\eta(\boldsymbol{x}) \in \arg\min_{\hat{\eta}} R_\ell(\hat{\eta} \,|\, \boldsymbol{x})$. Since it is often more convenient for prediction algorithms to work with a real-valued scoring function, $f : \mathcal{X} \mapsto \mathbb{R}$, than with an estimate bounded to interval $[0, 1]$, we transform $\hat{\eta}(\boldsymbol{x})$ using a strictly increasing (and therefore invertible) link function $\psi : [0, 1] \to \mathbb{R}$, that is, $f(\boldsymbol{x}) = \psi(\hat{\eta}(\boldsymbol{x}))$. We then consider a composite loss function $\ell_c : \{-1, 1\} \times \mathbb{R} \mapsto \mathbb{R}_+$ defined via a CPE loss as

$$\ell_c(y, f(\boldsymbol{x})) = \ell(y, \psi^{-1}(f(\boldsymbol{x}))).$$

The regret of f in terms of a loss function ℓ_c at point $\boldsymbol{x}$ is defined as:

$$\mathrm{reg}_{\ell_c}(f \,|\, \boldsymbol{x}) = R_\ell(\psi^{-1}(f) \,|\, \boldsymbol{x}) - R_\ell^*(\boldsymbol{x}),$$

where $R_\ell^*(\boldsymbol{x})$ is the minimum expected loss at point $\boldsymbol{x}$, achievable by $f^*(\boldsymbol{x}) = \psi(\eta(\boldsymbol{x}))$.

We say a loss function ℓ_c is λ-strongly proper composite loss, if for any $\eta(\boldsymbol{x}), \psi^{-1}(f(\boldsymbol{x})) \in [0, 1]$:

$$\left| \eta(\boldsymbol{x}) - \psi^{-1}(f(\boldsymbol{x})) \right| \le \sqrt{\frac{2}{\lambda}} \sqrt{\mathrm{reg}_{\ell_c}(f \,|\, \boldsymbol{x})}. \tag{16}$$

It can be shown under mild regularity assumptions that ℓ_c is λ-strongly proper composite if and only if its corresponding CPE loss is proper and function $H_\ell(\eta) = R_\ell(\eta \,|\, \boldsymbol{x})$ is λ-strongly concave, that is, $\left| \frac{d^2 H_\ell(\eta)}{d^2 \eta} \right| \ge \lambda$.

We apply the above results to node classifiers in a PLT tree. In each node $v \in V_T$ we consider a binary problem with $y = 2z_v - 1$ and pairs $(\boldsymbol{x}, z_v)$ generated i.i.d. according to $\mathbf{P}(\boldsymbol{x}, z_v \,|\, z_{\mathrm{pa}(v)} = 1)$. Moreover, let f_v be a scoring function in node $v \in V_T$ minimized by a strongly proper composite loss function ℓ_c. We obtain then the following result.

Theorem 3. *For any tree T, distribution $\mathbf{P}(\boldsymbol{x}, \boldsymbol{y})$, weights $W_j \in R$, $j \in \{1, \ldots, m\}$, a strongly proper composite loss function ℓ_c, and a set of scoring functions f_v, $v \in V_T$, the following holds:*

$$\frac{1}{m} \sum_{j=1}^m W_j \mathbb{E}_{\boldsymbol{x} \sim \mathbf{P}(\boldsymbol{x})} \left[|\eta_j(\boldsymbol{x}) - \hat{\eta}_j(\boldsymbol{x})| \right] \le \frac{\sqrt{2}}{m\sqrt{\lambda}} \sum_{v \in V} \sqrt{\mathbf{P}(z_{\mathrm{pa}(v)} = 1)\mathrm{reg}_{\ell_c}(f_v)} \sum_{j \in L_v} W_j, \tag{17}$$

15

where for the root node $\mathbf{P}(z_{\mathrm{pa}(r_T)} = 1) = 1$, *and* $\mathrm{reg}_{\ell_c}(f_v)$ *is the expected* ℓ_c-*regret of* f_v *taken over* $\mathbf{P}(\boldsymbol{x}, z_v \mid z_{\mathrm{pa}(v)} = 1)$. *For* $W_j = 1$, $j \in \{1, \ldots, m\}$, *we have:*

$$\frac{1}{m} \sum_{j=1}^{m} \mathbb{E}_{\boldsymbol{x} \sim \mathbf{P}(\boldsymbol{x})} \left[|\eta_j(\boldsymbol{x}) - \hat{\eta}_j(\boldsymbol{x})| \right] \leq \frac{\sqrt{2}}{m\sqrt{\lambda}} \sum_{v \in V} |L_v| \sqrt{\mathbf{P}(z_{\mathrm{pa}(v)} = 1) \mathrm{reg}_{\ell_c}(f_v)}. \tag{18}$$

The theorem justifies the use of strongly proper composite losses during the training of node classifiers. The technical details of the proof are presented in Appendix C. Here, we only notice that the weights of node errors follow from Theorem 2, while the squared root dependency from (16).

4.3   Generalized classification performance metrics

The results above show guarantees of PLTs for estimates of marginal probabilities of labels. In this subsection, we discuss a wide family of metrics often used to report performance of multi-label classification, such as (weighted) Hamming loss, AM metric, or macro- and micro-averaged F_β-measure. This family of metrics can be defined as a linear-fractional function of label-wise false positives $\mathrm{FP}_j(h_j) = \mathbf{P}(h_j(\boldsymbol{x}) = 1 \wedge y_j = 0)$ and false negatives $\mathrm{FN}_j(h_j) = \mathbf{P}(h_j(\boldsymbol{x}) = 0 \wedge y_j = 1)$. As already proven [Koyejo et al., 2015, Kotłowski and Dembczyński, 2017] the optimal strategy for these metrics is to find a threshold on the marginal probability $\eta_j(\boldsymbol{x})$ for each label $j \in \mathcal{L}$. From the practical point of view this boils down to setting thresholds to either predefined values, if they are known from theory (for example, this is 0.5 for Hamming loss), or to tune them on a validation set, if their optimal value depends on the optimum of the metric [Koyejo et al., 2015, Kotłowski and Dembczyński, 2017]. Both approaches can be applied to PLTs. The prediction procedure from Algorithm 3 can work with any set of thresholds. However, for small values of thresholds a problem of exploring a large part of a tree may appear. The results below show the theoretical aspects of these approaches, namely, we tailor the regret bounds for the general 1-vs-All approach, proven in [Kotłowski and Dembczyński, 2017], to PLTs.

Let us define the problem in a formal way. To this end we use a linear-factorial function Ψ of the following generic form:

$$\Psi(\mathrm{FP}, \mathrm{FN}) = \frac{a_0 + a_1 \mathrm{FP} + a_2 \mathrm{FN}}{b_0 + b_1 \mathrm{FP} + b_2 \mathrm{FN}}, \tag{19}$$

being non-increasing in its arguments. Moreover, we assume that there exists $\gamma > 0$, such that

$$b_0 + b_1 \mathrm{FP} + b_2 \mathrm{FN} \geq \gamma, \tag{20}$$

that is, the denominator of Ψ is positive and bounded away from 0. A macro-averaged generalized classification performance metric $\Psi_{\mathrm{macro}(\boldsymbol{x})}$ is defined then as:

$$\Psi_{\mathrm{macro}}(\boldsymbol{h}) = \frac{1}{m} \sum_{j=1}^{m} \Psi(h_j) = \frac{1}{m} \sum_{j=1}^{m} \Psi(\mathrm{FP}_j(h_j), \mathrm{FN}_j(h_j)). \tag{21}$$

It computes an average performance over single labels. Micro-averaged performance metrics, in turn, compute first the average false positives and false negatives:

$$\bar{\mathrm{FP}}(\boldsymbol{h}) = \frac{1}{m} \sum_{i=1}^{m} \mathrm{FP}_j(h_j), \quad \bar{\mathrm{FN}}(\boldsymbol{h}) = \frac{1}{m} \sum_{j=1}^{m} \mathrm{FN}_j(h_j).$$

16

Then, a micro-averaged metric $\Psi_{\text{micro}(\boldsymbol{x})}$ is defined as:

$$\Psi_{\text{micro}}(\boldsymbol{h}) = \Psi(\bar{\text{FP}}(\boldsymbol{h}), \bar{\text{FN}}(\boldsymbol{h})) \,. \tag{22}$$

The optimal classifier, being a member of class $\mathcal{H}_{\text{bin}}^m : \mathcal{X} \to \{0,1\}^m$, for the above generalized performance measures has the generic form:

$$\boldsymbol{h}_{\Psi}^*(\boldsymbol{x}) = \boldsymbol{h}_{\boldsymbol{\alpha}_{\Psi}^*}^*(\boldsymbol{x}) = \left(h_{1,\alpha_{\Psi,1}^*}^*(\boldsymbol{x}), h_{2,\alpha_{\Psi,2}^*}^*(\boldsymbol{x}), \ldots, h_{m,\alpha_{\Psi,m}^*}^*(\boldsymbol{x}) \right) , \tag{23}$$

where

$$h_{j,\alpha_{\Psi,j}^*}^*(\boldsymbol{x}) = [\![\eta_j(\boldsymbol{x}) > \alpha_{\Psi,j}^*]\!] \,, \text{with } \Psi\text{-optimal } \boldsymbol{\alpha}_{\Psi}^* = (\alpha_{\Psi,1}^*, \alpha_{\Psi,2}^*, \ldots, \alpha_{\Psi,m}^*) \in [0,1]^m \,.$$

In other words, for each metric there is an optimal vector $\boldsymbol{\alpha}_{\Psi}^*$ of thresholds defined over the marginal probabilities of labels, $\eta_j(\boldsymbol{x})$, for all $j \in \mathcal{L}$. The values of its elements are given by the following expression [Koyejo et al., 2015, Kotłowski and Dembczyński, 2017]:

$$\alpha_{\Psi}^* = \frac{\Psi(\text{FP}^*, \text{FN}^*)b_1 - a_1}{\Psi(\text{FP}^*, \text{FN}^*)(b_1 + b_2) - (a_1 + a_2)} \,,$$

where FP^*, FN^* are arguments maximizing either $\Psi(\text{FP}_j(h_j), \text{FN}_j(h_j))$, for each label $j \in \mathcal{L}$ separately, in case of a macro-averaged metric, or $\Psi(\bar{\text{FP}}(\boldsymbol{h}), \bar{\text{FN}}(\boldsymbol{h}))$ in case of a micro-averaged metric. This result shows that for macro-averaged metrics the threshold can be different for each label, while for micro-average metrics there is one common threshold shared by all labels. Therefore, we denote the optimal classifier for a macro-average metric by $\boldsymbol{h}_{\boldsymbol{\alpha}_{\Psi}^*}^*$, while for a micro-average metric by $\boldsymbol{h}_{\alpha_{\Psi}^*}^*$.

The thresholds in general depend on the optimal value of Ψ, which makes their value to be unknown beforehand. Only for metrics for which $b_1 = b_2 = 0$, the thresholds can be computed a priori. This is the case of Hamming loss, its cost-sensitive variant (in which there are different costs of false positive and false negative predictions), or the AM metric. In the other cases, thresholds have to be found on a validation set. For some metrics, such as the micro- and macro-F measure, this can be performed efficiently even in the XMLC setting, as only positive and positively predicted labels are needed to tune thresholds [Jasinska et al., 2016]. This can be even obtained using an online procedure [Busa-Fekete et al., 2015, Jasinska et al., 2016].

We present the form of $\Psi(\text{FP}, \text{FN})$ and α_{Ψ}^* for some popular generalized performance metrics in Table 1. We use there P to denote $\mathbf{P}(y_j = 1)$, for macro-averaging, and $\frac{1}{m} \sum_{j=1}^m \mathbf{P}(y_j = 1)$, for micro-averaging. Remark that this is a constant not depending on $\boldsymbol{h}$. All these metrics can be used with macro- and micro-averaging. Remark, however, that for Hamming loss both variants lead to the same form. A similar table can be found in [Kotłowski and Dembczyński, 2017].

The regret of the Ψ_{macro} metric decomposes into a weighted sum:

$$\text{reg}_{\Psi_{\text{macro}}}(\boldsymbol{h}) = \Psi_{\text{macro}}(\boldsymbol{h}_{\boldsymbol{\alpha}_{\Psi}^*}^*) - \Psi_{\text{macro}}(\boldsymbol{h}) = \frac{1}{m} \sum_{j=1}^m (\Psi(h_{j,\alpha_{\Psi,j}^*}^*) - \Psi(h_j)) \tag{24}$$

In turn, the regret of the Ψ_{micro} metric is given by:

$$\text{reg}_{\Psi_{\text{micro}}}(\boldsymbol{h}) = \Psi_{\text{micro}}(\boldsymbol{h}_{\alpha_{\Psi}^*}^*) - \Psi_{\text{micro}}(\boldsymbol{h}) \,. \tag{25}$$

We are interested in bounding these regrets with a performance of node classifiers of a PLT. We assume, similarly as in the previous subsection, that a score function $f_v(\boldsymbol{x})$ in a node $v \in V$ is

Metric	$\Psi(\mathrm{FP},\mathrm{FN})$	α^*_Ψ
Hamming loss	$1 - \mathrm{FP} - \mathrm{FN}$	0.5
F-measure	$\frac{(1+\beta^2)(P-\mathrm{FN})}{(1+\beta^2)P-\mathrm{FN}+\mathrm{FP}}$	$\Psi(\mathrm{FP}^*,\mathrm{FN}^*)/2$
Jaccard similarity	$\frac{P-\mathrm{FN}}{P+\mathrm{FP}}$	$\frac{\Psi(\mathrm{FP}^*,\mathrm{FN}^*)}{\Psi(\mathrm{FP}^*,\mathrm{FN}^*)+1}$
AM	$\frac{2P(1-P)-P\mathrm{FP}-(1-P)\mathrm{FN}}{2P(1-P)}$	P

Table 1: Examples of popular generalized performance metrics, with their form of $\Psi(\mathrm{FP},\mathrm{FN})$ and α^*_Ψ. P denotes $\mathbf{P}(y_j=1)$, for macro-averaging, or $\frac{1}{m}\sum_{j=1}^m \mathbf{P}(y_j=1)$, for micro-averaging.

trained via minimization of a strongly proper composite loss function ℓ_c. The estimates $\hat\eta(\boldsymbol{x},v)$, for all $v \in V$, are then computed as:

$$\hat\eta(\boldsymbol{x},v) = \psi^{-1}(f_v(\boldsymbol{x})).$$

The final prediction is computed by Algorithm 3 and has a form similar to the optimal classifier (23):

$$\boldsymbol{h}_{\boldsymbol{\tau}}(\boldsymbol{x}) = (h_{1,\tau_1}(\boldsymbol{x}), h_{2,\tau_2}(\boldsymbol{x}), \ldots, h_{m,\tau_m}(\boldsymbol{x})), \text{ where } h_{j,\tau_j}(\boldsymbol{x}) = [\![\hat\eta_j(\boldsymbol{x}) > \tau_j]\!],$$

for some vector $\boldsymbol{\tau} = (\tau_1, \tau_2, \ldots, \tau_m) \in [0,1]^m$ of thresholds. Estimates $\hat\eta_j(\boldsymbol{x})$ are computed as in (8), that is, $\hat\eta_j(\boldsymbol{x}) = \prod_{v \in \mathrm{Path}(l_j)} \hat\eta(\boldsymbol{x},v)$, where $l_j \in L_T$ is a node corresponding to label j. The theorems below present the main result of this section.

Theorem 4. *Let $\tau_j^* = \arg\max_\tau \Psi(h_{j,\tau})$, for each $j \in \mathcal{L}$, and $\boldsymbol{\tau}^* = (\tau_1^*, \tau_2^*, \ldots, \tau_m^*)$. For any tree T and distribution $\mathbf{P}(\boldsymbol{x},\boldsymbol{y})$, the classifier $\boldsymbol{h}_{\boldsymbol{\tau}^*}$ achieves the following upper bound on its Ψ_{macro}-regret:*

$$\mathrm{reg}_{\Psi_{\mathrm{macro}}}(\boldsymbol{h}_{\boldsymbol{\tau}^*}) \leq \frac{\sqrt{2}}{m\sqrt{\lambda}} \sum_{v \in V} \sqrt{\mathbf{P}(z_{\mathrm{pa}(v)}=1)\mathrm{reg}_{\ell_c}(f_v)} \sum_{j \in L_v} C_j,$$

where $C_j = \frac{1}{\gamma}(\Psi(h_\Psi^*,j)(b_1+b_2)-(a_1+a_2))$, for each $j \in \mathcal{L}$, with γ defined in (20), $\mathbf{P}(z_{\mathrm{pa}(r_T)}=1)=1$ for the root node, and $\mathrm{reg}_{\ell_c}(f_v)$ is the expected ℓ_c-regret of f_v taken over $\mathbf{P}(\boldsymbol{x}, z_v \,|\, z_{\mathrm{pa}(v)}=1)$.

Theorem 5. *Let $\boldsymbol{h}_\tau = (h_{1,\tau}, h_{2,\tau}, \ldots, h_{m,\tau})$ be a classifier which shares the same threshold τ over all labels $j \in \mathcal{L}$. For any tree T, distribution $\mathbf{P}(\boldsymbol{x},\boldsymbol{y})$, and $\tau^* = \arg\max_\tau \Psi_{\mathrm{micro}}(\boldsymbol{h}_\tau)$, classifier $\boldsymbol{h}_{\tau^*}$ achieves the following upper bound on its Ψ_{micro}-regret:*

$$\mathrm{reg}_{\Psi_{micro}}(\boldsymbol{h}_{\tau^*}) \leq \frac{C}{m}\sqrt{\frac{2}{\lambda}} \sum_{v \in V} |L_v|\sqrt{\mathbf{P}(z_{\mathrm{pa}(v)}=1)\mathrm{reg}_{\ell_c}(f_v)},$$

where $C = \frac{1}{\gamma}(\Psi_{\mathrm{micro}}(\boldsymbol{h}_\Psi^*)(b_1+b_2)-(a_1+a_2))$ with γ defined in (20), $\mathbf{P}(z_{\mathrm{pa}(r_T)}=1)=1$ for the root node, and $\mathrm{reg}_{\ell_c}(f_v)$ is the expected ℓ_c-regret of f_v taken over $\mathbf{P}(\boldsymbol{x}, z_v \,|\, z_{\mathrm{pa}(v)}=1)$.

The above theorems can be interpreted in the following way. For marginal probability estimates $\hat\eta_j(\boldsymbol{x})$, $j \in \mathcal{L}$, obtained as described just before the theorem, there exists a vector $\boldsymbol{\tau}$ of thresholds, for which the regret of a generalized performance metric is upperbounded solely by regrets of node classifiers, expressed in terms of a strongly proper composite loss function. Therefore, from the perspective of learning one needs to focus on the node classifiers to get as accurate as possible

18

estimates of marginal probabilities of labels, by minimizing a strongly proper composite loss function in each node. The next step, being independent of the previous one, is to obtain the right values of thresholds $\boldsymbol{\tau}^*$, following one of the approaches mentioned above.

Let us analyze the regret bounds more carefully. In the case of macro-averaged metrics, the regret of each node classifier is weighted by the sum of C_j-values of all labels in the corresponding subtree. In the case of micro-averaged metrics, there is only one global C-value, and each node classifier is weighted by the number of labels in the corresponding subtree. The values of C and γ for different metrics are given in Table 2 (a similar table can be found in [Kotłowski and Dembczyński, 2017]). It is easy to verify with these values that for the Hamming loss the regret bounds for macro- and micro-averaging are the same. This agrees with the fact that both averaging schemes boils down to the same metric in case of the Hamming loss. In general, the macro- and micro-averaging bounds coincide for all metrics with constant C. Interestingly, the bounds are different for the F_1-measure and the Jaccard similarity, while they both share the same optimal solution (since the Jaccard similarity is a strictly monotone transformation of the F_1-measure). As γ is the same for both metrics, this observation suggests that C could be defined more tightly. One can also observe that C grows with decreasing P. Therefore, for sparse problems and labels from the long-tail the value of C can be large, potentially leading to poor guarantees.

Metric	γ	C
Hamming loss	1	2
F_β-measure	$\beta^2 P$	$\frac{1+\beta}{\beta^2 P}$
Jaccard similarity	P	$\frac{\Psi(\mathrm{FP}^*,\mathrm{FN}^*)+1}{P}$
AM	$2P(1-P)$	$\frac{1}{2P(1-P)}$

Table 2: The values of γ and C values for some generalized classification performance metrics. As before, P denotes $\mathbf{P}(y_j = 1)$, for macro-averaging, or $\frac{1}{m}\sum_{j=1}^m \mathbf{P}(y_j = 1)$, for micro-averaging.

The proofs of both theorems are given in Appendix D. They are based on results previously obtained for the 1-vs-ALL approach in [Kotłowski and Dembczyński, 2017], combined together with Theorem 3. The result for the 1-vs-ALL approach relies on two observations. The first one states that the regret for a cost-sensitive binary classification can be upperbounded by the L_1 estimation error of the conditional probabilities, if a classification procedure uses a threshold which directly corresponds to the misclassification cost. The second shows that the regret of the generic function $\Psi(\mathrm{FP},\mathrm{FN})$ can be upperbounded by the regret of the cost-sensitive binary classification with costs related to α_Ψ^*. The actual value of the optimal thresholds is a direct consequence of the proof. Putting these two observations together along with Theorem 3 gives the final results.

4.4   Precision@k

In this section, we analyze precision@k which is of a different nature than the metrics discussed above. Let us consider a class of functions $\mathcal{H}_{@k}^m = \{\boldsymbol{h} \in \mathcal{H}_{\mathrm{bin}}^m : \sum_{j=1}^m h_j(\boldsymbol{x}) = k \,, \forall \boldsymbol{x} \in \mathcal{X}\}$, that is, functions that predict exactly k labels with $k \le m$. We then define precision@k for $\boldsymbol{h}_{@k} \in \mathcal{H}_{@k}^m$ as:

$$p@k(\boldsymbol{y}, \boldsymbol{h}_{@k}(\boldsymbol{x})) = \frac{1}{k} \sum_{j \in \hat{\mathcal{L}}_{\boldsymbol{x}}} [\![y_j = 1]\!]\,,$$

where $\hat{\mathcal{L}}_{\boldsymbol{x}} = \{j \in \mathcal{L} : h_j(\boldsymbol{x}) = 1\}$ is a set of k labels predicted by classifier $\boldsymbol{h}_{@k}$ for $\boldsymbol{x}$. In order to define conditional risk it is more convenient to consider the precision@k loss, $\ell_{p@k} = 1 - p@k(\boldsymbol{y}, \boldsymbol{h}_{@k}(\boldsymbol{x}))$. The conditional risk is then:

$$
\begin{aligned}
R_{p@k}(\boldsymbol{h}_{@k} \,|\, \boldsymbol{x}) &= \mathbb{E}_{\boldsymbol{y}} \ell_{p@k}(\boldsymbol{y}, \boldsymbol{h}_{@k}(\boldsymbol{x})) \\
&= 1 - \sum_{\boldsymbol{y} \in \mathcal{Y}} \mathbf{P}(\boldsymbol{y} \,|\, \boldsymbol{x}) \frac{1}{k} \sum_{j \in \hat{\mathcal{L}}_{\boldsymbol{x}}} [\![y_j = 1]\!] \\
&= 1 - \frac{1}{k} \sum_{j \in \hat{\mathcal{L}}_{\boldsymbol{x}}} \sum_{\boldsymbol{y} \in \mathcal{Y}} \mathbf{P}(\boldsymbol{y} \,|\, \boldsymbol{x}) [\![y_j = 1]\!] \\
&= 1 - \frac{1}{k} \sum_{j \in \hat{\mathcal{L}}_{\boldsymbol{x}}} \eta_j(\boldsymbol{x}) \,.
\end{aligned}
$$

From the above it is easy to notice that the optimal strategy for precision@k,

$$
\boldsymbol{h}^*_{p@k}(\boldsymbol{x}) = \left(h^*_{1,p@k}, h^*_{2,p@k}, \ldots, h^*_{m,p@k} \right) \,,
$$

is to predict k labels with the highest marginal probabilities $\eta_j(\boldsymbol{x})$,

$$
h^*_{j,p@k} = \begin{cases} 1, & j \in \hat{\mathcal{L}}^*_{\boldsymbol{x}} \\ 0, & \text{otherwise} \end{cases} \,, \tag{26}
$$

with $\hat{\mathcal{L}}^*_{\boldsymbol{x}} = \{j \in \mathcal{L} : \pi(j) \le k\}$ and π being a permutation of the labels ordered with respect to descending $\eta_j(\boldsymbol{x})$ with ties solved in any way. The conditional regret for precision@k is then:

$$
\text{reg}_{p@k}(\boldsymbol{h} \,|\, \boldsymbol{x}) = \frac{1}{k} \sum_{i \in \hat{\mathcal{L}}^*_{\boldsymbol{x}}} \eta_i(\boldsymbol{x}) - \frac{1}{k} \sum_{j \in \hat{\mathcal{L}}_{\boldsymbol{x}}} \eta_j(\boldsymbol{x}) \,.
$$

The conditional regret with respect to precision@k can be upperbounded by the L_1-estimation errors as stated by the following theorem, originally published in [Wydmuch et al., 2018].

Theorem 6. *For any tree T, distribution $\mathbf{P}(\boldsymbol{y} \,|\, \boldsymbol{x})$ and classifier $\boldsymbol{h}_{@k} \in \mathcal{H}^m_{@k}$ the following holds:*

$$
\text{reg}_{p@k}(\boldsymbol{h}_{@k} \,|\, \boldsymbol{x}) = \frac{1}{k} \sum_{i \in \hat{\mathcal{L}}^*_{\boldsymbol{x}}} \eta_i(\boldsymbol{x}) - \frac{1}{k} \sum_{j \in \hat{\mathcal{L}}_{\boldsymbol{x}}} \eta_j(\boldsymbol{x}) \le 2 \max_j |\eta_j(\boldsymbol{x}) - \hat{\eta}_j(\boldsymbol{x})| \,.
$$

Proof. Let us add and subtract the following two terms, $\frac{1}{k} \sum_{i \in \hat{\mathcal{L}}^*_{\boldsymbol{x}}} \hat{\eta}_i(\boldsymbol{x})$ and $\frac{1}{k} \sum_{j \in \hat{\mathcal{L}}_{\boldsymbol{x}}} \hat{\eta}_j(\boldsymbol{x})$, to the

regret and reorganize the expression in the following way:

$$\mathrm{reg}_{p@k}(\boldsymbol{h}_{@k}\,|\,\boldsymbol{x}) = \underbrace{\frac{1}{k}\sum_{i\in\hat{\mathcal{L}}_{\boldsymbol{x}}^{*}}\eta_i(\boldsymbol{x}) - \frac{1}{k}\sum_{i\in\hat{\mathcal{L}}_{\boldsymbol{x}}^{*}}\hat{\eta}_i(\boldsymbol{x})}_{\leq\frac{1}{k}\sum_{i\in\hat{\mathcal{L}}_{\boldsymbol{x}}^{*}}|\eta_i(\boldsymbol{x})-\hat{\eta}_i(\boldsymbol{x})|}$$

$$+ \underbrace{\frac{1}{k}\sum_{j\in\hat{\mathcal{L}}_{\boldsymbol{x}}}\hat{\eta}_j(\boldsymbol{x}) - \frac{1}{k}\sum_{j\in\hat{\mathcal{L}}_{\boldsymbol{x}}}\eta_j(\boldsymbol{x})}_{\leq\frac{1}{k}\sum_{j\in\hat{\mathcal{L}}_{\boldsymbol{x}}}|\hat{\eta}_j(\boldsymbol{x})-\eta_j(\boldsymbol{x})|}$$

$$+ \underbrace{\frac{1}{k}\sum_{i\in\hat{\mathcal{L}}_{\boldsymbol{x}}^{*}}\hat{\eta}_i(\boldsymbol{x}) - \frac{1}{k}\sum_{j\in\hat{\mathcal{L}}_{\boldsymbol{x}}}\hat{\eta}_j(\boldsymbol{x})}_{\leq 0}$$

$$\leq \frac{1}{k}\sum_{i\in\hat{\mathcal{L}}_{\boldsymbol{x}}^{*}}|\eta_i(\boldsymbol{x}) - \hat{\eta}_i(\boldsymbol{x})| + \frac{1}{k}\sum_{j\in\hat{\mathcal{L}}_{\boldsymbol{x}}}|\eta_j(\boldsymbol{x}) - \hat{\eta}_j(\boldsymbol{x})|$$

Next we bound each L_1 error, $|\eta_j(\boldsymbol{x}) - \hat{\eta}_j(\boldsymbol{x})|$ by $\max_j |\eta_j(\boldsymbol{x}) - \hat{\eta}_j(\boldsymbol{x})|$. There are at most $|\mathcal{Y}_k| + |\hat{\mathcal{Y}}_k| = 2k$ such terms. Therefore

$$\mathrm{reg}_{p@k}(\boldsymbol{h}\,|\,\boldsymbol{x}) \leq 2\max_j |\eta_j(\boldsymbol{x}) - \hat{\eta}_j(\boldsymbol{x})| \ .$$

$\square$

Interestingly, the bound does not depend neither on k nor m. However, if $k = m$ then $\mathrm{reg}_{p@m} = 0$ for any distribution, since $\hat{\mathcal{L}}_{\boldsymbol{x}}^{*} = \hat{\mathcal{L}}_{\boldsymbol{x}}$ in this case. In general, if $m < 2k$, then $\hat{\mathcal{L}}_{\boldsymbol{x}}^{*} \cap \hat{\mathcal{L}}_{\boldsymbol{x}} \neq \emptyset$. In other words, some of the labels from $\hat{\mathcal{L}}_{\boldsymbol{x}}$ are also in $\hat{\mathcal{L}}_{\boldsymbol{x}}^{*}$, so the bound can be tighter. For example, one can multiply the bound by $\frac{\min(k,m-k)}{k}$, assuming that $k \leq m$. However, in extreme classification usually $k \ll m$, so we do not use the more complex bound.

The above result suggests that PLTs are well-suited to optimization of precision@k. The next theorem shows this directly by providing an upper bound of the unconditional regret for a PLT. We use the same setting as in the above subsection with the difference that instead of thresholding probability estimates we use Algorithm 4 to compute predictions consisting of k labels with the highest $\hat{\eta}_j(\boldsymbol{x})$. The form of the final PLT classifier $\boldsymbol{h}_{@k}(\boldsymbol{x})$ is then similar to (26), but with permutation π defined over $\hat{\eta}_j(\boldsymbol{x})$, $j \in \mathcal{L}$. Unfortunately, the max operator from Theorem 6 needs to be replaced by sum in the derivations, therefore the theorem has the following form.

Theorem 7. *For any tree T and distribution $\mathbf{P}(\boldsymbol{x}, \boldsymbol{y})$, classifier $\boldsymbol{h}_{@k}(\boldsymbol{x})$ achieves the following upper bound on its precision@k regret:*

$$\mathrm{reg}_{p@k}(\boldsymbol{h}_{@k}) \leq \frac{2\sqrt{2}}{\sqrt{\lambda}}\sum_{v\in V}|L_v|\sqrt{\mathbf{P}(z_{\mathrm{pa}(v)}=1)\mathrm{reg}_{\ell_c}(f_v)}\,,$$

where $\mathbf{P}(z_{\mathrm{pa}(r_T)} = 1) = 1$ for the root node, and $\mathrm{reg}_{\ell_c}(f_v)$ is the expected ℓ_c-regret of f_v taken over $\mathbf{P}(\boldsymbol{x}, z_v\,|\,z_{\mathrm{pa}(v)} = 1)$.

Proof. By taking expectation over $\mathbf{P}(\boldsymbol{x})$ of the bound from Theorem 6 and replacing the max operator by sum, that is, $\max(a, b) \le a + b$, for $a, b \ge 0$, we obtain:

$$\text{reg}_{p@k}(\boldsymbol{h}_{@k}) \le 2 \sum_{j=1}^{m} \mathbb{E}_{\boldsymbol{x} \sim \mathbf{P}(\boldsymbol{x})} \left[|\eta_j(\boldsymbol{x}) - \hat{\eta}_j(\boldsymbol{x})| \right]$$

Next, by applying (18) from Theorem 3, we get the statement:

$$\text{reg}_{p@k}(\boldsymbol{h}_{@k}) \le \frac{2\sqrt{2}}{\sqrt{\lambda}} \sum_{v \in V} |L_v| \sqrt{\mathbf{P}(z_{\text{pa}(v)} = 1) \text{reg}_{\ell_c}(f_v)} \,.$$

$\square$

It is worth to compare the above bound with the one for the Hamming loss, taken either from Theorem 4 or Theorem 5, with $C = 2$ and $\gamma = 1$ (see Table 2). It turns out that the bound for precision@k is m times larger. The reason is that if there were k labels with the L_1-estimation error approaching 1, but with the actual probability close to 0, then the precision@k regret would get its maximum. On the other hand, the Hamming loss regret is an average of label-wise regrets. Therefore, it does not suffer much, as there were only k labels out of m with the highest regret.

4.5 Relation to hierarchical softmax

In this section, we show that PLTs are strictly related to hierarchical softmax designed for multi-class classification. Using our notation, we have $\sum_{i=1}^{m} y_i = 1$ for multi-class problems, that is, there is one and only one label assigned to an instance $(\boldsymbol{x}, \boldsymbol{y})$. The marginal probabilities $\eta_j(\boldsymbol{x})$ in this case sum up to 1. Since in multi-class classification always one label is assigned to an instance, there is no need to learn a root classifier which verifies whether there exists a positive label for an instance. Nevertheless, the factorization of the conditional probability of label j is given by the same equation (3) as for multi-label case:

$$\eta_j(\boldsymbol{x}) = \prod_{v' \in \text{Path}(l_j)} \eta(\boldsymbol{x}, v') \,.$$

However, in this case $\eta(\boldsymbol{x}, v') = 1$, for v' being the root, and

$$\sum_{v' \in \text{Ch}(v)} \eta(\boldsymbol{x}, v') = 1 \,,$$

since $\sum_{i=1}^{m} y_i = 1$. One can easily verify that the model above is the same as the one presented in [Morin and Bengio, 2005], where the parent nodes are identified by a code indicating a path from the root to this node. When used with a sigmoid function to model the conditional probabilities, we obtain the popular formulation of hierarchical softmax.

To deal with multi-label problems, some popular tools, such as FASTTEXT [Joulin et al., 2017] and its extension LEARNED TREE [Jernite et al., 2017], apply hierarchical softmax with a simple heurustic, we call *pick-one-label*, which randomly picks one of the positive labels from a given training instance. The resulting instance is then treated as a multi-class instance. During prediction, the heuristic returns a multi-class distribution and the k most probable labels. We show below that this specific reduction of the multi-label problem to multi-class classification is not consistent in general.

Since the probability of picking a label j from $\boldsymbol{y}$ is equal to $y_j / \sum_{j'=1}^m y_{j'}$, the pick-one-label heuristic maps the multi-label distribution to a multi-class distribution in the following way:

$$\eta_j'(\boldsymbol{x}) = \mathbf{P}'(y_j = 1 \,|\, \boldsymbol{x}) = \sum_{\boldsymbol{y} \in \mathcal{Y}} \frac{y_j}{\sum_{j'=1}^m y_{j'}} \mathbf{P}(\boldsymbol{y} \,|\, \boldsymbol{x}) \,, j \in \mathcal{L} \,. \tag{27}$$

It can be easily checked that the resulting $\eta_j'(\boldsymbol{x})$ form a multi-class distribution as the probabilities sum up to 1. It is obvious that the heuristic changes the marginal probabilities of labels, unless the initial distribution is multi-class. Therefore this method cannot lead to a consistent classifier in terms of estimating $\eta_j(\boldsymbol{x})$. As we show below, it is also not consistent for precision@k in general.

Proposition 3. *A classifier $\boldsymbol{h}_{@k} \in \mathcal{H}_{@k}^m$ predicting k labels with highest $\eta_j'(\boldsymbol{x})$, $j \in \mathcal{L}$, defined in (27), has in general a non-zero regret in terms of precision@k.*

Proof. We prove the proposition by giving a simple counterexample. Consider the following conditional distribution for some $\boldsymbol{x}$:

$$\mathbf{P}(\boldsymbol{y} = (1, 0, 0) \,|\, \boldsymbol{x}) = 0.1 \,, \quad \mathbf{P}(\boldsymbol{y} = (1, 1, 0) \,|\, \boldsymbol{x}) = 0.5 \,, \quad \mathbf{P}(\boldsymbol{y} = (0, 0, 1) \,|\, \boldsymbol{x}) = 0.4 \,.$$

The optimal top 1 prediction for this example is obviously label 1, since the marginal probabilities are $\eta_1(\boldsymbol{x}) = 0.6, \eta_2(\boldsymbol{x}) = 0.5, \eta_3(\boldsymbol{x}) = 0.4$. However, the pick-one-label heuristic will transform the original distribution to the following one: $\eta_1'(\boldsymbol{x}) = 0.35, \eta_2'(\boldsymbol{x}) = 0.25, \eta_3'(\boldsymbol{x}) = 0.4$. The predicted top label will be then label 3, giving the regret of 0.2 for precision@1. $\square$

The proposition shows that the heuristic is in general inconsistent for precision@k. Interestingly, the situation changes when the labels are conditionally independent, that is, $\mathbf{P}(\boldsymbol{y} \,|\, \boldsymbol{x}) = \prod_{j=1}^m \mathbf{P}(y_i \,|\, \boldsymbol{x})$.

Proposition 4. *Given conditionally independent labels, $\boldsymbol{h}_{@k} \in \mathcal{H}_{@k}^m$ predicting k labels with highest $\eta_j'(\boldsymbol{x})$, $j \in \mathcal{L}$, defined in (27), has zero regret in terms of the precision@k loss.*

We show here only a sketch of the proof. The full proof is given in Appendix E. It is enough to show that in the case of conditionally independent labels the pick-one-label heuristic does not change the order of marginal probabilities. Let y_i and y_j be so that $\eta_i(\boldsymbol{x}) \geq \eta_j(\boldsymbol{x})$. Then in the summation over all $\boldsymbol{y}$s in (27), we are interested in four different subsets of $\mathcal{Y}$, $S_{i,j}^{u,w} = \{\boldsymbol{y} \in \mathcal{Y} : y_i = u \wedge y_j = w\}$, where $u, w \in \{0, 1\}$. Remark that during mapping none of $\boldsymbol{y} \in S_{i,j}^{0,0}$ plays any role, and for each $\boldsymbol{y} \in S_{i,j}^{1,1}$, the value of

$$y_t / (\sum_{t'=1}^m y_{t'}) \times \mathbf{P}(\boldsymbol{y} \,|\, \boldsymbol{x}) \,,$$

for $t \in \{i, j\}$, is the same for both y_i and y_j. Now, let $\boldsymbol{y}' \in S_{i,j}^{1,0}$ and $\boldsymbol{y}'' \in S_{i,j}^{0,1}$ be the same on all elements except the i-th and the j-th one. Then, because of the label independence and the assumption that $\eta_i(\boldsymbol{x}) \geq \eta_j(\boldsymbol{x})$, we have $\mathbf{P}(\boldsymbol{y}' \,|\, \boldsymbol{x}) \geq \mathbf{P}(\boldsymbol{y}'' \,|\, \boldsymbol{x})$. Therefore, after mapping (27) we obtain $\eta_i'(\boldsymbol{x}) \geq \eta_j'(\boldsymbol{x})$. Thus, for independent labels, the pick-one-label heuristic is consistent for precision@k.

5 Online PLT

A PLT model can be trained either in batch mode or incrementally. The batch algorithm has been presented in Algorithm 1 in Section 3. It can be easily transformed into an incremental algorithm operating sequentially on observations from $\mathcal{D} = \{(\boldsymbol{x}_i, \boldsymbol{y}_i)\}_{i=1}^n$. To this end, we need to use an incremental learning algorithm A_{online} in the tree nodes. Such *incremental PLT* (IPLT) is given in Algorithm 5.

Algorithm 5 IPLT.TRAIN$(T, A_{\text{online}}, \mathcal{D})$

1: $H_T = \emptyset$ ▷ Initialize a set of node probabilistic classifiers
2: **for** each node $v \in V_T$ **do**   ▷ For each node in the tree
3:      $\hat{\eta}(v) = \text{NEWCLASSIFIER}(), H_T = H_T \cup \{\hat{\eta}(v)\}$ ▷ Initialize its binary classifier.
4: **for** $i = 1 \rightarrow n$ **do**   ▷ For each observation in the training sequence
5:      $(P, N) = \text{ASSIGNTONODES}(T, \boldsymbol{x}_i, \mathcal{L}_{\boldsymbol{x}_i})$ ▷ Compute its positive and negative nodes
6:      **for** $v \in P$ **do**   ▷ For all positive nodes
7:          $A_{\text{online}}.\text{UPDATE}(\hat{\eta}(v), (\boldsymbol{x}_i, 1))$ ▷ Update classifiers with a positive update with $\boldsymbol{x}_i$.
8:      **for** $v \in N$ **do**   ▷ For each negative node
9:          $A_{\text{online}}.\text{UPDATE}(\hat{\eta}(v), (\boldsymbol{x}_i, 0))$ ▷ Update classifiers with a negative update with $\boldsymbol{x}_i$.
10:      **return** H_T ▷ Return the set of node probabilistic classifiers

---

The above algorithm, similarly as its batch counterpart, works on a finite training set and requires a tree structure T to be given in advance. To construct T at least the number m of labels needs to be known. More advance tree construction procedures, as discussed in Section 6.5, exploit additional information like feature values or label co-occurrence [Prabhu et al., 2018]. In all such algorithms, the tree is built in a batch mode prior to the learning of node classifiers. Here, we analyze a different scenario in which an algorithm operates on a possibly infinite sequence of training instances and the tree is constructed online, simultaneously with incremental training of node classifiers, without any prior knowledge of the set of labels or training data. We refer to such approach as online probabilistic label trees.

Let us denote a sequence of observations by $\mathcal{S} = \{(\boldsymbol{x}_i, \mathcal{L}_{\boldsymbol{x}_i})\}_{i=1}^{\infty}$ and a subsequence consisting of the first t instances by $\mathcal{S}_t$. We refer here to labels of $\boldsymbol{x}_i$ only by $\mathcal{L}_{\boldsymbol{x}_i}$, not using the vector notation $\boldsymbol{y}_i$. This is because the number of labels m increases over time, which would also change the length of $\boldsymbol{y}_i$.[3] Furthermore, let the set of labels observed in $\mathcal{S}_t$ be denoted by $\mathcal{L}_t$, with $\mathcal{L}_0 = \emptyset$. An online algorithm returns at step t a tree structure T_t constructed over labels in $\mathcal{L}_t$ and a set of node classifiers H_t. Notice that the tree structure and the set of classifiers change in each iteration in which one or more new labels are observed. Below we discuss two properties that are desired for such online algorithm, defined in relation to the IPLT algorithm given above.

Definition 1 (A proper online PLT algorithm). *Let T_t and H_t be respectively a tree structure and a set of node classifiers trained on a sequence $\mathcal{S}_t$ using an online algorithm A. We say that A is a proper online PLT algorithm, when for any $\mathcal{S}$ and t we have that*

- *$l_j \in L_{T_t}$ iff $j \in \mathcal{L}_t$, that is, leaves of T_t correspond to all labels observed in S_t,*

---

[3]The same applies to $\boldsymbol{x}_t$ as the number of features also increases. We keep however the vector notation in this case, as it does not impact the description of the algorithm.

- *and H_t is exactly the same as $H = \text{IPLT.TRAIN}(T_t, A_{online}, \mathcal{S}_t)$, that is, node classifiers from H_t are the same as the ones trained incrementally by Algorithm 5 on $\mathcal{D} = \mathcal{S}_t$ and tree T_t given as input parameter.*

In other words, we require that whatever tree an online algorithm produces, the node classifiers should be trained the same way as the tree would be know from the very beginning of training. Thanks to that we can control the quality of each node classifier, as we are not missing any update. Moreover, since the result of a proper online PLT is the same as of IPLT, the same statistical guarantees apply to both of them.

The above definition can be satisfied by a naive algorithm that stores all observations seen so far, use them in each iteration to build a tree, and train node classifiers with the IPLT algorithm. This approach is costly in terms of both memory, used for storing S_t, and time, as all computations are run from scratch in each iteration. Therefore, we also demand an online algorithm to be space and time-efficient in the following sense.

Definition 2 (An efficient online PLT algorithm). *Let T_t and H_t be respectively a tree structure and a set of node classifiers trained on a sequence $\mathcal{S}_t$ using an online algorithm A. Let C_s and C_t be the space and time training cost of IPLT trained on sequence $\mathcal{S}_t$ and tree T_t. An online algorithm is an* efficient online PLT algorithm *when for any S and t we have its space and time complexity to be in a constant factor of C_s and C_t, respectively.*

In this definition, we abstract from the actual implementation of IPLT. In other words, the complexity of an efficient online PLT algorithm depends directly on design choices for an IPLT. Let us recall that the training cost for a single training example can be expressed by (11), as discussed in Section 3.3. By summing it over all examples in $\mathcal{S}_t$, we obtain the cost C_t of an IPLT. The space complexity is upperbounded by $2m - 1$ (the maximum number of node models), but it also depends on the chosen type of node models and the way of storing them (see Section 6 for a detailed discussion on implementation choices). Let us also notice that the definition implies that the update of a tree structure has to be in a constant factor of the training cost of a single instance, given by (11).

5.1 Online tree building and training of node classifiers

Below we describe an online algorithm that, as we show in the next subsection, satisfies both properties defined above. It is similar to the conditional probability tree (CPT) [Beygelzimer et al., 2009a], introduced for multi-class problems and binary trees, but extends it to multi-label problems and trees of any arity. We refer to this algorithm as OPLT.

The pseudocode is presented in Algorithms 6-11. In a nutshell, OPLT processes observations from $\mathcal{S}$ sequentially, updating node classifiers. For new incoming labels it creates new nodes according to a chosen tree building policy which is responsible for the main logic of the algorithm. Each new node v is associated with two classifiers, a regular one $\hat{\eta}(v) \in H_T$, and an *auxiliary* one $\hat{\theta}(v) \in \Theta_T$, where H_T and Θ_T denote the corresponding sets of node classifiers. The task of the auxiliary classifiers is to accumulate positives updates. The algorithm uses them later to initialize classifiers in new nodes added to a tree. They can be removed if a given node will not be used anymore to extend the tree. A particular criterion for removing an auxiliary classifier depends, however, on a tree building policy.

OPLT.TRAIN, outlined in Algorithm 6, administrates the entire process. It first initializes a tree with a root node r_T only and creates two corresponding classifiers, $\hat{\eta}(v_{r_T})$ and $\hat{\theta}(v_{r_T})$. Notice that the root has both classifiers initialized from the very beginning without a label assigned to it. Thanks to this, the algorithm can properly estimate the probability of $\mathbf{P}(\mathcal{L}_{\boldsymbol{x}} = \emptyset \,|\, \boldsymbol{x})$. Observations from $\mathcal{S}$ are processed sequentially in the main loop of OPLT.TRAIN. If a new observation contains one or more new labels then the tree structure is appropriately extended by calling UPDATETREE. The node classifiers are updated in UPDATECLASSIFIERS. After each iteration t, the algorithm sends H_T along with the tree structure T, respectively as H_t and T_t, to be used outside the algorithm for prediction tasks. We assume that tree T along with sets of its all nodes V_T and leaves L_T, as well as sets of classifiers H_T and Θ_T, are accessible to all subroutines discussed below.

Algorithm 6 OPLT.TRAIN($\mathcal{S}, A_{\text{online}}, A_{\text{policy}}$)

1: $r_T = \text{NEWNODE}()$, $V_T = \{r_T\}$ ▷ Create the root of the tree
2: $\hat{\eta}(r_T) = \text{NEWCLASSIFIER}()$, $H_T = \{\hat{\eta}_T(r_T)\}$ ▷ Initialize a new classifier in the root
3: $\hat{\theta}(r_T) = \text{NEWCLASSIFIER}()$, $\Theta_T = \{\theta(r_T)\}$ ▷ Initialize an auxiliary classifier in the root
4: **for** $(\boldsymbol{x}_t, \mathcal{L}_{\boldsymbol{x}_t}) \in \mathcal{S}$ **do**   ▷ For each observation in $\mathcal{S}$
5:      **if** $\mathcal{L}_{\boldsymbol{x}_t} \setminus \mathcal{L}_{t-1} \neq \emptyset$ **then**   ▷ If the observation contains new labels
6:          UPDATETREE($\boldsymbol{x}_t, \mathcal{L}_{\boldsymbol{x}_t}, A_{\text{policy}}$)   ▷ Add them to the tree
7:      UPDATECLASSIFIERS($\boldsymbol{x}_t, \mathcal{L}_{\boldsymbol{x}_t}, A_{\text{online}}$)   ▷ Update the classifiers
8:      **send** $H_t, T_t = H_T, V_T$ ▷ Send the node classifiers and the tree structure.

(a) Tree T_{t-1} after $t-1$ iterations.

(b) Variant 1: A leaf node v_1'' for label j added as a child of an internal node v_1.

(c) Variant 2: A leaf node v_1'' for label j and an internal node v_1' (with all children of v_1 reassigned to it) added as children of v_1.

(d) Variant 3: A leaf node v_2'' for label j and a leaf node v_2' (with a reassigned label of v_2) added as children of v_2.
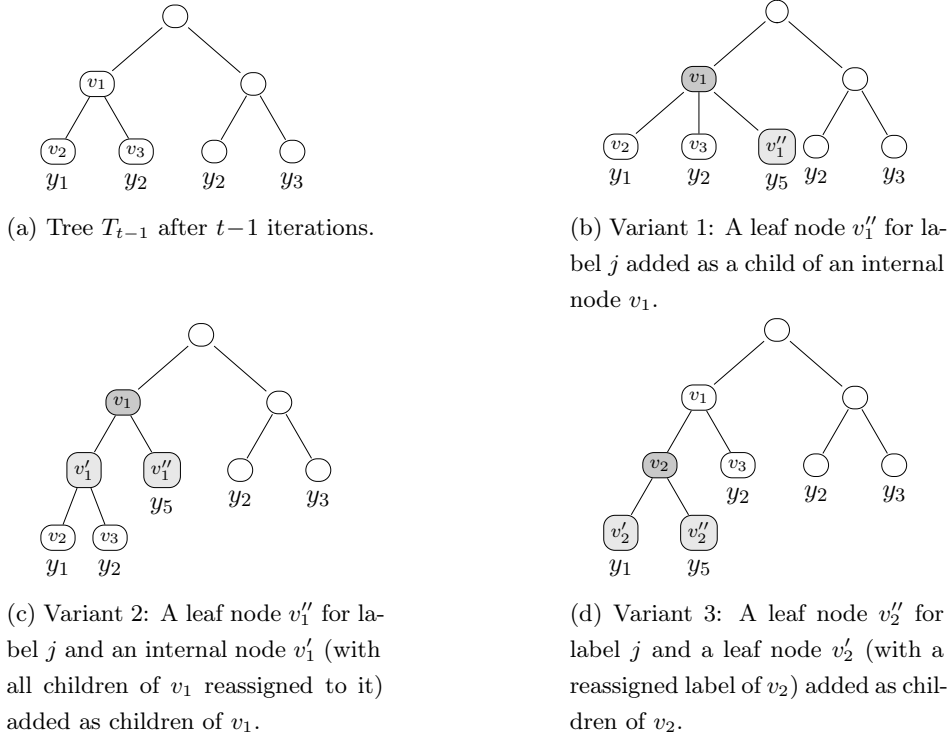
Figure 3: Three variants of tree extension for a new label j.

Algorithm 7, UPDATETREE, builds the tree structure. It iterates over all new labels from $\mathcal{L}_{\boldsymbol{x}}$. If

there were no labels in the sequence $\mathcal{S}$ before, the first new label taken from $\mathcal{L}_{\boldsymbol{x}}$ is assigned to the root note. Otherwise, the tree needs to be extended by one or two nodes according to a selected tree building policy. One of these nodes is a leaf to which the new label will be assigned. There are in general three variants of performing this step illustrated in Figure 3. The first one relies on selecting an internal node v whose number of children is lower than the accepted maximum, and adding to it a child node v'' with the new label assigned to it. In the second one, two new child nodes, v' and v'', are added to a selected internal node v. Node v' becomes a new parent of child nodes of the selected node v, that is, the subtree of v is moved down by one level. Node v'' is a leaf with the new label assigned to it. The third variant is a modification of the second one. The difference is that the selected node v is a leaf node. Therefore there are no children nodes to be moved to v', but label of v is reassigned to v'. The A_{policy} method encodes the tree building policy, that is, it decides which of the three variants to follow and selects the node v. The additional node v' is inserted by the INSERTNODE method. Finally, a leaf node is added by the ADDLEAF method. We discuss the three methods in more detail below.

Algorithm 7 OPLT.UPDATETREE($\boldsymbol{x}, \mathcal{L}_{\boldsymbol{x}}, A_{\text{policy}}$)

1: **for** $j \in \mathcal{L}_{\boldsymbol{x}} \setminus \mathcal{L}_{t-1}$ **do**   ▷ For each new label in the observation
2:      **if** $\mathcal{L}_T$ is $\emptyset$ **then**   ▷ If no labels have been seen so far
3:          LABEL(r_T) $= j$ ▷ Assign label j to the root node
4:      **else**   ▷ If there are already labels in the tree.
5:          $v, \ insert = A_{\text{policy}}(\boldsymbol{x}, j, \mathcal{L}_{\boldsymbol{x}})$ ▷ Select a variant of extending the tree
6:          **if** $insert$ **then** INSERTNODE(v)   ▷ Insert an additional node if needed.
7:          ADDLEAF(j, v)   ▷ Add a new leaf for label j.

A_{policy} returns the selected node v and a Boolean variable $insert$ which indicates whether an additional node v' has to be added to the tree. For the first variant, v is an internal node and $insert$ is set to false. For the second variant, v is an internal node and $insert$ is set to true. For the third variant, v is a leaf node and $insert$ is set to true. In general, the policy can be guided by $\boldsymbol{x}$, current label j, and set $\mathcal{L}_{\boldsymbol{x}}$ of all labels of $\boldsymbol{x}$. As an instance of the tree building policy, we consider, however, a much simpler method presented in Algorithm 8. It creates a b-ary complete tree. In this case, the selected node is either the leftmost internal node with the number of children less than b or the leftmost leaf of the lowest depth. The $insert$ variable is then $false$ or $true$, respectively. So, only the first and the third variants occur here. Notice, however, that this policy can be efficiently performed in amortized constant time per label if the complete tree is implemented using a dynamic array with doubling. Nevertheless, more advanced and computationally complex policies can be applied. As mentioned before, the complexity of this step should be at most proportional to the complexity of updating the node classifiers for one label, that is, it should be proportional to the depth of the tree.

Algorithm 8 BUILDCOMPLETETREE(b)

1: array $= T$.array   ▷ Let nodes of complete tree T be stored in a dynamic array T.array
2: $s = $ array.length   ▷ Read the number of nodes in T
3: $pa = \lceil \frac{s}{b} \rceil - 1$ ▷ Get the index of a parent of a next added node; the array is indexed from 0
4: $v = $ array(pa)   ▷ Get the parent node
5: **return** v, ISLEAF(v)   ▷ Return the node and whether it is a leaf.

The INSERTNODE and ADDLEAF procedures involve specific operations concerning initialization of classifiers in the new nodes. INSERTNODE is given in Algorithm 9. It inserts a new node v' as a child of the selected node v. If v is a leaf then its label is reassigned to the new node. Otherwise, all children of v become the children of v'. In both cases, v' becomes the only child of v. Figure 3 illustrates inserting v' as either a child of an internal node (c) or a leaf node (d). Since, the node classifier of v' aims at estimating $\eta(\boldsymbol{x}, v')$, defined as $\mathbf{P}(z_{v'} = 1 \,|\, z_{\mathrm{pa}(v')} = 1, \boldsymbol{x})$, its both classifiers, $\hat{\eta}(v')$ and $\hat{\theta}(v')$, are initialized as copies (by calling the COPY function) of the auxiliary classifier $\hat{\theta}(v)$ of the parent node v. Recall that the task of auxiliary classifiers is to accumulate all positive updates in nodes, so the conditioning $z_{\mathrm{pa}(v')} = 1$ is satisfied in that way.

Algorithm 9 OPLT.INSERTNODE(v)

1: $v' = \text{NEWNODE}()$, $V_T = V_T \cup \{v'\}$ ▷ Create a new node and add it to the tree nodes
2: **if** ISLEAF(v) **then**   ▷ If node v is a leaf
3:     LABEL(v') = LABEL(v), LABEL(v) = NULL   ▷ Reassign label of v to v'
4: **else**   ▷ Otherwise
5:     Ch(v') = Ch(v)   ▷ All children of v become children of v'
6:     **for** $v_{\mathrm{ch}} \in$ Ch(v') **do** pa(v_{ch}) = v' ▷ And v' becomes their parent
7: Ch(v) = $\{v'\}$, pa(v') = v ▷ The new node v' becomes the only child of v
8: $\hat{\eta}(v') = \text{COPY}(\hat{\theta}(v))$, $H_T = H_T \cup \{\hat{\eta}(v')\}$ ▷ Create a classifier.
9: $\hat{\theta}(v') = \text{COPY}(\hat{\theta}(v))$, $\Theta_T = \Theta_T \cup \{\hat{\theta}(v')\}$ ▷ And an auxiliary classifier.

Algorithm 10 outlines the ADDLEAF procedure. It adds a new leaf node v'' for label j as a child of node v . The classifier $\hat{\eta}(v'')$ is created as an "inverse" of the auxiliary classifier $\hat{\theta}(v)$ from node v. More precisely, the INVERSECLASSIFIER procedure creates a wrapper inverting the behavior of the base classifier. It predicts $1 - \hat{\eta}$, where $\hat{\eta}$ is the prediction of the base classifier, and flips the updates, that is, positive updates become negative and negative updates become positive. Finally, the auxiliary classifier $\hat{\theta}(v'')$ of the new leaf node is initialized.

Algorithm 10 OPLT.ADDLEAF(j, v)

1: $v'' = \text{NEWNODE}()$, $V_T = V_T \cup \{v''\}$ ▷ Create a new node and add it to the tree nodes
2: Ch(v) = Ch(v) $\cup \{v''\}$, pa(v'') = v ▷ Add this node to children of v.
3: LABEL(v'') = j ▷ Assign label j to the node v''
4: $\hat{\eta}(v'') = \text{INVERSECLASSIFIER}(\hat{\theta}(v))$, $H_T = H_T \cup \{\hat{\eta}(v'')\}$ ▷ Initialize a classifier for v''
5: $\hat{\theta}(v'') = \text{NEWCLASSIFIER}()$, $\Theta_T = \Theta_T \cup \{\hat{\theta}(v'')\}$ ▷ Initialize an auxiliary classifier for v''

The final step in the main loop of OPLT.TRAIN updates the node classifiers. The regular classifiers, $\hat{\eta}(v) \in H_T$, are updated exactly as in IPLT.TRAIN given in Algorithm 5. The auxiliary classifiers, $\theta(v) \in \Theta_T$, are updated only in positive nodes according to their definition and purpose.

Algorithm 11 OPLT.UPDATECLASSIFIERS($\boldsymbol{x}, \mathcal{L}_{\boldsymbol{x}}, A_{\text{online}}$)

1: $(P, N) = \text{ASSIGNTONODES}(T, \boldsymbol{x}, \mathcal{L}_{\boldsymbol{x}})$	▷ Compute its positive and negative nodes
2: **for** $v \in P$ **do**	▷ For all positive nodes
3: $\quad A_{\text{online}}.\text{UPDATE}(\hat{\eta}(v), (\boldsymbol{x}, 1))$	▷ Update classifiers with a positive update with $\boldsymbol{x}$.
4: $\quad$ **if** $\hat{\theta}(v) \in \Theta$ **then**	▷ Update auxiliary classifier if it exists.
5: $\qquad A_{\text{online}}.\text{UPDATE}(\hat{\theta}(v), (\boldsymbol{x}, 1))$	▷ With a positive online update with $\boldsymbol{x}_i$.
6: **for** $v \in N$ **do**	▷ For each negative node
7: $\quad A_{\text{online}}.\text{UPDATE}(\hat{\eta}(v), (\boldsymbol{x}, 0))$	▷ Update classifiers with a negative update with $\boldsymbol{x}$.

5.2 Theoretical analysis of OPLT

The OPLT algorithm has been designed to satisfy the properness and efficiency property of online probabilistic label trees. The theorem below states this fact formally.

Theorem 8. OPLT *is an proper and efficient* OPLT *algorithm.*

The proof is quite technical and we present it in Appendix F. To show the properness, it uses induction for both the outer and inner loop of the algorithm, where the outer loop iterates over observations $(\boldsymbol{x}_t, \mathcal{L}_{\boldsymbol{x}_t})$, while the inner loop over new labels in $\mathcal{L}_{\boldsymbol{x}_t}$. The key elements used to prove this property are the use of the auxiliary classifiers and the analysis of the three variants of the tree structure extension. The efficiency is proved by noticing that each node has two classifiers, and the algorithm creates and updates no more than one additional classifier per node comparing to IPLT. Moreover, any node selection policy which cost is proportional to the cost of updating IPLT classifiers for a single label meets the efficiency requirement. Particularly, the policy building a complete tree presented above satisfies this constraint.

The OPLT algorithm aims at constructing the node classifiers in such a way that its properness can be met by a wide range of tree building policies. The naive complete tree policy was introduced mainly for ease of presentation. One can, for example, easily adapt and further extend the policy originally used in CPT [Beygelzimer et al., 2009a]. In short, the CPT policy selects a node v which trade-offs balancedness of the tree and a fit of $\boldsymbol{x}$, that is, the value of $\hat{\eta}_v(\boldsymbol{x})$. Since it works with binary trees only, the policy uses solely the third variant of the tree extension. Moreover, it was designed for multi-class problems. In [Jasinska-Kobus et al., 2020] we have considered such extension. From this point of view, the presented framework significantly extends CPT. It solves both types of problems, multi-class and multi-label, and can be used with more advanced policies that exploit all three variants of the tree extension.

6 Implementation

There are several popular packages that implement the PLT model, for example, XMLC-PLT [Jasinska et al., 2016],[4] PLT-VW,[5] PARABEL [Prabhu et al., 2018],[6] EXTREME-TEXT [Wydmuch et al., 2018],[7] ATTENTIONXML [You et al., 2019],[8] BONSAI [Khandagale et al.,

---

[4] https://github.com/busarobi/XMLC

[5] https://github.com/VowpalWabbit/vowpal_wabbit

[6] http://manikvarma.org/code/Parabel/download.html

[7] https://github.com/mwydmuch/extremeText

[8] https://github.com/yourh/AttentionXML

2019],[9] or NAPKINXC[10] that we introduce in this paper. In this section, we discuss the differences between them in terms of training node classifiers, dealing with sparse and dense features, efficient prediction, tree structure learning, and ensembling. Table 3 summarizes the differences between the discussed implementations. At the end of this section we also shortly discuss a different approach to obtain $\hat{\eta}_v(\boldsymbol{x})$, which uses multi-class probability estimation instead of binary probability estimation.

Implementation	node classifiers	represen- tation	prediction	tree structure	ensem- bling
XMLC-PLT/ PLT-VW	online	sparse	online/ unif.-cost search	complete tree based on freq.	no
PARABEL	batch	sparse	batch/ beam search	balanced h. 2-means	yes
BONSAI	batch	sparse	batch/ beam search	unbalanced h. k-means	yes
EXTREMETEXT	online	dense	online/ unif.-cost search.	h. k-means	yes
ATTENTIONXML	online & leveled	dense	batch & leveled/ beam search	shallow h. k-means	no
NAPKINXC	both	both	online/ unif.-cost search, thresholds-based	any	yes

Table 3: Comparison of different implementations of the PLT model in terms of node classifiers (online, batch, or both), representation of features (sparse, dense, both), prediction algorithm (online, batch, leveled/beam search, uniform cost search, thresholds-based), tree structure learning (complete tree based on frequencies, hierarchical k means, their shallow variant, or any), ensembling (yes, no). All the options are described in text.

6.1 Training of node classifiers

Given the tree structure, the node classifiers of PLTs can be trained either in online or batch mode. Both training modes have their pros and cons. The batch variant, implemented for example in PARABEL, can benefit from using well-known batch solvers, such as LIBLINEAR [Fan et al., 2008]. These variants are relatively easy to train and achieve high predictive performance. Moreover, each model can be trained independently which enables a simple parallelization of training.

In turn, the online variant, such as XMLC-PLT, PLT-VW, or EXTREMETEXT, can be applied to stream data. However, all those implementations demand a tree structure to be known prior to the training of node classifiers. Nevertheless, the online node learners give the possibility of combining them with the online tree construction, as discussed in the previous section. Moreover, they can benefit from using deep networks to learn complex representation of input instances. Parallelization can be performed similarly as in the case of batch models. If accepting additional conflicts during updates of the node models, we can apply parallelization on the level of single examples as in EXTREMETEXT. Each thread consumes a part of the training examples and updates model allocated in shared memory.

---

[9]https://github.com/xmc-aalto/bonsai
[10]https://github.com/mwydmuch/napkinXC

napkinXC follows a modular design, therefore it can be easily used with either batch or online node learners. In the latter case, it has an implemented functionality of collaborating with external learners to exchange the "forward" and "backward" signals. It also supports the online tree construction.

6.2 Sparse features

For problems with sparse features, such as text classification, PLTs can be efficiently implemented using different approaches. The simplest and naive one relies on transforming sparse representation to dense one, training a given classifier using this representation, and then storing the final model in the sparse representation again. For example, if someone wants to use the popular LIBLINEAR package, this is the approach to go as this package uses dense representation internally. The resulting model can be stored as sparse, mainly if the model has been trained with L_1 regularization. However, in the case of L_2 regularization one can remove all weights being close to zero, similarly as in DISMEC [Babbar and Schölkopf, 2017]. Since the node classifiers can be trained independently, the runtime memory of this approach can also be optimized.

Alternatively, one can use sparse learning algorithms. Such algorithms follow usually the online/incremental learning paradigm, in which training instances are processed sequentially one-by-one. Instances of such algorithms are Fobos [Duchi and Singer, 2009] or AdaGrad [Duchi et al., 2011]. To store and update weights they use either hash maps or feature hashing [Weinberger et al., 2009]. The latter, implemented for example in the popular VOWPAL WABBIT package [Langford et al., 2007], relies on allocating a constant memory space for features weights. Since the allocated space can be too small, conflicts can exist between different weights. They are not resolved, that is, a weight is shared by all conflicting features. If used with PLTs, the allocated memory can be shared by all node models. In case of hash maps, one needs to reallocate the memory if the map is close to be full. In our implementation we follow the ROBIN HOOD HASHING [Celis et al., 1985] which allows for very efficient insert and find operations, having at the same time minimal memory overhead. It uses open addressing, but compared to hash maps with linear and quadratic probing, it significantly reduces the expected average and maximum probe lengths. This is achieved by shifting the keys around in such a way that all keys stay reasonably close to the slot they hash to. When inserting a new element, if the probe length for the existing element is less than the current probe length for the element being inserted, ROBIN HOOD swaps the two elements and continues the procedure. This results in much lower average probe lengths as well as its variance. This also allows for a straightforward lookup algorithm that ignores empty slots and keeps looking for a key until it reaches the known maximum probe length for the whole table. This property also allows usage of high load factors (higher than 0.9). Since it uses open addressing, the memory usage for the whole map is very close to memory needed to store its content as a sparse vector.

It is worth noticing that for sparse data the weights sparsity increases with the depth of a tree. This implies a significant reduction of space of the final PLT model. Paradoxically, this reduction can be the largest in case of binary trees, although the number of nodes is the highest in this case, (equal to $2m - 1$, being as much as twice the number of models in the 1-VS-ALL approach). This is because the models use only non-zero features of the sibling nodes, and there are only two such nodes in binary trees. No other features are needed to build the corresponding classifiers.

6.3   Dense features

PLTs can also work with dense features, however, the dimensionality of the feature space cannot be too high. Otherwise, the memory used for models would be too large. The dense representation is usually connected with deep or shallow neural networks.

One possibility is to use pretrained embeddings. For text classification, one can use word representations trained by WORD2VEC [Mikolov et al., 2013] or GLOVE [Pennington et al., 2014] on large text corpuses. The document representation can be then created from these word embeddings in many ways, for example, as an average or as the maximum or minimum value of each element of the embeddings [De Boom et al., 2016]. Alternatively, one can train the word embeddings simultaneously with the node classifiers, similarly as in FASTTEXT [Joulin et al., 2017]. This approach is taken in EXTREMETEXT. Another option is to initiate the network with the pretrained embeddings and then update all the parameters of both the node classifiers and text representations.

To improve the document representation, instead of a simple aggregation over words, one can use word embeddings in a more advanced deep architecture, such as LSTM [Hochreiter and Schmidhuber, 1997] or the text-based convolution neural network [Liu et al., 2017]. PLTs can be used with such architecture as the output layer. However, the speed advantage of this architecture might not be so visible in the case of GPU-based training, as matrix multiplication can be efficiently performed on GPUs. Nevertheless, in the case of complex and memory-intensive approaches, the PLT approach can be used to decompose the problem in such a way that computations are performed level-by-level in a tree (with additional decomposition possible on a given level). All the layers except the PLT one are initialized using the trained values from the preceding level. This idea is followed in ATTENTIONXML.

6.4   Prediction

The top-k prediction, discussed in Section 3.2 as Algorithm 4, is a variant of the uniform-cost search. It is used in XMLC-PLT, EXTREMETEXT, and NAPKINXC. It has the advantage of being very efficient for online prediction. The algorithm also allows for extending k at any time, without restarting the whole procedure from the beginning. If one does not need to change k, the algorithm can be improved by adding to the priority queue only those nodes whose probability is greater than the probability of the k-th top leaf already added to the queue. In case of sparse models, they should be stored either in hash maps or use the feature hashing to allow random access to model weights.

Unpacking a sparse model to dense representation, as implemented in PARABEL, can be very costly in case of online prediction. However, for sufficiently large batches, the approach taken in PARABEL can benefit from beam search. In this case, a node classifier is unpacked once for a batch of test examples allowing a very efficient computation of the dot products. If models are dense and they can be all load to the main memory, then both search methods perform similarly in terms of computational times. However, beam search is an approximate method and it may not find the actual top k labels with the highest estimates of label probabilities. Therefore it may suffer regret for precision@k [Zhuo et al., 2020]. In the case of memory-intensive deep models, such as the one used in ATTENTIONXML, the prediction is usually performed level-by-level, similarly as training, and, therefore, it uses beam search. Nevertheless, there also exists a variant of uniform-cost search efficiently operating in a batch mode [Jasinska, 2018].

6.5 Tree structure

The tree structure of a PLT is a crucial modeling decision. The theoretical results from Section 4 concerning the vanishing regret of PLT hold regardless of the tree structure, however, this theory requires the regret of the node classifiers also to vanish. In practice, we can only estimate the conditional probabilities in the nodes, therefore the tree structure does indeed matter as it affects the difficulty of the node learning problems. In Section 5, we already discussed the problem of building a tree in the online setting. Here, we focus on batch approaches which assume that labels are known. The original PLT paper [Jasinska et al., 2016] uses simple complete trees with labels assigned to leaves according to their frequencies. Another option, routinely used in HSM [Joulin et al., 2017], is the Huffman tree built over the label frequencies. Such tree takes into account the computational complexity by putting the most frequent labels close to the root. This approach has been further extended to optimize GPU operations in [Grave et al., 2017]. Unfortunately, for multi-label classification the Huffman tree is no longer optimal in terms of computational cost. As already mentioned in Section 3.3, an exhaustive analysis of computational complexity of PLTs has been performed by Busa-Fekete et al. [2019]. Furthermore, Huffman trees ignore the statistical properties of the tree structure. There exist, however, other methods that focus on building a tree with high overall accuracy [Tagami, 2017, Prabhu et al., 2018].

The method of [Prabhu et al., 2018], implemented in PARABEL, performs a simple top-down hierarchical clustering. Each label in this approach is represented by a profile vector being an average of the training vectors tagged by this label. Then the profile vectors are clustered using balanced k-means which divides the labels into two or more clusters with approximately the same size. This procedure is then repeated recursively until the clusters are smaller than a given value (for example, 100). The nodes of the resulting tree are then of different arities. The internal nodes up to the pre-leaf nodes have k children, but the pre-leaf nodes are usually of higher arity. Thanks to this clustering, similar labels are close to each other in the tree. Moreover, the tree is balanced, so its depth is logarithmic in terms of the number of labels. Variants of this method have been used in EXTREMETEXT [Wydmuch et al., 2018], BONSAI TREES [Khandagale et al., 2019] and ATTENTIONXML [You et al., 2019]. The two latter algorithms promote shallow trees, that is, trees of a much higher arity.

6.6 Ensemble of PLTs

Various ensemble techniques, such as bagging, are routinely applied with tree-based learners. A simple ensemble approach can also be implemented for PLTs. One can use several PLT instances of a different structure, which share the same feature space. This can be obtained by running the k-means-based top-down hierarchical clustering. Since k-means can be initialized randomly, each time a different tree can be produced. Depending on the tree structure, the accuracy of a single PLT for specific labels may vary. Thus the aggregation of predictions of this diverse pool of PLTs should lead to improvement of the overall predictive performance. Such ensemble technique has been used in PARABEL.

Classification of test examples with multiple trees can be still performed very efficiently. Each tree can be queried for its top k predictions. Then, the labels are pooled and their average scores are computed. Based on them, the final prediction is made. If a label does not have a probability estimate from a given tree (it is not included in the top-k predictions), then the estimate is either set to 0 or computed by traversing a single path in the tree corresponding to the label. The good

trade-off between the improvement of the results and the required computational resources is usually obtained for around 3 or 5 trees.

6.7 Node probabilities via multi-class classification

So far we assumed that each node $v \in V$ is associated with a binary probabilistic classifier that seeks for estimating $\eta_v(\boldsymbol{x})$. As already mentioned in Section 3.2, this may require the additional normalization step (10), as all models of siblings nodes are trained independently. To avoid this problem, one can train a joint multi-class classifier over the sibling nodes. Let $v \in V$ be a parent of the sibling nodes $\mathrm{Ch}(v)$. Then, the class labels of the multi-class problem correspond to binary codes of vector $\boldsymbol{c}$ whose elements correspond to $z_{v'}$, $v' \in \mathrm{Ch}(v)$. The classifier estimates $\mathbf{P}(\boldsymbol{c} \,|\, \boldsymbol{x}, z_v = 1)$, for all $\boldsymbol{c} \in \{0,1\}^{|\mathrm{Ch}(v)|}$. Probability $\eta_{v'}(\boldsymbol{x})$, for $v' \in \mathrm{Ch}(v)$, is obtained by proper marginalization of the multi-class distribution over vectors $\boldsymbol{c}$:

$$\eta_{v'}(\boldsymbol{x}) = \sum_{z_{v'}=1} \mathbf{P}(\boldsymbol{c} \,|\, \boldsymbol{x}, z_v = 1) \,.$$

This approach has been investigated in PARABEL [Prabhu et al., 2018]. It can be applied to trees of small arity only as the number of class labels grows exponentially with the number of sibling nodes.

7 Empirical validation of PLTs

In this section, we show results of a wide empirical study we performed to comprehensively evaluate the described algorithms and theoretical findings. We mainly report the results of the predictive performance in terms of precision@k, as this is the most used metric in XMLC experiments. Moreover, as shown in Section 4, PLTs are well-suited for this metric. We also present training and test times, as well as memory consumption. Whenever it was necessary, we repeated an experiment 5 times to eliminate the impact of the randomness of algorithms. In such cases, we report the mean performance along with standard errors. All computations were conducted on an Intel Xeon E5-2697 v3 2.60GHz (14 cores) machine with 128GB RAM. In most experiments, we use TF-IDF versions of the real-word benchmark data sets from the Extreme Classification Repository [Bhatia et al., 2016],[11] for which we use the original train and test splits. Table 4 gives basic statistics of the data sets.

In the first part of the study, we analyze different design choices for PLTs. To this end, we mainly use NAPKINXC, because of its modular architecture. However, whenever a tested configuration agrees with another PLT implementation, we use this one in the experiment. In the next part, we evaluate PLTs on Hamming loss and micro-F measure, to verify our theoretical results concerning generalized performance metrics. Later, we empirically confirm the suboptimality of hierarchical softmax with pick-one-label heuristic. The next experiment studies the performance of the fully online variant of PLTs, in which both node classifiers and tree structure are built incrementally on a sequence of training examples. Finally, we compare PLTs to relevant state-of-the-art algorithms.[12]

---

[11]http://manikvarma.org/downloads/XC/XMLRepository.html

[12]The experiments with NAPKINXC are reproducible by running scripts available from https://github.com/mwydmuch/napkinXC/experiments

Dataset	dim $\mathcal{X}$	dim $\mathcal{Y}$ (m)	N_{train}	N_{test}	avg. $|\mathcal{L}_{\boldsymbol{x}}|$
EurLex-4K	5000	3993	15539	3809	5.31
AmazonCat-13K	203882	13330	1186239	306782	5.04
Wiki10-30K	101938	30938	14146	6616	18.64
DeliciousLarge-200K	782585	205443	196606	100095	75.54
WikiLSHTC-325K	1617899	325056	1778351	587084	3.19
WikipediaLarge-500K	2381304	501070	1813391	783743	4.77
Amazon-670K	135909	670091	490449	153025	5.45
Amazon-3M	337067	2812281	1717899	742507	36.17

Table 4: The number of unique features, labels, examples in train and test splits, and the average number of true labels per example in the benchmark data sets.

7.1 PLTs with different design choices

We analyze different design choices for PLTs. To this end, we use NAPKINXC, as thanks to its modular design, we can easily experiment with different settings. However, whenever a given configuration agrees with an existing PLT implementation, we use this one in the experiment. This is the case of PARABEL and EXTREMETEXT. The former uses a dual coordinate descent method from LIBLINEAR with squared hinge loss to train node classifiers. It uses weight pruning at threshold 0.1, that is, it sets model weights less than 0.1 to zero. The prediction algorithm is based on beam search. EXTREMETEXT is built over FASTTEXT [Grave et al., 2017]. It uses dense representation, shared by all nodes, which is a result of a 1-layer network implementing the CBOW architecture [Mikolov et al., 2013]. This representation is trained along with the node models using stochastic gradient descent with L_2 regularization and logistic loss. Both implementations use hierarchical k-means clustering. PARABEL uses $k = 2$, while EXTREMETEXT allows for different values of k. Both use pre-leaves of high degree equal to 100. In the experiment, we do not use ATTENTIONXML, as it uses a complex deep architecture requiring powerful GPUs and runs over raw textual data. By comparing the results from the original paper [You et al., 2019], we admit that it achieves the best results among PLT-based approaches. Nevertheless, in this study, we focus on efficient CPU implementations and the TF-IDF versions of the benchmark data sets.

We start with a comparison of batch and incremental learning of node classifiers. For both, we use logistic and squared hinge loss. Next, we verify two different methods of prediction. The first one is based on uniform-cost search, while the second on the beam search. We then compare training and prediction with sparse and dense representation. In the next experiment, we analyze different tree-building strategies. Finally, we check the impact of ensembling.

7.1.1 Batch and incremental learning

For batch learning, we use LIBLINEAR, the dual coordinate descent method, with either logistic loss or squared hinge loss. We use L_2 regularization for both and tune its C parameter for each data set. For incremental learning, we use ADAGRAD [Duchi et al., 2011] with 3 epochs and tune the base learning rate ϵ for each data set. As above, we use either logistic loss or squared hinge loss. In all algorithms, we prune the weights at 0.1 to obtain smaller models and use uniform-cost search to obtain top-k predictions. Let us point out that the configuration based on LIBLINEAR with squared hinge loss is similar to PARABEL. The difference is that PARABEL uses beam search, thus we run the implementation from NAPKINXC here.

Optimizer	$p@1$ [%]	$p@3$ [%]	$p@5$ [%]	T_{train} [h]	T/N_{test} [ms]	M_{size} [GB]
			EurLex-4K			
NXC-B,log	**80.51±0.16**	65.65±0.40	53.33±0.68	0.02±0.00	0.39±0.03	0.02±0.00
NXC-B,s.h.	80.17±0.27	65.33±0.53	53.01±0.87	**0.01±0.00**	**0.24±0.02**	**0.00±0.00**
NXC-I,log	80.43±0.09	**66.08±0.26**	**53.87±0.58**	0.01±0.00	0.25±0.02	0.05±0.00
NXC-I,s.h.	78.72±0.18	61.54±0.34	48.09±0.51	0.01±0.00	0.33±0.03	0.03±0.00
			AmazonCat-13K			
NXC-B,log	93.04±0.02	78.44±0.02	63.70±0.02	0.72±0.02	0.32±0.03	0.35±0.00
NXC-B,s.h.	92.40±0.04	78.49±0.02	63.88±0.02	0.29±0.00	**0.19±0.00**	**0.19±0.00**
NXC-I,log	**93.23±0.02**	**78.76±0.03**	**64.05±0.02**	0.17±0.00	0.32±0.02	0.72±0.00
NXC-I,s.h.	92.62±0.05	76.39±0.06	60.67±0.06	**0.16±0.00**	0.38±0.01	0.55±0.00
			Wiki10-30K			
NXC-B,log	85.36±0.09	73.90±0.07	63.84±0.07	0.21±0.00	5.35±0.32	0.58±0.00
NXC-B,s.h.	84.17±0.10	72.43±0.10	63.12±0.04	0.11±0.00	**2.87±0.08**	**0.06±0.00**
NXC-I,log	84.92±0.10	**74.52±0.09**	**65.29±0.04**	0.11±0.00	5.24±0.42	0.91±0.00
NXC-I,s.h.	**85.64±0.10**	70.37±0.09	59.43±0.13	**0.10±0.00**	7.19±0.06	0.35±0.00
			DeliciousLarge-200K			
NXC-B,log	**49.55±0.05**	**43.08±0.03**	**39.90±0.02**	**2.58±0.15**	**9.89±0.89**	**0.95±0.00**
NXC-B,s.h.	46.30±0.07	39.76±0.08	36.54±0.07	5.51±0.29	10.07±0.23	1.82±0.00
NXC-I,log	45.27±0.06	38.26±0.03	34.88±0.02	2.97±0.03	11.51±0.57	15.05±0.00
NXC-I,s.h.	45.29±0.34	38.15±0.50	34.44±0.58	3.13±0.10	27.11±1.55	9.59±0.00
			WikiLSHTC-325K			
NXC-B,log	61.96±0.03	40.77±0.02	30.19±0.02	2.95±0.15	1.77±0.11	2.73±0.00
NXC-B,s.h.	**62.78±0.03**	**41.17±0.02**	**30.25±0.02**	1.60±0.06	**0.86±0.06**	**0.97±0.00**
NXC-I,log	60.99±0.04	39.85±0.02	29.50±0.01	1.52±0.00	2.44±0.02	4.93±0.00
NXC-I,s.h.	59.55±0.05	37.33±0.04	27.02±0.03	**1.41±0.05**	1.70±0.17	3.64±0.00
			WikipediaLarge-500K			
NXC-B,log	66.20±0.05	47.14±0.02	36.83±0.01	16.10±0.44	6.67±0.23	8.89±0.00
NXC-B,s.h.	**66.77±0.08**	**47.63±0.04**	**36.94±0.02**	9.48±0.33	**2.86±0.07**	**1.78±0.00**
NXC-I,log	65.68±0.15	46.62±0.09	36.52±0.06	**8.11±0.18**	7.86±0.19	19.11±0.00
NXC-I,s.h.	65.05±0.08	44.35±0.03	33.74±0.05	8.22±0.06	6.66±0.06	24.71±0.00
			Amazon-670K			
NXC-B,log	43.54±0.01	38.71±0.02	35.15±0.03	0.56±0.00	4.13±0.28	2.26±0.00
NXC-B,s.h.	43.31±0.03	38.19±0.03	34.31±0.03	**0.40±0.01**	**1.32±0.08**	**0.63±0.00**
NXC-I,log	**43.82±0.01**	**38.88±0.03**	**35.31±0.03**	0.42±0.00	5.93±0.11	6.22±0.00
NXC-I,s.h.	41.46±0.02	36.16±0.04	32.34±0.03	0.41±0.00	2.08±0.17	5.26±0.00
			Amazon-3M			
NXC-B,log	46.09±0.02	43.11±0.01	40.98±0.01	7.07±0.56	3.26±0.08	20.84±0.00
NXC-B,s.h.	**46.23±0.01**	**43.48±0.01**	**41.41±0.01**	5.44±0.13	**1.96±0.05**	**9.86±0.00**
NXC-I,log	43.61±0.12	40.44±0.09	38.32±0.06	**4.44±0.10**	4.42±0.00	52.16±0.00
NXC-I,s.h.	43.73±0.07	40.19±0.06	37.75±0.05	4.45±0.04	11.03±0.02	24.77±0.01

Table 5: Comparison of NAPKINXC (NXC) with different modes of node classifiers training. We perform batch LIBLINEAR (B) or incremental ADAGRAD (I) training with logistic loss (log) or squared hinge loss (s.h.).

36

The results are given in Table 5. None of the configurations strictly dominates the others. It seems, however, that ADAGRAD with squared hinge loss usually performs the worst. This agrees with the fact that stochastic gradient approaches perform usually better with logistic loss. This configuration also leads to models with substantially longer testing times. In turn, significantly larger models for some data sets are built by ADAGRAD with logistic loss, while the training time can be doubled by LIBLINEAR with the same loss. It seems from this analysis that the batch training with squared hinge loss is the most reliable, without outlying results. Moreover, it performs the best on both WIKIPEDIA data sets. Nevertheless, incremental learning is a valid competitor that can be easily combined with training of dense representation or online tree structure building.

7.1.2 Prediction methods

We compare two prediction algorithms, the uniform-cost search and the beam search. The former is well-suited for online predictions and is implemented as a default method in NAPKINXC. It exploits efficient ROBIN HOOD hash maps to perform fast predictions. The latter method, used in PARABEL, benefits from using larger batches of test examples. In each node it decompresses its sparse model to a dense form before evaluation of test examples (see discussion on both algorithms in Section 6.4). We use the default size of the beam equal to 10. Besides the prediction method, NAPKINXC is set in the experiment to have the same setting as PARABEL. As shown in Table 7, both methods perform very similarly in terms of precision@k. This means that the beam of size 10 is indeed sufficient to approximate well the exact solution. The small deviations in the results between both prediction methods are likely caused by small differences in their implementations and randomness present in the experiment. Moreover, selecting top k labels with respect to the estimates does not necessarily lead to the best result.

In the remainder, we focus on computational costs. Figure 4 shows the average prediction time per a single test example, T/N_{test}, as a function of the batch size N_{test}. For each batch, we create 50 samples of observations by selecting them uniformly from the test set. We measure the average prediction time over 5 different NAPKINXC and PARABEL models, giving 250 measurements in total per each batch size. The prediction time of the uniform-cost search, processing example by example, is independent of the batch size and it is lower than 10ms for most of the data sets. Beam search, working on batches of examples, is more than 100 times slower than the uniform-cost search for small batches. To reach the prediction time of uniform-cost search it requires often batch sizes greater than 1000.

7.1.3 Sparse and dense representation

In the next experiment, we test the performance of PLTs with sparse and dense representation. To this end, we use NAPKINXC and EXTREMETEXT, respectively. Besides representation, we use a similar setting for both algorithms. Trees are built with hierarchical k-means clustering. Node classifiers are trained incrementally by minimizing logistic loss, however, NAPKINXC uses ADAGRAD, while EXTREMETEXT stochastic gradient descent with L_2 regularization. Prediction in both is based on uniform-cost search.

Prediction method	p@1 [%]		p@3 [%]		p@5 [%]	
	u-c search	beam search	u-c search	beam search	u-c search	beam search
EurLex-4K	80.17±0.27	**80.66±0.16**	65.33±0.53	**67.76±0.05**	53.01±0.87	**56.57±0.07**
AmazonCat-13K	92.40±0.04	**92.58±0.02**	78.49±0.02	**78.53±0.00**	63.88±0.02	**63.90±0.01**
Wiki10-30K	**84.17±0.10**	**84.17±0.03**	**72.43±0.10**	72.12±0.04	63.12±0.04	**63.30±0.05**
DeliciousLarge-200K	46.30±0.07	**46.44±0.07**	**39.76±0.08**	39.66±0.06	**36.54±0.07**	36.19±0.05
WikiLSHTC-325K	**62.78±0.03**	**62.78±0.02**	41.17±0.02	**41.22±0.02**	30.25±0.02	**30.27±0.01**
WikipediaLarge-500K	66.77±0.08	**67.05±0.14**	47.63±0.04	**47.75±0.10**	36.94±0.02	**36.99±0.08**
Amazon-670K	**43.31±0.03**	43.13±0.02	**38.19±0.03**	37.94±0.03	**34.31±0.03**	34.00±0.00
Amazon-3M	**46.23±0.01**	46.14±0.01	**43.48±0.01**	43.32±0.01	**41.41±0.01**	41.20±0.01

Table 7: Precision@k of uniform-cost (u-c) search (NAPKINXC) and beam search (PARABEL).
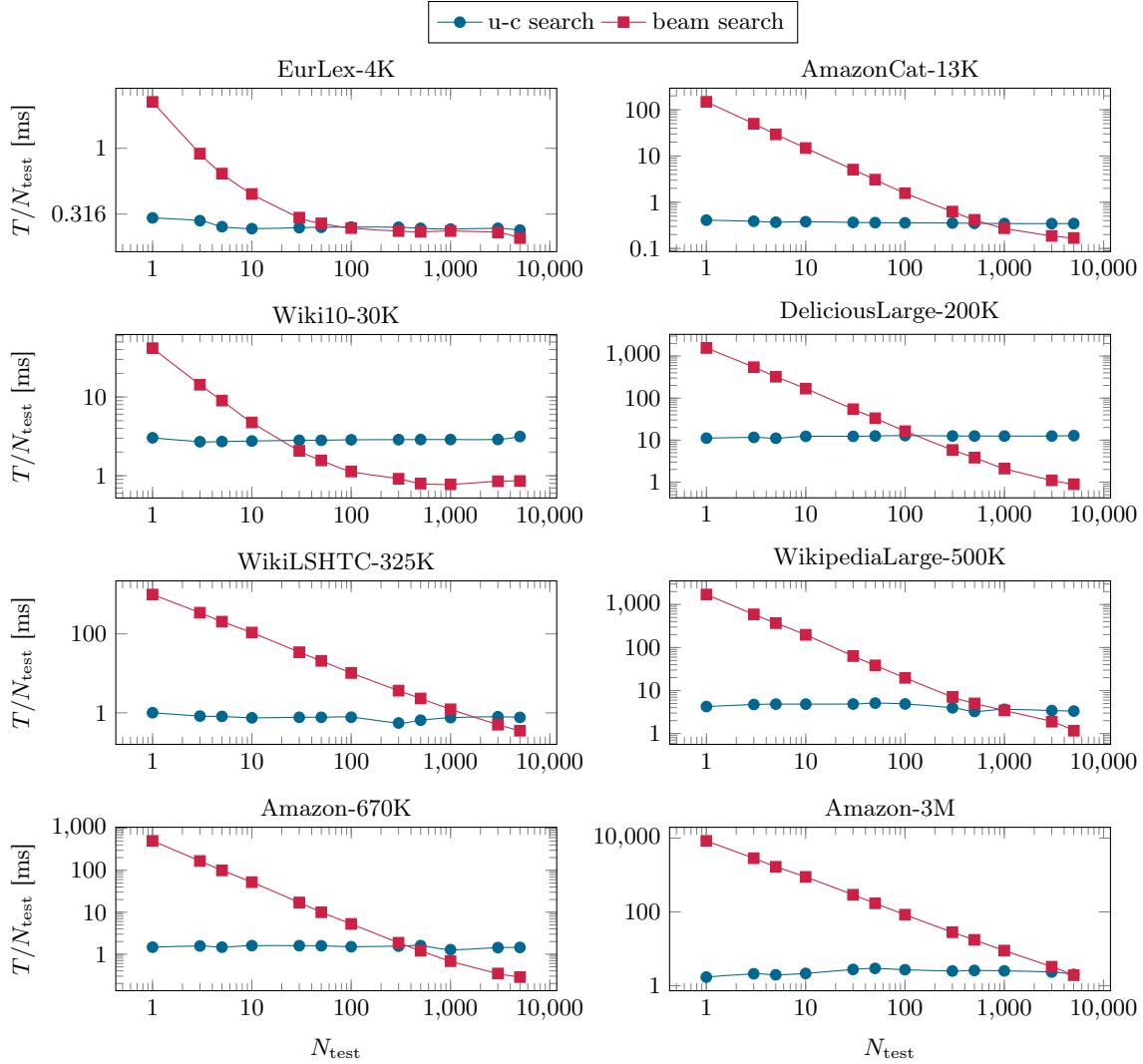

Figure 4: Average prediction times of uniform-cost search (NAPKINXC) and beam search (PARABEL) as a function of batch size N_{test}.

Representation	dense	sparse	dense	sparse	dense	sparse
	$p@1$ [%]		$p@3$ [%]		$p@5$ [%]	
EurLex-4K	77.29±0.21	**80.43±0.09**	64.41±0.11	**66.08±0.26**	53.56±0.11	**53.87±0.58**
AmazonCat-13K	91.96±0.02	**93.23±0.02**	77.41±0.01	**78.76±0.03**	62.75±0.02	**64.05±0.02**
Wiki10-30K	**85.76±0.06**	84.92±0.10	74.37±0.10	**74.52±0.09**	64.44±0.05	**65.29±0.04**
DeliciousLarge-200K	**47.95±0.03**	45.27±0.06	**41.69±0.02**	38.26±0.03	**38.60±0.01**	34.88±0.02
WikiLSHTC-325K	57.58±0.06	**60.99±0.04**	38.01±0.04	**39.85±0.02**	28.33±0.02	**29.50±0.01**
WikipediaLarge-500K	64.56±0.06	**65.68±0.15**	46.04±0.06	**46.62±0.09**	36.06±0.04	**36.52±0.06**
Amazon-670K	40.24±0.03	**43.82±0.01**	35.84±0.04	**38.88±0.03**	32.61±0.05	**35.31±0.03**
Amazon-3M	39.29±0.03	**43.61±0.12**	36.53±0.02	**40.44±0.09**	34.65±0.01	**38.32±0.06**
	T_{train} [h]		T/N_{test} [ms]		M_{size} [GB]	
EurLex-4K	0.21±0.00	**0.01±0.00**	0.36±0.00	**0.25±0.02**	**0.02±0.00**	0.05±0.00
AmazonCat-13K	10.75±0.71	**0.17±0.00**	**0.17±0.01**	0.32±0.02	**0.41±0.00**	0.72±0.00
Wiki10-30K	0.72±0.06	**0.11±0.00**	**0.91±0.06**	5.24±0.42	**0.25±0.00**	0.91±0.00
DeliciousLarge-200K	38.32±1.84	**2.97±0.03**	**1.69±0.05**	11.51±0.57	**1.90±0.00**	15.05±0.00
WikiLSHTC-325K	2.34±0.17	**1.52±0.00**	**0.57±0.01**	2.44±0.02	**3.30±0.00**	4.93±0.00
WikipediaLarge-500K	28.23±1.41	**8.11±0.18**	**0.64±0.01**	7.86±0.19	**5.50±0.00**	19.11±0.00
Amazon-670K	6.27±0.49	**0.42±0.00**	**1.18±0.01**	5.93±0.11	**1.60±0.00**	6.22±0.00
Amazon-3M	36.07±2.05	**4.44±0.10**	**0.91±0.01**	4.42±0.00	**6.20±0.00**	52.16±0.00

Table 6: Comparison of dense (EXTREMETEXT) and sparse (NAPKINXC) representation.

Table 6 shows the results. NAPKINXC with sparse representation achieves higher precision@k than EXTREMETEXT on almost all data sets. This agrees with a common observation that learning a powerful dense representation for XMLC problems is difficult. Nevertheless, the results of EXTREMETEXT are approaching those of NAPKINXC, despite its very simple architecture and gradient updates. Because of the additional layer, EXTREMETEXT needs more time for training, but the dense representation allows for faster predictions and smaller models. Let us comment, however, on the last observation. The size of a model in EXTREMETEXT is determined by the dimension of dense representation, the number of labels, features, and tree nodes. In NAPKINXC with sparse representation, the model size is influenced by the distribution of features among the labels, the tree structure, the chosen loss function and regularization. Moreover, aggressive weight pruning can be applied without a significant drop in predictive performance, as we show in Appendix I.

7.1.4 Tree structure

The choice of the tree structure is crucial as it affects all aspects of the performance: the accuracy of predictions, execution times, and model sizes. In this experiment, we investigate different tree building strategies described in Section 6.5. We first compare two types of balanced binary trees in which labels are split either randomly or using k-means clustering in a top-down procedure. In trees of both types, pre-leaf nodes are set to have a high degree equal to 100, that is, the splitting procedure stops when a cluster contains less than 100 labels which are then transformed into leaves. Both algorithms create trees of the same depth, but with a different arrangement of labels. The results are given in Table 8. In all cases, the k-means tree outperforms the random one in terms of precision@k. On some data sets this difference is not substantial, but in several cases, k-means clustering leads to a huge boost of almost 20 percent. Also training time and model size benefit from the clustering. The power of k-means trees can be explained by the fact that co-occurring and

similar labels are grouped. Thanks to this a training example is used in fewer nodes on average, the training tasks in tree nodes become simpler, and less features are necessary to solve them.

Tree type	random	k-means	random	k-means	random	k-means
	$p@1$ [%]		$p@3$ [%]		$p@5$ [%]	
EurLex-4K	76.22±0.21	**80.51±0.16**	54.54±0.13	**65.65±0.40**	39.20±0.09	**53.33±0.68**
AmazonCat-13K	91.39±0.04	**93.04±0.02**	75.86±0.03	**78.44±0.02**	61.00±0.02	**63.70±0.02**
Wiki10-30K	84.26±0.07	**85.36±0.09**	71.68±0.06	**73.90±0.07**	60.16±0.12	**63.84±0.07**
DeliciousLarge-200K	49.13±0.03	**49.55±0.05**	42.68±0.01	**43.08±0.03**	39.47±0.02	**39.90±0.02**
WikiLSHTC-325K	44.04±0.02	**61.96±0.03**	24.69±0.45	**40.77±0.02**	18.20±0.18	**30.19±0.02**
WikipediaLarge-500K	48.40±0.02	**66.20±0.05**	32.05±0.01	**47.14±0.02**	24.82±0.01	**36.83±0.01**
Amazon-670K	33.76±0.06	**43.54±0.01**	28.25±0.02	**38.71±0.02**	24.88±0.01	**35.15±0.03**
Amazon-3M	37.77±0.05	**46.09±0.02**	34.55±0.01	**43.11±0.01**	32.49±0.01	**40.98±0.01**
	T_{train} [h]		T/N_{test} [ms]		M_{size} [GB]	
EurLex-4K	**0.02±0.00**	0.02±0.00	**0.27±0.02**	0.39±0.03	**0.02±0.00**	0.02±0.00
AmazonCat-13K	0.84±0.03	**0.72±0.02**	0.37±0.02	**0.32±0.03**	0.40±0.00	**0.35±0.00**
Wiki10-30K	**0.19±0.01**	0.21±0.00	**2.59±0.21**	5.35±0.32	0.62±0.00	**0.58±0.00**
DeliciousLarge-200K	5.26±0.26	**2.58±0.15**	**5.24±0.43**	9.89±0.89	1.30±0.00	**0.95±0.00**
WikiLSHTC-325K	3.01±0.16	**2.95±0.15**	**1.36±0.13**	1.77±0.11	3.25±0.00	**2.73±0.00**
WikipediaLarge-500K	22.07±0.59	**16.10±0.44**	10.65±0.52	**6.67±0.23**	12.00±0.00	**8.89±0.00**
Amazon-670K	1.02±0.02	**0.56±0.00**	4.74±0.22	**4.13±0.28**	3.00±0.00	**2.26±0.00**
Amazon-3M	48.09±1.72	**7.07±0.56**	8.05±0.17	**3.26±0.08**	29.00±0.00	**20.84±0.00**

Table 8: Precision@k for $k = 1, 3, 5$, training time, average test time per example, and model size for random and k-means trees.

In the next two experiments, we evaluate the impact of tree depth on predictive and computational performance of PLTs. In the first experiment, we increase the degree of tree nodes to 16 and 64, but keep the degree of pre-leaves equal to 100. Such an approach is similar to the one used in BONSAI TREE [Khandagale et al., 2019]. The results for k-means trees and logistic loss are given in Table 9a. In the second experiment, we use binary trees, but change the degree of pre-leaves from 100 to 25 and 400. The results are given in Table 9b.[13] In both experiments, precision@k slightly increases with a decrease in the tree depth. This behavior is expected as suggested by the theoretical results from Section 4. The shorter paths should result in tighter upper bounds. On the other hand, a shallower tree leads to longer training times, as an example is used for training in more nodes. Notice that the 1-VS-ALL approach can be treated as an extremely shallow tree, with each training example used in all nodes. Similarly to the training time, we should expect prediction time to increase with the decreasing tree depth. This is, however, clearly visible only in the second experiment, in which we change the degree of pre-leaf nodes. Interestingly, the size of the resulting models does not significantly change over the different tree structures. The larger number of nodes is likely compensated by sparser models.

7.1.5 Ensemble of PLTs

In the last experiment focused on design choices, we analyze the predictive performance of small ensembles of PLTs. In Figure 5, we compare ensembles of size 3 and 5 to a single tree. Each tree

---

[13]For completeness, we present the results for the squared hinge loss in Appendix J.

Arity	2	16	64	2	16	64
	$p@1$ [%]			T/N_{test} [ms]		
WikiLSHTC-325K	61.96±0.03	63.16±0.03	**63.62±0.03**	1.77±0.11	**1.26±0.03**	1.91±0.19
WikipediaLarge-500K	66.20±0.05	67.36±0.10	**67.49±0.05**	6.67±0.23	**6.47±0.30**	9.02±0.39
Amazon-670K	**43.54±0.01**	43.33±0.04	43.53±0.05	4.13±0.28	**2.91±0.17**	5.12±0.24
Amazon-3M	46.09±0.02	46.74±0.01	**46.97±0.01**	3.26±0.08	**3.06±0.04**	4.19±0.16
	T_{train} [h]			M_{size} [GB]		
WikiLSHTC-325K	**2.95±0.15**	3.71±0.13	7.13±0.41	2.73±0.00	2.65±0.00	**2.62±0.00**
WikipediaLarge-500K	**16.10±0.44**	26.28±0.40	46.84±2.94	8.89±0.00	8.20±0.00	**8.13±0.00**
Amazon-670K	**0.56±0.00**	0.78±0.03	2.17±0.12	2.26±0.00	1.68±0.00	**1.60±0.00**
Amazon-3M	**7.07±0.56**	9.80±0.10	23.69±1.09	20.84±0.00	20.32±0.00	**20.17±0.00**

(a) Results for arity equal to 2, 16 or 64 and pre-leaf node degree equal to 100.

Pre-leaf degree	25	100	400	25	100	400
	$p@1$ [%]			T/N_{test} [ms]		
WikiLSHTC-325K	61.42±0.03	61.96±0.03	**62.16±0.05**	**0.66±0.04**	1.77±0.11	4.21±0.10
WikipediaLarge-500K	65.72±0.12	**66.20±0.05**	65.95±0.10	**3.52±0.05**	6.67±0.23	20.13±1.07
Amazon-670K	41.83±0.02	**43.54±0.01**	43.21±0.03	**1.61±0.04**	4.13±0.28	11.74±0.46
Amazon-3M	46.07±0.01	46.09±0.02	**46.13±0.01**	**1.47±0.00**	3.26±0.08	11.45±0.22
	T_{train} [h]			M_{size} [GB]		
WikiLSHTC-325K	**2.36±0.05**	2.95±0.15	4.83±0.29	3.28±0.00	2.73±0.00	**2.47±0.00**
WikipediaLarge-500K	**12.40±0.08**	16.10±0.44	34.15±0.46	10.60±0.01	8.89±0.00	**7.94±0.00**
Amazon-670K	**0.42±0.01**	0.56±0.00	1.01±0.05	2.20±0.00	2.26±0.00	**1.52±0.00**
Amazon-3M	**5.18±0.25**	7.07±0.56	16.41±0.52	24.00±0.00	20.84±0.00	**19.35±0.01**

(b) Results arity equal to 2 and pre-leaf node degree equal to 25, 100, or 400.

Table 9: Precision@k1, average prediction time per example, training time and model size for k-means trees if different depths with logistic loss.

is trained using 2-means clustering with the degree of pre-leaf nodes set to 100. The tree nodes are trained using LIBLINEAR with either logistic loss or squared hinge loss. The results show that the gain of using 3 trees instead of one is much greater than the gain of using 5 trees instead of 3. This makes the ensemble of size 3 a reasonable trade-off between predictive and computational cost, as the size of the models and computational cost grow linearly with the number of trees. It seems also that ensembles with squared hinge loss gain slightly more than the ensembles trained with logistic loss.

7.2 Generalized performance metrics

The previous experiments concern PLTs with top-k predictions suited for precision@k. In this section, we focus on threshold-based predictions and generalized performance metrics, discussed in Section 4.3. We constrain our analysis to Hamming loss and micro F_1-measure. A similar experiment for the macro F_1-measure has been conducted in [Jasinska et al., 2016]. For each metric, we report the results of two approaches. The first one uses a fixed threshold of 0.5, which is theoretically
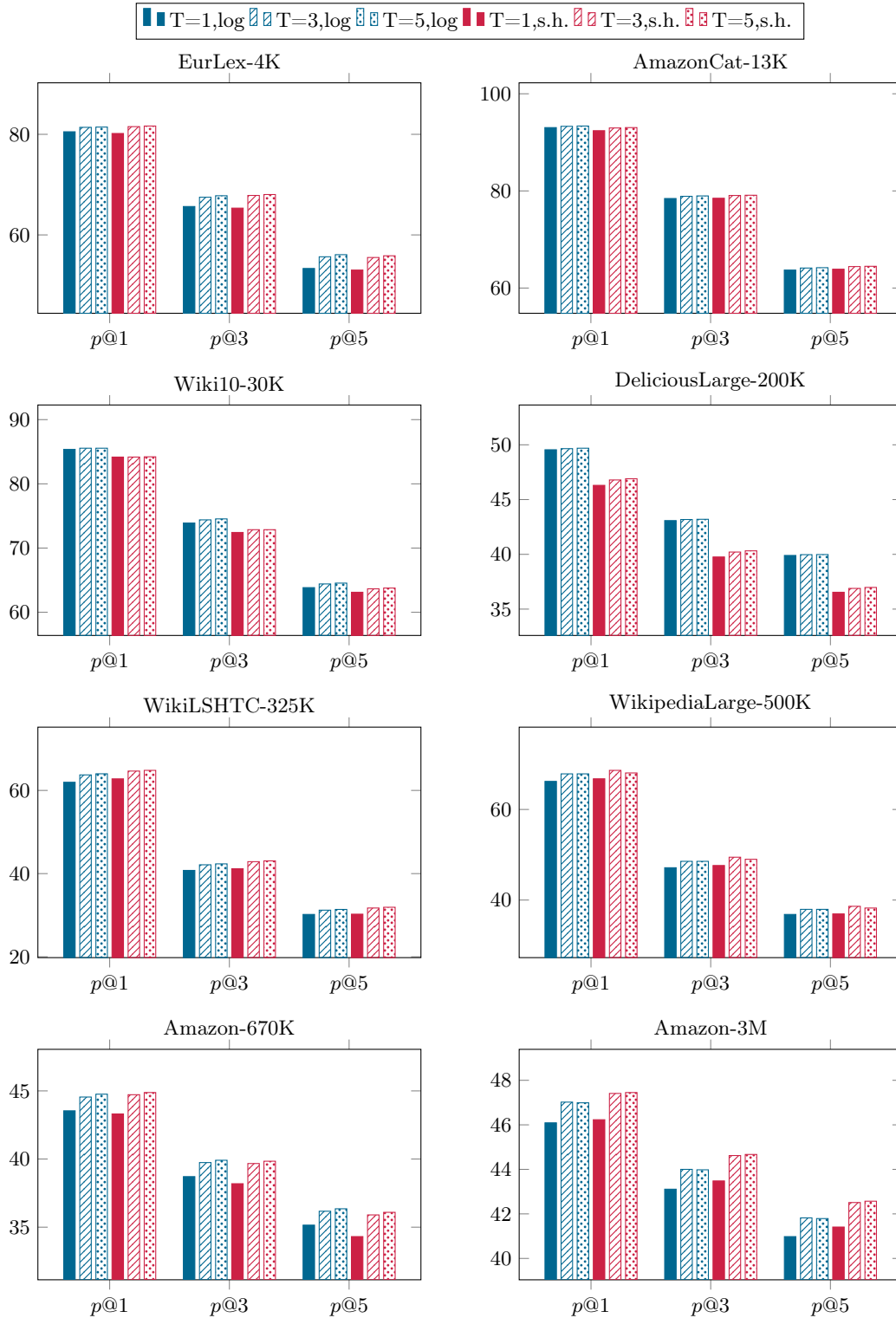
Figure 5: Precision@k for ensembles of $T = 1$, 3, and 5 trees trained using either logistic loss (log) or squared hinge loss (s.h.).

optimal for Hamming loss. Remark, however, that for estimated probabilities the optimal threshold can be different. The second one optimizes the micro F_1-measure by tuning one global threshold, as suggested by theory. To this end, it uses 70% of original training data to train a PLT model, and the rest to tune the threshold by running online F-measure optimization (OFO) [Busa-Fekete et al., 2015]. The same method has been used in [Jasinska et al., 2016] to optimize the macro F-measure. We repeat computations 5 times and report the average results along with standard errors. Table 10 presents the results. Notice that for Hamming loss the lower the value the better is the performance, while for the micro F-measures it is the opposite, the higher the value the better. As expected from the theoretical analysis, a procedure suited for a given metric leads to significantly better results, with only one exception.

	Hamming loss[1]		micro-F_1 [%]	
	thr=0.5	micro-OFO	thr=0.5	**micro-OFO**
EurLex-4K	**4.01±0.00**	7.42±0.59	**46.81±0.08**	40.30±2.08
AmazonCat-13K	**2.79±0.00**	2.94±0.01	67.00±0.02	**68.55±0.12**
Wiki10-30K	**17.43±0.01**	23.60±0.30	24.95±0.10	**32.27±0.18**
DeliciousLarge-200K	**97.15±0.00**	554.37±0.35	0.84±0.01	**13.08±0.00**
WikiLSHTC-325K	**2.94±0.00**	4.14±0.08	31.76±0.07	**32.73±0.44**
WikipediaLarge-500K	**4.12±0.01**	4.60±0.00	31.88±0.12	**38.76±0.00**
Amazon-670K	**4.69±0.00**	6.22±0.13	18.87±0.03	**28.95±0.48**
Amazon-3M	**34.87±0.00**	73.32±0.00	12.79±0.02	**28.20±0.00**

[1] multiplied by the number of labels to avoid presentation of very small numbers

Table 10: The results of PLTs with threshold-based predictions for Hamming loss, micro F_1-measures. The name of the column with the theoretically optimal tuning strategy for a given metric is given in bold.

7.3 Comparison to hierarchical softmax

In this experiment, we verify our theoretical findings from Section 4.5. As we have shown, hierarchical softmax with the pick-one-label heuristic (HSM-POL) leads to a suboptimal solution with respect to precision@k. To demonstrate this empirically, we run two experiments. In the first one, we compare the performance of PLTs and HSM-POL on synthetic data. In the second experiment, we evaluate both algorithms on benchmark data sets. To conduct the experiments, we implemented HSM-POL in NAPKINXC. We made it as similar as possible to the implementation of PLTs, with the only differences coming from the model definition. For both algorithms, we use LIBLINEAR with L2-regularized logistic loss to train node classifiers. In the experiment on benchmark data, we additionally use weight pruning to reduce model sizes. This is not necessary for synthetic data. To simulate the pick-one-label heuristic in batch learning, we transform a multi-label example with $||\boldsymbol{y}||_1$ positive labels to $||\boldsymbol{y}||_1$ weighted multi-class examples, each with a different positive label assigned and weight equal $\frac{1}{||\boldsymbol{y}||_1}$.

The results for precision@1 are given in Table 11. We use three types of synthetic data generated from different distributions: multi-label with conditionally independent labels, multi-label with conditionally dependent labels, and multi-class. The detailed description of the data generation process is given in Appendix G. The presented values are averages over 50 runs along with standard errors. Notice, however, that the data generation processes may lead to very diverse problems, with a different level of noise. Therefore, standard errors indicate rather the diversity of the generated problems.

43

	HSM-POL	PLT	# of losses	# of ties	# of wins	p-value
multi-label dependent	71.29±0.98	72.31±0.94	5	0	45	4.21e-09
multi-label independent	32.66±0.08	32.64±0.08	25	3	22	0.4799
multi-class	61.23±1.14	61.23±1.14	0	50	0	-

Table 11: Precision@1 of PLTs and HSM-POL on synthetic data. Reported are mean values over 50 runs along with standard errors, the number of wins, ties, and losses of PLTs, and p-value of the sign test.

To overcome this issue, we report the number of wins, ties, and losses, as well as p-values of the very conservative sign test. On data with conditionally dependent labels, PLTs clearly outperform HSM-POL as indicated by the p-value. This agrees with our theoretical results. On data with conditionally independent labels, both algorithms perform similarly without statistically significant differences. This also agrees with the theory, as we have proven that under label independence HSM-POL performs optimally for precision@k. The results on multi-class data completely match, as for this distribution the PLT model boils down to HSM.

	p@1 [%]		r@1 [%]		r@5 [%]	
	HSM	PLT	HSM	PLT	HSM	PLT
EurLex-4K	67.89±0.26	**80.51±0.16**	13.64±0.06	**16.20±0.04**	44.64±0.45	**51.71±0.67**
AmazonCat-13K	88.19±0.16	**93.04±0.02**	24.73±0.06	**26.37±0.01**	69.38±0.09	**74.64±0.02**
Wiki10-30K	54.69±1.00	**85.36±0.09**	3.18±0.07	**5.06±0.01**	12.58±0.18	**18.26±0.02**
WikiLSHTC-325K	58.35±0.04	**61.96±0.03**	26.41±0.02	**27.41±0.01**	49.81±0.01	**52.96±0.03**
WikipediaLarge-500K	60.48±0.09	**66.20±0.05**	20.16±0.03	**21.50±0.01**	43.17±0.03	**47.12±0.03**
Amazon-670K	40.38±0.04	**43.54±0.01**	8.53±0.01	**9.01±0.01**	29.52±0.04	**32.83±0.02**

Table 12: Precision@1 and recall@k of hierarchical softmax with pick-one-label heuristic (HSM) and PLT on benchmark datasets.

Table 12 gives the results on benchmark data sets. The difference in performance between PLTs and HSM-POL is clearly visible. It is even more substantial than in the previous experiment. Besides precision@1, the table contains also results for recall@k (with $k = 1, 5$),

$$r@k(\boldsymbol{y}, \boldsymbol{h}_{@k}(\boldsymbol{x})) = \frac{1}{||\boldsymbol{y}||_1} \sum_{j \in \hat{\mathcal{L}}_{\boldsymbol{x}}} [\![y_j = 1]\!] \,,$$

where $\hat{\mathcal{L}}_{\boldsymbol{x}} = \{j \in \mathcal{L} : h_j(\boldsymbol{x}) = 1\}$ is a set of k labels predicted by classifier $\boldsymbol{h}_{@k}$ for $\boldsymbol{x}$. The pick-one-label heuristic should lead to optimal results for this metric, as shown by Menon et al. [2019]. Nevertheless, PLTs obtain better results also for this metric, but the difference is much smaller. This suggests that indeed HSM-POL can be well-suited for recall@k, but the pick-one-label heuristic may lead to corrupted learning problems in tree nodes. As discussed in [Menon et al., 2019], there exist other strategies for optimizing recall@k, which may perform better than PLTs.

7.4   Online PLTs

We empirically verify online probabilistic label trees in which both node classifiers and tree structure are built incrementally. We implemented the OPLT algorithm, introduced in Section 5, in

NAPKINXC. The tree is constructed using the simple complete tree policy from Algorithm 8. To train node classifiers, we use ADAGRAD with logistic loss. The incremental learning in the online setting requires quick access to model weights, preferably storing all of them at once in memory. Unfortunately, maintaining an array for all possible weights in a dense format would require, for many data sets, thousands of GB of memory. As described in Section 6.2, either hash maps, such as ROBIN HOOD, or feature hashing should be applied to overcome this problem. In the experiment, we compare both approaches.

Feature hashing allows us to directly control the amount of memory used, but it may result with many unresolved collisions if the allocated space is too small. We consider setups with 64GB, 128GB, and 256GB of RAM. The ROBIN HOOD hash map avoids collisions, but does not allow for restraining memory consumption. The number of hashed features which can be allocated without collisions is given in Table 13. We report this number for each data set and memory setup. It takes into account memory needed for $2m - 1$ nodes, each containing model weights and cumulative gradients required by ADAGRAD, and auxiliary classifiers which number can be limited to m for the chosen tree building policy. Additionally, we present in the same table the amount of memory required by OPLT with ROBIN HOOD and OPLT with dense vectors.

	#features	#hashed features			RAM [GB]	
		64GB	128GB	256GB	ROBIN HOOD	dense vector
EurLex-4K	5000	*	*	*	0.6	0.2
AmazonCat-13K	203882	*	*	*	9	60
Wiki10-30K	101938	*	*	*	18	70
DeliciousLarge-200K	782585	13000	26000	52000	240	3593
WikiLSHTC-325K	1617899	8000	16000	32000	30	11754
WikipediaLarge-500K	2381304	5000	10000	20000	240	26670
Amazon-670K	135909	4000	8000	16000	36	2035
Amazon-3M	337067	1000	2000	4000	280	21187

Table 13: Number of features, hashed features for OPLT with complete tree policy and memory required to train OPLT with complete tree policy with ROBIN HOOD hash maps and dense vectors. With symbol '*' we denote data sets for which feature hashing is not needed to fit the available memory.

To simulate the online/streaming setting, the OPLT algorithms run three times over training examples, each time permuted randomly. We evaluate the performance on the original test sets in terms of precision@1. The results are given in Table 14. For reference, we also present the results of a batch PLT trained with logistic loss on a complete binary tree. OPLT with ROBIN HOOD performs similarly to PLT. This agrees with the results from Section 7.1.1 showing that incremental learning under logistic loss is competitive to its batch counterpart. Interestingly, ROBIN HOOD allows us to train OPLT in 256GB of RAM for all data sets, with the only exception of Amazon-3M for which 280GB is required. The performance of OPLT with feature hashing drops significantly for large data sets, even when using the same amount of memory as OPLT with ROBIN HOOD. One may observe that the smaller is the hashing space compared to the original feature space, the larger is the drop.

| Algorithm | OPLT | | | | PLT |
| Representation | feature hashing | | | ROBIN HOOD | |
RAM	64GB	128GB	256GB	unlimited	unlimited
EurLex-4K	$*$	$*$	$*$	76.69±0.21	**76.82±0.35**
AmazonCat-13K	$*$	$*$	$*$	**91.35±0.06**	**91.20±0.05**
Wiki10-30K	$*$	$*$	$*$	**84.41±0.19**	82.74±0.14
DeliciousLarge-200K	44.61±0.03	44.52±0.04	44.58±0.06	46.29±0.05	**47.81±0.03**
WikiLSHTC-325K	32.18±0.04	34.71±0.01	36.90±0.00	**44.42±0.03**	43.91±0.02
WikipediaLarge-500K	25.39±0.03	29.04±0.02	32.90±0.06	**49.35±0.03**	47.25±0.02
Amazon-670K	23.18±0.05	26.64±0.02	29.53±0.05	**37.02±0.01**	35.12±0.03
Amazon-3M	10.31±0.01	14.18±0.01	18.49±0.03	37.80±0.01	**38.05±0.02**

Table 14: Performance of OPLT with different memory management strategies: feature hashing of 64GB, 128GB and 256GB, and ROBIN HOOD hash maps. Results of a batch counterpart are given for reference. With symbol '$*$' we denote data sets where feature hashing is not needed to fit the available memory.

A better tree building policy may improve the predictive performance of OPLT. By comparing the results presented here to the ones of k-means trees, we observe a large gap. The online tree building algorithms are not able to fully eliminate it, but we believe that the regret can be much smaller. Also, memory usage could be improved by better utilization of auxiliary classifiers.

7.5 PLT vs. state-of-the-art

In the final part of the empirical study, we compare PLTs with state-of-the-art algorithms. In the comparison, we use two decision tree methods. Their main difference to label trees is that they split the feature space, not the set of labels. FASTXML, introduced in [Prabhu and Varma, 2014], uses sparse linear classifiers in internal tree nodes, also trained using LIBLINEAR. Each linear classifier decides between two classes, the left or the right child. These two classes are initiated by a random assignment of training examples to the children nodes. In the next steps, the assignment is reshaped by optimizing the normalized discounted cumulative gain (nDCG) over both children. Once the assignment stabilizes, a sparse linear classifier is trained using logistic loss. To improve the overall accuracy FASTXML uses an ensemble of trees. PFASTREXML [Jain et al., 2016] is a modification of FASTXML that optimizes propensity scored nDCG at each tree node and re-ranks the predicted labels. Besides decision trees, we also use two 1-VS-ALL algorithms which are known to be the best *no-deep* (or CPU-based) XMLC methods. DiSMEC trains a single classifier per label under L_2 regularized squared hinge loss, also using LIBLINEAR. It prunes weights of final models at threshold equal 0.01 to reduce the memory needed to store a 1-VS-ALL classifier. It uses distributed training over multiple cores and processors to speed up computations. PPD-SPARSE [Yen et al., 2017], in turn, parallelizes PD-SPARSE [Yen et al., 2016] which optimizes a max-margin loss by exploiting the primal-dual sparsity, resulting from the use of the max-margin loss under L_1 regularization, given that for each training example the set of highly scored incorrect labels is small. We exclude from the comparison all XMLC algorithms based on complex deep networks, requiring the use of GPUs and raw versions of text data. We remark, however, that some of such methods, for example XML-CNN [Liu et al., 2017], perform worse than the best methods used in this study. As instances of PLTs, we use PARABEL and NAPKINXC. For the former, we use an ensemble of three trees trained with squared hinge loss. This is the first label tree

algorithm being competitive to state-of-the-art, as reported in Prabhu et al. [2018]. For NAPKINXC, we use a configuration, suggested by the results of the previous experiments, which uses also an ensemble of three trees, but with arity of 16, providing a significant predictive performance boost over binary trees, at the same keeping training and prediction times reasonably low. For training node classifiers, we use LIBLINEAR with logistic loss for 3 datasets (AmazonCat-13K, Wiki10-30K and DeliciousLarge-200K) and squared hinge loss for the rest of the datasets.

The results are given in Table 15. We report precision@k, training and prediction times, and model sizes. For each not deterministic algorithm, we repeat the experiment 5 times and report means with standard errors. We use original implementations of all competitors. The hyperparameters used to tune the final models are given in Appendix H. For DiSMEC and PPDSPARSE we report the best results found in the literature, namely from [Babbar and Schölkopf, 2017, Yen et al., 2017, Prabhu et al., 2018, Bhatia et al., 2016]. We use the provided implementations to approximate training and prediction times on our hardware. From the results, we see that PLTs are indeed competitive to the 1-VS-ALL approaches, achieving the best precision@1 on 5 from 8 data sets and is only slightly worse on the rest of the data sets. They outperform the decision tree-based methods. PLTs are almost always the fastest in training and prediction and achieve the smallest model sizes. They can be even a thousand times faster in training and prediction than 1-VS-ALL. The variant of NAPKINXC used in this experiment outperforms PARABEL in terms of precision@k by sacrificing the computational performance of training and prediction. However, it can predict in an online setting at the same time often consuming less memory.

	p@1 [%]	p@3 [%]	p@5 [%]	T_{train} [h]	T/N_{test} [ms]	M_{size} [GB]
			EurLex-4K			
FASTXML	71.26±0.19	59.80±0.12	50.28±0.02	0.07±0.00	0.97±0.15	0.22±0.00
PFASTREXML	70.21±0.09	59.26±0.10	50.59±0.08	0.08±0.00	1.30±0.09	0.26±0.00
PPDSPARSE	**83.83**	**70.72**	**59.21**	≈ 0.02	≈ 0.70	0.07
DiSMEC	83.67	70.70	59.14	≈ 0.70	≈ 4.60	0.04
PARABEL-T=3	81.80±0.10	68.67±0.03	57.45±0.06	**0.02±0.00**	**0.93±0.04**	0.03±0.00
NXC-T=3	81.94±0.24	68.94±0.07	57.49±0.14	0.03±0.00	0.97±0.06	**0.02±0.00**
			AmazonCat-13K			
FASTXML	93.03±0.00	78.22±0.01	63.38±0.00	5.53±0.15	1.06±0.08	18.35±0.00
PFASTREXML	85.62±0.01	75.31±0.00	62.83±0.01	5.45±0.12	**0.99±0.06**	19.01±0.00
PPDSPARSE	92.72	78.14	63.41	≈ 2.97	≈ 1.20	**0.50**
DiSMEC	92.72	78.11	63.40	≈ 138.60	≈ 2.9	1.50
PARABEL-T=3	93.24±0.01	79.17±0.00	64.51±0.00	**0.64±0.03**	1.05±0.04	0.62±0.00
NXC-T=3	**93.37±0.05**	**79.01±0.03**	**64.27±0.04**	2.30±0.13	**0.99±0.10**	1.01±0.00

	$p@1$ [%]	$p@3$ [%]	$p@5$ [%]	T_{train} [h]	T/N_{test} [ms]	M_{size} [GB]
			Wiki10-30K			
FastXML	82.97±0.02	67.58±0.07	57.68±0.03	0.23±0.01	8.21±0.52	0.54±0.00
PfastreXML	75.58±0.07	64.38±0.11	57.25±0.07	0.23±0.00	10.40±0.41	1.13±0.00
PPDSparse	73.80	60.90	50.40	≈ 1.20	≈ 22.00	0.80
DiSMEC	85.20	**74.60**	**65.90**	≈ 26.80	≈ 112.40	2.40
Parabel-T=3	84.49±0.05	72.57±0.04	63.66±0.10	**0.20±0.00**	**2.67±0.06**	**0.18±0.00**
nXC-T=3	**85.90±0.02**	74.45±0.11	64.84±0.09	0.39±0.01	11.76±0.19	2.16±0.00
			DeliciousLarge-200K			
FastXML	43.17±0.03	38.70±0.01	36.22±0.02	3.86±0.09	12.27±0.36	6.95±0.00
PfastreXML	17.44±0.02	17.28±0.01	17.19±0.01	3.71±0.02	19.64±0.35	15.34±0.00
PPDSparse	45.05	38.34	34.90	≈ 17.00	≈ 64.00	3.40
DiSMEC	45.50	38.70	35.50	≈ 24000.00	≈ 68.20	160.10
Parabel-T=3	46.62±0.02	39.78±0.04	36.37±0.04	9.01±0.20	**2.61±0.03**	6.36±0.00
nXC-T=3	**49.65±0.03**	**43.18±0.02**	**39.97±0.01**	**7.90±0.48**	31.10±2.87	**2.86±0.00**
			WikiLSHTC-325K			
FastXML	49.85±0.00	33.16±0.01	24.49±0.01	6.41±0.13	4.10±0.04	12.93±0.00
PfastreXML	58.50±0.02	37.69±0.01	27.57±0.01	6.25±0.13	4.00±0.20	14.20±0.00
PPDSparse	64.13	42.10	31.14	≈ 16.00	≈ 51.00	5.10
DiSMEC	64.94	42.71	31.50	≈ 2320.00	≈ 340.00	3.80
Parabel-T=3	64.95±0.02	43.21±0.02	32.01±0.01	**0.81±0.02**	**1.27±0.03**	3.10±0.00
nXC-T=3	**65.57±0.10**	**43.64±0.11**	**32.33±0.11**	7.10±0.13	1.70±0.13	**2.68±0.00**
			WikipediaLarge-500K			
FastXML	49.32±0.03	33.48±0.03	25.84±0.01	51.48±0.65	15.35±0.56	59.69±0.01
PfastreXML	59.58±0.02	40.26±0.01	30.73±0.01	51.07±0.92	15.24±0.24	69.33±0.01
PPDSparse	70.16	50.57	39.66	≈ 26.00	≈ 130.00	4.00
DiSMEC	**70.20**	**50.60**	**39.70**	≈ 26800.00	≈ 1200.00	14.80
Parabel-T=3	68.66±0.06	49.48±0.05	38.60±0.04	**7.33±0.12**	**3.44±0.13**	5.69±0.00
nXC-T=3	69.24±0.20	49.82±0.16	38.81±0.14	41.11±1.34	5.53±0.10	**4.68±0.01**
			Amazon-670K			
FastXML	36.90±0.02	33.22±0.01	30.44±0.01	2.80±0.03	8.57±0.20	9.54±0.00
PfastreXML	36.97±0.02	34.18±0.01	32.05±0.01	3.01±0.03	9.96±0.14	10.98±0.00
PPDSparse	45.32	40.37	36.92	≈ 2.00	≈ 90.00	6.00
DiSMEC	**45.37**	**40.40**	**36.96**	≈ 1830.00	≈ 380.00	3.80
Parabel-T=3	44.70±0.04	39.66±0.04	35.85±0.04	**0.39±0.00**	**1.57±0.05**	1.95±0.00
nXC-T=3	45.10±0.11	40.00±0.12	36.22±0.13	2.17±0.10	1.84±0.42	**1.66±0.00**
			Amazon-3M			
FastXML	45.26±0.01	41.96±0.00	39.80±0.01	18.19±1.01	68.77±4.16	30.70±0.00
PfastreXML	32.62±0.01	32.67±0.01	32.35±0.01	19.07±0.92	78.83±3.93	41.88±0.00
PPDSparse	-	-	-	-	-	-
DiSMEC	47.77	44.96	42.80	≈ 18800.00	≈ 2050.00	39.70
Parabel-T=3	47.52±0.01	44.69±0.01	42.57±0.00	**5.20±0.01**	**1.53±0.02**	31.43±0.00
nXC-T=3	**47.83±0.09**	**45.08±0.09**	**42.98±0.09**	25.43±1.02	4.93±0.60	**28.08±0.00**

Table 15: PLTs compared to state-of-the-art algorithms.

8 Summary

We presented and investigated probabilistic label trees, a computationally efficient and statistically well-justified model for solving extreme multi-label classification problems. The in-depth analysis shows that PLTs can scale logarithmically with the number of labels and are suitable for optimizing a wide spectrum of performance metrics commonly used in extreme multi-label classification. We also considered a fully online algorithm which incrementally trains both node classifiers and tree structure in a streaming setting, without any prior knowledge of training examples and the set of labels. The presented discussion on existing implementations of a PLT model systematizes the knowledge about different design choices and allows for a better understanding of their performance. We introduced NAPKINXC, a new modular implementation of PLTs. It supports batch and incremental training, the fully online setting, sparse and dense representation of features, as well as prediction suited for various performance metrics. Thanks to this it can be easily tailored for a wide spectrum of applications. In the comprehensive experimental study, we showed that PLTs are indeed a state-of-the-art method performing on par with the 1-vs-ALL approaches, but being at the same time orders of magnitude faster. The existing implementations of the PLT model along with the empirical results indicate that this approach is currently the most successful for extreme multi-label classification.

We hope that our work will contribute to development of label tree methods, by creating a common basis for this approach. Nevertheless, there exist many open problems related to probabilistic label trees. The tree structure learning is one of them. The k-means trees have made a significant contribution, but certainly they are not the ultimate solution to this problem. The ideal tree structure should also take training and prediction costs into account, as well as the long-tail labels. Another challenge are new tree building policies for online probabilistic label trees. An open problem is to make PLTs suitable for such performance metrics as recall@k and NDCG@k. Another interesting research direction is the use of PLTs as an efficient index structure for negative sampling in the 1-vs-ALL approaches.

A   Proofs of the results from Section 3.3

We present proofs of Proposition 2 and Theorem 1 concerning the computational costs of PLTs. The first proof has been originally published in [Busa-Fekete et al., 2019]. The second is based on a proof of a more general result concerning actual label probabilities from the same paper.

Proposition 2. *For any tree T and vector $\boldsymbol{y}$ it holds that:*

$$c(T, \boldsymbol{y}) \leq 1 + \|\boldsymbol{y}\|_1 \cdot \mathrm{depth}_T \cdot \mathrm{deg}_T \,,$$

where $\mathrm{depth}_T = \max_{v \in L_T} \mathrm{len}_v - 1$ is the depth of the tree, and $\mathrm{deg}_T = \max_{v \in V_T} \mathrm{deg}_v$ is the highest degree of a node in T.

Proof. First notice that a training example is always used in the root node, either as a positive example $(\boldsymbol{x}, 1)$, if $\|\boldsymbol{y}\|_1 > 0$, or as a negative example $(\boldsymbol{x}, 0)$, if $\|\boldsymbol{y}\|_1 = 0$. Therefore the cost is bounded by 1. If $\|\boldsymbol{y}\|_1 > 0$, the training example is also used as a positive example in all the nodes on paths from the root to leaves corresponding to labels j for which $y_j = 1$ in $\boldsymbol{y}$. As the root has been already counted, we have at most $\mathrm{depth}_T = \max_v \mathrm{len}_v - 1$ such nodes for each positive label in $\boldsymbol{y}$. Moreover, the training example is used as a negative example in all siblings of the nodes on the paths determined above, unless it is already a positive example in the sibling node. The highest degree of a node in the tree is deg_T. Taking the above into account, the cost $c(T, \boldsymbol{y})$ is bounded from above by $1 + \|\boldsymbol{y}\|_1 \cdot \mathrm{depth}_T \cdot \mathrm{deg}_T$. The bound is tight, for example, if $\|\boldsymbol{y}\|_1 = 1$ and T is a perfect deg_T-ary tree (all non-leaf nodes have an equal degree and the paths to the root from all leaves are of the same length). □

Theorem 1. *For Algorithm 3 with all thresholds τ_v, $v \in V_T$, set to τ and any $\boldsymbol{x} \in \mathcal{X}$, we have that:*

$$c_\tau(T, \boldsymbol{x}) \leq 1 + \lfloor \hat{P}/\tau \rfloor \cdot \mathrm{depth}_T \cdot \mathrm{deg}_T \,, \tag{12}$$

where $\hat{P}$ is a constant upperbounding $\sum_{j=1}^m \hat{\eta}_j(\boldsymbol{x})$, $\mathrm{depth}_T = \max_{v \in L_T} \mathrm{len}_v - 1$, and $\mathrm{deg}_T = \max_{v \in V_T} \mathrm{deg}_v$.

Proof. The proof is similar to the one of Theorem 6.1 in [Busa-Fekete et al., 2019]. As stated before the theorem, we assume that the estimates are properly normalized, that is, they satisfy:

$$\hat{\eta}_v(\boldsymbol{x}) \leq \min \left\{ 1, \sum_{v' \in \mathrm{Ch}(v)} \hat{\eta}_{v'}(\boldsymbol{x}) \right\} \,, \tag{28}$$

and

$$\max \left\{ \hat{\eta}_{v'}(\boldsymbol{x}), v' \in \mathrm{Ch}(v) \right\} \leq \hat{\eta}_v(\boldsymbol{x}) \,. \tag{29}$$

Consider the subtree T' of T, which consists of all nodes $v \in V_T$ for which $\hat{\eta}_v(\boldsymbol{x}) \geq \tau$. If there are no such nodes, from the pseudocode of Algorithm 3, we see that only the root classifier is called. The upperbound (12) in this case obviously holds. However, it might not be tight as $\hat{\eta}_v(\boldsymbol{x}) < \tau$ does not imply $\hat{P} \leq \tau$ because of (28).

If T' has at least one node, Algorithm 3 visits each node of T' (calls a corresponding classifier and add the node to a stack), since for each parent node we have (29). Moreover, Algorithm 3 visits all children of nodes T' (some of them are already in T'). Let the subtree T'' consist of all nodes of T' and their child nodes. Certainly $T' \subseteq T'' \subseteq T$. To prove the theorem we count first the number of nodes in T' and then the number of nodes in T'', which gives as the final result.

50

If the number of nodes in T' is greater than or equal to 1, then certainly r_T is in T'. Let us consider next the number of leaves of T'. Observe that $\sum_{v \in L_{T'}} \hat{\eta}_v(\boldsymbol{x}) \leq \hat{P}$. This is because $\sum_{v \in L_{T'}} \hat{\eta}_v(\boldsymbol{x}) \leq \sum_{v \in L_T} \hat{\eta}_v(\boldsymbol{x}) \leq \hat{P}$, that is, $v \in L_{T'}$ might be an internal node in T and its $\hat{\eta}_v(\boldsymbol{x})$ is at most the sum of probability estimates of the leaves underneath v according to (28). From this we get the following upper bound on the number of leaves in T':

$$|L_{T'}| \leq \lfloor \hat{P}/\tau \rfloor. \tag{30}$$

Since the degree of internal nodes in T' might be 1, to upperbound the number of all nodes in T' we count the number of nodes on all paths from leaves to the root, but counting the root node only once:

$$|V_{T'}| \leq 1 + \sum_{v \in L_{T'}} (\mathrm{len}_v - 1).$$

Next, notice that for each $v \in T'$ its all siblings are in T'' unless v is the root node. This is because if non-root node v is in T' then its parent is also in T' according to (29) and T'' contains all child nodes of nodes in T'. The rest of nodes in T'' are the child nodes of leaves of T', unless a leaf of T' is also a leaf of T. Therefore, we have

$$|V_{T''}| \leq 1 + \sum_{v \in L_{T'}} \deg_T(\mathrm{len}_v - 1) + \sum_{v \in L_{T'}} \deg_T [\![v \notin L_T]\!],$$

with $\deg_T$ being the highest possible degree of a node. Since (30) and

$$\mathrm{len}_v - 1 + [\![v \notin L_T]\!] \leq \mathrm{depth}_T,$$

that is, the longest path cannot be longer than the depth of the tree plus 1, we finally get:

$$|V_{T''}| \leq 1 + \lfloor \hat{P}/\tau \rfloor \cdot \mathrm{depth}_T \cdot \deg_T.$$

This ends the proof as the number of nodes in T'' is equivalent to the number of calls to the node classifiers, that is, $c_\tau(T, \boldsymbol{x})$. $\qquad \square$

B   Proofs of the results from Section 4.1

We prove here Theorem 2, the main result of Section 4.1. To this end we first show two additional results. The first lemma concerns expectation of $\eta_{\mathrm{pa}(v')}(\boldsymbol{x}) |\eta(\boldsymbol{x}, v') - \hat{\eta}(\boldsymbol{x}, v')|$, the weighted L_1 error in node v used in upper bounds from Lemma 1 and Corollary 1. We express this expectation by the expected L_1 error in node v multiplied by $\mathbf{P}(z_{\mathrm{pa}(\boldsymbol{x})} = 1)$. Based on this result, we proof the second lemma in which we bound the expected L_1-estimation error of label j by a weighted sum of expected L_1 errors on $\mathrm{Path}(l_j)$.

Lemma 2. *For any tree T and distribution $\mathbf{P}(\boldsymbol{x}, \boldsymbol{y})$, the following holds for $v \in V_T$:*

$$\mathbb{E}_{\boldsymbol{x} \sim \mathbf{P}(\boldsymbol{x})} \left[\eta_{\mathrm{pa}(v)}(\boldsymbol{x}) |\eta(\boldsymbol{x}, v) - \hat{\eta}(\boldsymbol{x}, v)| \right] = \mathbf{P}(z_{\mathrm{pa}(v)} = 1) \mathbb{E}_{\boldsymbol{x} \sim \mathbf{P}(\boldsymbol{x}|z_{\mathrm{pa}(v)}=1)} \left[|\eta(\boldsymbol{x}, v) - \hat{\eta}(\boldsymbol{x}, v)| \right],$$

where for the root node $\mathbf{P}(z_{\mathrm{pa}(r_T)} = 1) = 1$.

Proof. By using the definition of expectation, replacing $\eta_{\mathrm{pa}(v)}(\boldsymbol{x})$ by its definition, applying Bayes' theorem, and rearranging terms, we obtain:

$$\mathbb{E}_{\boldsymbol{x}\sim\mathbf{P}(\boldsymbol{x})}\big[\eta_{\mathrm{pa}(v)}(\boldsymbol{x})\,|\eta(\boldsymbol{x},v)-\hat{\eta}(\boldsymbol{x},v)|\big]=\int\mathbf{P}(\boldsymbol{x})\eta_{\mathrm{pa}(v)}(\boldsymbol{x})\,|\eta(\boldsymbol{x},v)-\hat{\eta}(\boldsymbol{x},v)|\,d\boldsymbol{x}$$

$$=\int\mathbf{P}(\boldsymbol{x})\mathbf{P}(z_{\mathrm{pa}(v)}=1|\boldsymbol{x})\,|\eta(\boldsymbol{x},v)-\hat{\eta}(\boldsymbol{x},v)|\,d\boldsymbol{x}$$

$$=\mathbf{P}(z_{\mathrm{pa}(v)}=1)\!\int\mathbf{P}(\boldsymbol{x}|z_{\mathrm{pa}(v)}=1)\,|\eta(\boldsymbol{x},v)-\hat{\eta}(\boldsymbol{x},v)|\,d\boldsymbol{x}\,.$$

Since

$$\int\mathbf{P}(\boldsymbol{x}|z_{\mathrm{pa}(v)}=1)\,|\eta(\boldsymbol{x},v)-\hat{\eta}(\boldsymbol{x},v)|\,d\boldsymbol{x}$$

is nothing else than the expected L_1 estimation error in node v, denoted by

$$\mathbb{E}_{\boldsymbol{x}\sim\mathbf{P}(\boldsymbol{x}|z_{\mathrm{pa}(v)}=1)}\left[|\eta(\boldsymbol{x},v)-\hat{\eta}(\boldsymbol{x},v)|\right]\,,$$

we obtain the final result. $\qquad\square$

Lemma 3. *For any tree T and distribution $\mathbf{P}(\boldsymbol{x},\boldsymbol{y})$ the following holds for $j\in\mathcal{L}$:*

$$\mathbb{E}_{\boldsymbol{x}\sim\mathbf{P}(\boldsymbol{x})}\left[|\eta_j(\boldsymbol{x})-\hat{\eta}_j(\boldsymbol{x})|\right]\leq\sum_{v\in\mathrm{Path}(l_j)}\mathbf{P}(z_{\mathrm{pa}(v)}=1)\mathbb{E}_{\boldsymbol{x}\sim\mathbf{P}(\boldsymbol{x}|z_{\mathrm{pa}(v)}=1)}\left[|\eta(\boldsymbol{x},v)-\hat{\eta}(\boldsymbol{x},v)|\right]\,,$$

where for the root node $\mathbf{P}(z_{\mathrm{pa}(r_T)}=1)=1$.

Proof. Take expectation of both hand sides of (14) and use linearity of expectation for the right hand side:

$$\mathbb{E}_{\boldsymbol{x}\sim\mathbf{P}(\boldsymbol{x})}\left[|\eta_j(\boldsymbol{x})-\hat{\eta}_j(\boldsymbol{x})|\right]$$

$$\leq\mathbb{E}_{\boldsymbol{x}\sim\mathbf{P}(\boldsymbol{x})}\left[\sum_{v\in\mathrm{Path}(l_j)}\eta_{\mathrm{pa}(v)}(\boldsymbol{x})\,|\eta(\boldsymbol{x},v)-\hat{\eta}(\boldsymbol{x},v)|\right]$$

$$=\sum_{v\in\mathrm{Path}(l_j)}\mathbb{E}_{\boldsymbol{x}\sim\mathbf{P}(\boldsymbol{x})}\left[\eta_{\mathrm{pa}(v)}(\boldsymbol{x})\,|\eta(\boldsymbol{x},v)-\hat{\eta}(\boldsymbol{x},v)|\right]$$

The rest follows from Lemma 2. $\qquad\square$

Using the above results, we finally prove Theorem 2. It bounds the expectation of the L_1-estimation error averaged over all labels by the expected L_1-estimation errors of node classifiers. The expectation is defined over the entire distribution $\Pr(\boldsymbol{x})$. We present the result in a general form of a weighted average as such form is used later in proofs for the generalized performance metrics.

Theorem 2. *For any tree T, distribution $\mathbf{P}(\boldsymbol{x},\boldsymbol{y})$, and weights $W_j\in R$, $j\in\{1,\ldots,m\}$, the following holds:*

$$\frac{1}{m}\sum_{j=1}^{m}W_j\mathbb{E}_{\boldsymbol{x}\sim\mathbf{P}(\boldsymbol{x})}\left[|\eta_j(\boldsymbol{x})-\hat{\eta}_j(\boldsymbol{x})|\right]\leq$$

$$\frac{1}{m}\sum_{v\in V}\mathbf{P}(z_{\mathrm{pa}(v)}=1)\mathbb{E}_{\boldsymbol{x}\sim\mathbf{P}(\boldsymbol{x}|z_{\mathrm{pa}(v)}=1)}\left[|\eta(\boldsymbol{x},v')-\hat{\eta}(\boldsymbol{x},v')|\right]\sum_{j\in L_v}W_j\,,\qquad(15)$$

where for the root node $\mathbf{P}(z_{\mathrm{pa}(r_T)} = 1) = 1$. *For* $W_j = 1$, $j \in \{1, \ldots, m\}$, *we have:*

$$\frac{1}{m} \sum_{j=1}^{m} \mathbb{E}_{\boldsymbol{x} \sim \mathbf{P}(\boldsymbol{x})} \left[|\eta_j(\boldsymbol{x}) - \hat{\eta}_j(\boldsymbol{x})| \right] \leq$$
$$\frac{1}{m} \sum_{v \in V} \mathbf{P}(z_{\mathrm{pa}(v)} = 1) \mathbb{E}_{\boldsymbol{x} \sim \mathbf{P}(\boldsymbol{x}|z_{\mathrm{pa}(v)}=1)} \left[|\eta(\boldsymbol{x}, v') - \hat{\eta}(\boldsymbol{x}, v')| \right] |L_v|.$$

Proof. From Lemma 3 we obtain:

$$\frac{1}{m} \sum_{j=1}^{m} W_j \mathbb{E}_{\boldsymbol{x} \sim \mathbf{P}(\boldsymbol{x})} \left[|\eta_j(\boldsymbol{x}) - \hat{\eta}_j(\boldsymbol{x})| \right] \leq$$
$$\frac{1}{m} \sum_{j=1}^{m} W_j \sum_{v \in \mathrm{Path}(l_j)} \mathbf{P}(z_{\mathrm{pa}(v)} = 1) \mathbb{E}_{\boldsymbol{x} \sim \mathbf{P}(\boldsymbol{x}|z_{\mathrm{pa}(v)}=1)} \left[|\eta(\boldsymbol{x}, v) - \hat{\eta}(\boldsymbol{x}, v)| \right].$$

The RHS can be further transformed to:

$$\frac{1}{m} \sum_{j=1}^{m} \sum_{v \in \mathrm{Path}(l_j)} W_j \mathbf{P}(z_{\mathrm{pa}(v)} = 1) \mathbb{E}_{\boldsymbol{x} \sim \mathbf{P}(\boldsymbol{x}|z_{\mathrm{pa}(v)}=1)} \left[|\eta(\boldsymbol{x}, v) - \hat{\eta}(\boldsymbol{x}, v)| \right] =$$
$$\frac{1}{m} \sum_{v \in V} \mathbf{P}(z_{\mathrm{pa}(v)} = 1) \mathbb{E}_{\boldsymbol{x} \sim \mathbf{P}(\boldsymbol{x}|z_{\mathrm{pa}(v)}=1)} \left[|\eta(\boldsymbol{x}, v) - \hat{\eta}(\boldsymbol{x}, v)| \right] \sum_{j \in L_v} W_j.$$

where the last equation follows from the fact that each $v \in V_T$ appears in the double sum $|L_v|$ times (where $|L_v|$ is the number of leaves in a subtree rooted in v; in other words, this is the number of paths from leaves to the root that contain node v). Changing the double sum to sum over all nodes and multiplying the expected L_1 estimation error for v by $\sum_{j \in L_v} W_j$ gives the final result. $\qquad \square$

C   Proofs of the results from Section 4.2

We present the proof of Theorem 3. It expresses the bound from Theorem 2 in terms of node regrets of a strongly proper composite loss function.

Theorem 3. *For any tree* T, *distribution* $\mathbf{P}(\boldsymbol{x}, \boldsymbol{y})$, *weights* $W_j \in R$, $j \in \{1, \ldots, m\}$, *a strongly proper composite loss function* ℓ_c, *and a set of scoring functions* f_v, $v \in V_T$, *the following holds:*

$$\frac{1}{m} \sum_{j=1}^{m} W_j \mathbb{E}_{\boldsymbol{x} \sim \mathbf{P}(\boldsymbol{x})} \left[|\eta_j(\boldsymbol{x}) - \hat{\eta}_j(\boldsymbol{x})| \right] \leq \frac{\sqrt{2}}{m\sqrt{\lambda}} \sum_{v \in V} \sqrt{\mathbf{P}(z_{\mathrm{pa}(v)} = 1) \mathrm{reg}_{\ell_c}(f_v)} \sum_{j \in L_v} W_j, \qquad (17)$$

where for the root node $\mathbf{P}(z_{\mathrm{pa}(r_T)} = 1) = 1$, *and* $\mathrm{reg}_{\ell_c}(f_v)$ *is the expected* ℓ_c-*regret of* f_v *taken over* $\mathbf{P}(\boldsymbol{x}, z_v \,|\, z_{\mathrm{pa}(v)} = 1)$. *For* $W_j = 1$, $j \in \{1, \ldots, m\}$, *we have:*

$$\frac{1}{m} \sum_{j=1}^{m} \mathbb{E}_{\boldsymbol{x} \sim \mathbf{P}(\boldsymbol{x})} \left[|\eta_j(\boldsymbol{x}) - \hat{\eta}_j(\boldsymbol{x})| \right] \leq \frac{\sqrt{2}}{m\sqrt{\lambda}} \sum_{v \in V} |L_v| \sqrt{\mathbf{P}(z_{\mathrm{pa}(v)} = 1) \mathrm{reg}_{\ell_c}(f_v)}. \qquad (18)$$

Proof. As ψ is an invertible function satisfying $f(\boldsymbol{x}) = \psi(\mathbf{P}(y = 1 \,|\, \boldsymbol{x}))$, we can assume that $\hat{\eta}(\boldsymbol{x}, v) = \psi^{-1}(f_v(\boldsymbol{x}))$. We then obtain from (16):

$$\eta_{\mathrm{pa}(v)}(\boldsymbol{x}) \,|\eta(\boldsymbol{x}, v) - \hat{\eta}(\boldsymbol{x}, v)| \leq \eta_{\mathrm{pa}(v)}(\boldsymbol{x})\sqrt{\frac{2}{\lambda}}\sqrt{\mathrm{reg}_{\ell_c}(f_v \,|\, \boldsymbol{x})}, \tag{31}$$

for any $v \in V_T$. We take the expectation with respect to $\mathbf{P}(\boldsymbol{x})$ of (31). Based on Lemma 2, given in Appendix B, the left hand side is equal to:

$$\mathbf{P}(z_{\mathrm{pa}(v)} = 1)\mathbb{E}_{\boldsymbol{x} \sim \mathbf{P}(\boldsymbol{x}|z_{\mathrm{pa}(v)}=1)}\left[|\eta(\boldsymbol{x}, v) - \hat{\eta}(\boldsymbol{x}, v)|\right].$$

For the left hand side we obtain the following upper bound:

$$\mathbb{E}_{\boldsymbol{x} \sim \mathbf{P}(\boldsymbol{x})}\left[\eta_{\mathrm{pa}(v)}(\boldsymbol{x})\sqrt{\frac{2}{\lambda}}\sqrt{\mathrm{reg}_{\ell_c}(f_v \,|\, \boldsymbol{x})}\right] = \sqrt{\frac{2}{\lambda}}\mathbb{E}_{\boldsymbol{x} \sim \mathbf{P}(\boldsymbol{x})}\left[\mathbf{P}(z_{\mathrm{pa}(v)} = 1|\boldsymbol{x})\sqrt{\mathrm{reg}_{\ell_c}(f_v \,|\, \boldsymbol{x})}\right]$$

$$= \sqrt{\frac{2}{\lambda}}\mathbb{E}_{\boldsymbol{x} \sim \mathbf{P}(\boldsymbol{x})}\left[\sqrt{\mathbf{P}(z_{\mathrm{pa}(v)} = 1|\boldsymbol{x})^2\mathrm{reg}_{\ell_c}(f_v \,|\, \boldsymbol{x})}\right]$$

$$\leq \sqrt{\frac{2}{\lambda}}\mathbb{E}_{\boldsymbol{x} \sim \mathbf{P}(\boldsymbol{x})}\left[\sqrt{\mathbf{P}(z_{\mathrm{pa}(v)} = 1|\boldsymbol{x})\mathrm{reg}_{\ell_c}(f_v \,|\, \boldsymbol{x})}\right].$$

Using Jensen's inequality we further get:

$$\sqrt{\frac{2}{\lambda}}\mathbb{E}_{\boldsymbol{x} \sim \mathbf{P}(\boldsymbol{x})}\left[\sqrt{\mathbf{P}(z_{\mathrm{pa}(v)} = 1|\boldsymbol{x})\mathrm{reg}_{\ell_c}(f_v \,|\, \boldsymbol{x})}\right] \leq \sqrt{\frac{2}{\lambda}\mathbb{E}_{\boldsymbol{x} \sim \mathbf{P}(\boldsymbol{x})}\left[\mathbf{P}(z_{\mathrm{pa}(v)} = 1|\boldsymbol{x})\mathrm{reg}_{\ell_c}(f_v \,|\, \boldsymbol{x})\right]}$$

The next step is similarly to the proof of Lemma 1. We use first the definition of expectation, then Bayes' theorem, and finally we rearrange the terms:

$$\sqrt{\frac{2}{\lambda}\mathbb{E}_{\boldsymbol{x} \sim \mathbf{P}(\boldsymbol{x})}\left[\mathbf{P}(z_{\mathrm{pa}(v)} = 1|\boldsymbol{x})\mathrm{reg}_{\ell_c}(f_v \,|\, \boldsymbol{x})\right]} = \sqrt{\frac{2}{\lambda}\int \mathbf{P}(\boldsymbol{x})\mathbf{P}(z_{\mathrm{pa}(v)} = 1|\boldsymbol{x})\mathrm{reg}_{\ell_c}(f_v \,|\, \boldsymbol{x})d\boldsymbol{x}}$$

$$= \sqrt{\frac{2}{\lambda}\int \mathbf{P}(z_{\mathrm{pa}(v)} = 1)\mathbf{P}(\boldsymbol{x}|z_{\mathrm{pa}(v)} = 1)\mathrm{reg}_{\ell_c}(f_v \,|\, \boldsymbol{x})d\boldsymbol{x}}$$

$$= \sqrt{\frac{2}{\lambda}\mathbf{P}(z_{\mathrm{pa}(v)} = 1)\int \mathbf{P}(\boldsymbol{x}|z_{\mathrm{pa}(v)} = 1)\mathrm{reg}_{\ell_c}(f_v \,|\, \boldsymbol{x})d\boldsymbol{x}}.$$

Notice that:

$$\int \mathbf{P}(\boldsymbol{x}|z_{\mathrm{pa}(v)} = 1)\mathrm{reg}_{\ell}(f_v \,|\, \boldsymbol{x})d\boldsymbol{x} = \mathbb{E}_{\boldsymbol{x} \sim \mathbf{P}(\boldsymbol{x}|z_{\mathrm{pa}(v)=1})}\left[\mathrm{reg}_{\ell_c}(f_v \,|\, \boldsymbol{x})\right]$$

This is the expected regret of f_v taken over $\mathbf{P}(\boldsymbol{x}, z_v \,|\, z_{\mathrm{pa}(v)} = 1)$, denoted by $\mathrm{reg}_{\ell_c}(f_v)$. We thus obtain the following by taking the expectation of (31):

$$\mathbf{P}(z_{\mathrm{pa}(v)} = 1)\mathbb{E}_{\boldsymbol{x} \sim \mathbf{P}(\boldsymbol{x}|z_{\mathrm{pa}(v)=1})}\left[|\eta(\boldsymbol{x}, v') - \hat{\eta}(\boldsymbol{x}, v')|\right] \leq \sqrt{\frac{2}{\lambda}}\sqrt{\mathbf{P}(z_{\mathrm{pa}(v)} = 1)\mathrm{reg}_{\ell_c}(f_v)}$$

By using the above in Eq. (15) from Theorem 2, we obtain the final result. $\qquad\square$

D   Proofs of the results from Section 4.3

This appendix contains proofs of Theorems 4 and 5 which state the regret bounds of PLTs for generalized performance metrics. We start with presenting two other results being the building blocks of the main proofs. Both are based on [Kotłowski and Dembczyński, 2017]. The first one states that the regret for a cost-sensitive binary classification can be upperbounded by L_1 estimation error of the conditional probabilities by using a proper threshold that corresponds to the misclassification cost. The second one shows that the regret of the generic function $\Psi(\mathrm{FP}, \mathrm{FN})$ can be upperbounded by the regret of the cost-sensitive binary classification with costs being a function of the optimal value of $\Psi(\mathrm{FP}, \mathrm{FN})$.

Given a real number $\alpha \in [0, 1]$, let us first define an α-cost-sensitive loss function for a single binary label y, $\ell_\alpha : \{0, 1\} \times \{0, 1\} \to [0, 2]$, as:

$$\ell_\alpha(y, \hat{y}) = 2\alpha[\![y = 0]\!][\![\hat{y} = 1]\!] + 2(1 - \alpha)[\![y = 1]\!][\![\hat{y} = 0]\!]$$

The cost-sensitive loss assigns different costs of misclassification depending on whether the label is relevant ($y = 1$) or not ($y = -1$). The multiplier of 2 makes $\ell_{0.5}(y, \hat{y})$ to be the typical binary 0/1 loss. Given classifier h, the α-cost-sensitive risk of h is:

$$R_\alpha(h) = \mathbb{E}_{(y,\boldsymbol{x}) \sim \mathbf{P}(y,\boldsymbol{x})}[\ell_\alpha(y, \hat{y})] = 2\alpha\mathrm{FP}(h) + 2(1 - \alpha)\mathrm{FN}(h) \tag{32}$$

The α-cost-sensitive regret of h is then:

$$\mathrm{reg}_\alpha(h) = R_\alpha(h) - R_\alpha(h_\alpha^*), \tag{33}$$

where $h_\alpha^* = \arg\min_h R_\alpha(h)$.

Proposition 5. *For any distribution* $\mathbf{P}$ *over* $(y, \boldsymbol{x}) \in \{0, 1\} \times \mathcal{X}$, *with* $\eta(\boldsymbol{x}) = \mathbf{P}(y = 1 \,|\, \boldsymbol{x})$, *any* $\alpha \in [0, 1]$, *and classifier* h, *such that* $h(\boldsymbol{x}) = [\![\hat{\eta}(\boldsymbol{x}) > \alpha]\!]$ *with* $\hat{\eta}(\boldsymbol{x}) \in [0, 1]$, *the following holds:*

$$\mathrm{reg}_\alpha(h) \leq 2\mathbb{E}_{\boldsymbol{x} \sim \mathbf{P}(\boldsymbol{x})}[|\eta(\boldsymbol{x}) - \hat{\eta}(\boldsymbol{x})|]$$

Proof. The proof is a part of the derivation of the bound from Proposition 2 in Kotłowski and Dembczyński [2017]. Given $\eta \in [0, 1]$ and $h \in [0, 1]$, the conditional α-cost-sensitive risk is:

$$R_\alpha(h \,|\, \boldsymbol{x}) = \mathbb{E}_{y \sim \mathbf{P}(y \,|\, \boldsymbol{x})}[\ell_\alpha(y, h)] = 2\alpha(1 - \eta)[\![h = 1]\!] + 2(1 - \alpha)\eta[\![h = 0]\!].$$

Let $h_\alpha^* \in \arg\min_h \mathrm{risk}_\alpha(\eta, h)$. It is easy to check that one of possible solutions is

$$h_\alpha^* = [\![\eta > \alpha]\!]. \tag{34}$$

The α-conditional cost-sensitive regret is

$$\mathrm{reg}_\alpha(h \,|\, \boldsymbol{x}) = R_\alpha(h \,|\, \boldsymbol{x}) - R_\alpha(h_\alpha^* \,|\, \boldsymbol{x}).$$

If $h = h_\alpha^*$, then $\mathrm{reg}_\alpha(\eta, h) = 0$, otherwise, $\mathrm{reg}_\alpha(\eta, h) = 2|\eta - \alpha|$, so

$$\mathrm{reg}_\alpha(h \,|\, \boldsymbol{x}) = 2[\![h \neq h_\alpha^*]\!]|\eta - \alpha|.$$

In the statement of the theorem, we assume $h(\boldsymbol{x}) = [\![\hat{\eta}(\boldsymbol{x}) > \alpha]\!]$, for some $\hat{\eta}(\boldsymbol{x}) \in [0,1]$, that is, $h(\boldsymbol{x})$ has the same form as $h^*_\alpha(\boldsymbol{x})$ in (34). For such $h(\boldsymbol{x})$ we have:

$$\mathrm{reg}_\alpha(h \,|\, \boldsymbol{x}) \leq 2|\eta - \hat{\eta}|\,.$$

This statement trivially holds when $h = h^*_\alpha$. If $h \neq h^*_\alpha$, then η and $\hat{\eta}$ are on the opposite sides of α, hence $|\eta - \alpha| \leq |\eta - \hat{\eta}|$.

The unconditional statement is obtained by taking the expectation with respect to $\boldsymbol{x}$ of both sides of the above equation:

$$\mathrm{reg}_\alpha(h) = \mathbb{E}_{\boldsymbol{x} \sim \mathbf{P}(\boldsymbol{x})}[\mathrm{reg}_\alpha(h \,|\, \boldsymbol{x})] \leq 2\mathbb{E}_{\boldsymbol{x} \sim \mathbf{P}(\boldsymbol{x})}[|\eta(\boldsymbol{x}) - \hat{\eta}(\boldsymbol{x})|]\,.$$

$\square$

The second result is a modified version of Proposition 1 from [Kotłowski and Dembczyński, 2017], which in turn generalizes Proposition 6 in [Puthiya Parambath et al., 2014].

Proposition 6. *Let Ψ be a linear-factorial function as defined in (19) with the denominator bounded away from 0 by γ as in (20). Take any real values* FP, FN *and* FP*, FN* *in the domain of Ψ such that:*

$$\Psi(\mathrm{FP}^*, \mathrm{FN}^*) - \Psi(\mathrm{FP}, \mathrm{FN}) \geq 0\,.$$

Then, we obtain:

$$\Psi(\mathrm{FP}^*, \mathrm{FN}^*) - \Psi(\mathrm{FP}, \mathrm{FN}) \leq C(\alpha^*_\Psi(\mathrm{FP} - \mathrm{FP}^*) + (1 - \alpha^*_\Psi)(\mathrm{FN} - \mathrm{FN}^*))$$

where:

$$\alpha^*_\Psi = \frac{\Psi(\mathrm{FP}^*, \mathrm{FN}^*)b_1 - a_1}{\Psi(\mathrm{FP}^*, \mathrm{FN}^*)(b_1 + b_2) - (a_1 + a_2)}\,,$$

and

$$C = \frac{1}{\gamma}\left(\Psi(\mathrm{FP}^*, \mathrm{FN}^*)(b_1 + b_2) - (a_1 + a_2)\right) > 0\,.$$

Proof. For the sake of clarity, we use a shorthand notation $\Psi^* = \Psi(\mathrm{FP}^*, \mathrm{FN}^*)$, $\Psi = \Psi(\mathrm{FP}, \mathrm{FN})$, $A = a_0 + a_1\mathrm{FP} + a_2\mathrm{FN}$, $B = b_0 + b_1\mathrm{FP} + b_2\mathrm{FN}$, for the numerator and denominator of Ψ, and analogously A^* and B^* for Ψ^*. With this notation, we have:

$$\begin{aligned}
\Psi^* - \Psi &= \frac{\Psi^* B - A}{B} = \frac{\Psi^* B - A - \overbrace{(\Psi^* B^* - A^*)}^{=0}}{B} \\
&= \frac{\Psi^*(B - B^*) - (A - A^*)}{B} \\
&= \frac{(\Psi^* b_1 - a_1)(\mathrm{FP} - \mathrm{FP}^*) + (\Psi^* b_2 - a_2)(\mathrm{FN} - \mathrm{FN}^*)}{B} \\
&\leq \frac{(\Psi^* b_1 - a_1)(\mathrm{FP} - \mathrm{FP}^*) + (\Psi^* b_2 - a_2)(\mathrm{FN} - \mathrm{FN}^*)}{\gamma}\,,
\end{aligned} \tag{35}$$

where the last inequality follows from the assumptions that $B \geq \gamma$ and $\Psi^* - \Psi \geq 0$. Since Ψ is non-increasing in FP and FN, we have:

$$\frac{\partial \Psi^*}{\partial \mathrm{FP}^*} = \frac{a_1 B^* - b_1 A^*}{(B^*)^2} = \frac{a_1 - b_1 \Psi^*}{B^*} \leq 0$$

56

and similarly $\frac{\partial \Psi^*}{\partial FN^*} = \frac{a_2 - b_2 \Psi^*}{B^*} \leq 0$. This and the assumption $B^* \geq \gamma$ implies that both $\Psi b_1 - a_1$ and $\Psi^* b_2 - a_2$ are non-negative. If we normalize them by defining:

$$\alpha_\Psi^* = \frac{\Psi^* b_1 - a_1}{\Psi^*(b_1 + b_2) - (a_1 + a_2)},$$

we obtain then from (35):

$$\Psi^* - \Psi \leq C(\alpha_\Psi^*(FP - FP^*) + (1 - \alpha_\Psi^*)(FN - FN^*))$$

with C being $\frac{1}{\gamma}(\Psi^*(b_1 + b_2) - (a_1 + a_2))$. $\qquad \square$

With the above results we can prove the main theorems of Section 4.3.

Theorem 4. *Let $\tau_j^* = \arg\max_\tau \Psi(h_{j,\tau})$, for each $j \in \mathcal{L}$, and $\boldsymbol{\tau}^* = (\tau_1^*, \tau_2^*, \ldots, \tau_m^*)$. For any tree T and distribution $\mathbf{P}(\boldsymbol{x}, \boldsymbol{y})$, the classifier $\boldsymbol{h}_{\boldsymbol{\tau}^*}$ achieves the following upper bound on its Ψ_{macro}-regret:*

$$\mathrm{reg}_{\Psi_{\mathrm{macro}}}(\boldsymbol{h}_{\boldsymbol{\tau}^*}) \leq \frac{\sqrt{2}}{m\sqrt{\lambda}} \sum_{v \in V} \sqrt{\mathbf{P}(z_{\mathrm{pa}(v)} = 1)\mathrm{reg}_{\ell_c}(f_v)} \sum_{j \in L_v} C_j,$$

where $C_j = \frac{1}{\gamma}(\Psi(h_\Psi^*, j)(b_1 + b_2) - (a_1 + a_2))$, for each $j \in \mathcal{L}$, with γ defined in (20), $\mathbf{P}(z_{\mathrm{pa}(r_T)} = 1) = 1$ for the root node, and $\mathrm{reg}_{\ell_c}(f_v)$ is the expected ℓ_c-regret of f_v taken over $\mathbf{P}(\boldsymbol{x}, z_v \,|\, z_{\mathrm{pa}(v)} = 1)$.

Proof. From the definitions of the macro-average performance measure (21) and the regret of Ψ_{macro} (24), as well as from Proposition 6 we have for any $\boldsymbol{h}(\boldsymbol{x}) = (h_1(\boldsymbol{x}), h_2(\boldsymbol{x}), \ldots, h_m(\boldsymbol{x}))$ that:

$$\mathrm{reg}_{\Psi_{\mathrm{macro}}}(\boldsymbol{h}) \leq \frac{1}{m} \sum_{j=1}^m C_j(\alpha_\Psi^*(FP_j - FP_j^*) + (1 - \alpha_\Psi^*)(FN_j - FN_j^*)),$$

with FP_j and FN_j being the false positives and false negatives of h_j. It can be easily notice $(\alpha_\Psi^*(FP_j - FP_j^*) + (1 - \alpha_\Psi^*)(FN_j - FN_j^*))$ is half of the α_Ψ^*-regret (33) for label j. Therefore, we can write:

$$\mathrm{reg}_{\Psi_{\mathrm{macro}}}(\boldsymbol{h}) \leq \frac{1}{2m} \sum_{j=1}^m C_j \mathrm{reg}_{\alpha_\Psi^*}(h_j).$$

If we now take $h_j = h_{j, \alpha_{\Psi,j}^*}$, then by using Proposition 5 and the bound (17) from Theorem 3 we obtain:

$$\begin{aligned}
\mathrm{reg}_{\Psi_{\mathrm{macro}}}(\boldsymbol{h}_{\boldsymbol{\alpha}_\Psi^*}) &\leq \frac{1}{m} \sum_{j=1}^m C_j \mathbb{E}_{\boldsymbol{x} \sim \mathbf{P}(\boldsymbol{x})}[|\eta(\boldsymbol{x}) - \hat{\eta}(\boldsymbol{x})|] \\
&\leq \frac{\sqrt{2}}{m\sqrt{\lambda}} \sum_{v \in V} \sqrt{\mathbf{P}(z_{\mathrm{pa}(v)} = 1)\mathrm{reg}_{\ell_c}(f_v)} \sum_{j \in L_v} C_j.
\end{aligned}$$

Finally, since

$$\boldsymbol{\tau}^* = \arg\max_{\boldsymbol{\tau}} \Psi_{\mathrm{macro}}(\boldsymbol{h}_{\boldsymbol{\tau}}) = \arg\min_{\boldsymbol{\tau}} \mathrm{reg}_{\Psi_{\mathrm{macro}}}(\boldsymbol{h}_{\boldsymbol{\tau}}),$$

we have that $\mathrm{reg}_{\Psi_{\mathrm{macro}}}(\boldsymbol{h}_{\boldsymbol{\tau}^*}) \leq \mathrm{reg}_{\Psi_{\mathrm{macro}}}(\boldsymbol{h}_{\boldsymbol{\alpha}_\Psi^*})$. $\qquad \square$

Theorem 5. *Let $\boldsymbol{h}_\tau = (h_{1,\tau}, h_{2,\tau}, \ldots, h_{m,\tau})$ be a classifier which shares the same threshold τ over all labels $j \in \mathcal{L}$. For any tree T, distribution $\mathbf{P}(\boldsymbol{x}, \boldsymbol{y})$, and $\tau^* = \arg\max_\tau \Psi_{\mathrm{micro}}(\boldsymbol{h}_\tau)$, classifier $\boldsymbol{h}_{\tau^*}$ achieves the following upper bound on its Ψ_{micro}-regret:*

$$\mathrm{reg}_{\Psi_{micro}}(\boldsymbol{h}_{\tau^*}) \leq \frac{C}{m}\sqrt{\frac{2}{\lambda}} \sum_{v \in V} |L_v| \sqrt{\mathbf{P}(z_{\mathrm{pa}(v)} = 1)\mathrm{reg}_{\ell_c}(f_v)},$$

where $C = \frac{1}{\gamma}(\Psi_{\mathrm{micro}}(\boldsymbol{h}_\Psi^*)(b_1 + b_2) - (a_1 + a_2))$ with γ defined in (20), $\mathbf{P}(z_{\mathrm{pa}(r_T)} = 1) = 1$ for the root node, and $\mathrm{reg}_{\ell_c}(f_v)$ is the expected ℓ_c-regret of f_v taken over $\mathbf{P}(\boldsymbol{x}, z_v \mid z_{\mathrm{pa}(v)} = 1)$.

Proof. Using Proposition 6, which applies to any real values FP, FN, FP*, FN*, and from definitions of the micro-averaged performance measure (22) and the regret of Ψ_{micro} (25), we can write for any $\boldsymbol{h}(\boldsymbol{x}) = (h_1(\boldsymbol{x}), h_2(\boldsymbol{x}), \ldots, h_m(\boldsymbol{x}))$ that:

$$\begin{aligned}
\mathrm{reg}_{\Psi_{micro}}(\boldsymbol{h}) &= \Psi(\bar{\mathrm{FP}}(\boldsymbol{h}_{\alpha_\Psi^*}^*), \bar{\mathrm{FN}}(\boldsymbol{h}_{\alpha_\Psi^*}^*)) - \Psi(\bar{\mathrm{FP}}(\boldsymbol{h}), \bar{\mathrm{FN}}(\boldsymbol{h})) \\
&\leq C\big(\alpha_\Psi^*(\bar{\mathrm{FP}}(\boldsymbol{h}) - \bar{\mathrm{FP}}(\boldsymbol{h}_{\alpha_\Psi^*}^*)) + (1 - \alpha_\Psi^*)(\bar{\mathrm{FN}}(\boldsymbol{h}) - \bar{\mathrm{FN}}(\boldsymbol{h}_{\alpha_\Psi^*}^*))\big) \\
&= \frac{C}{m} \sum_{j=1}^m \alpha_\Psi^*(\mathrm{FP}_j(h_j) - \mathrm{FP}_j(\boldsymbol{h}_{\alpha_\Psi^*}^*)) + (1 - \alpha_\Psi^*)(\mathrm{FN}_j(h_j) - \bar{\mathrm{FN}}_j(\boldsymbol{h}_{\alpha_\Psi^*}^*)).
\end{aligned}$$

Further from α-cost-sensitive risk (32) and regret (33), we have:

$$\begin{aligned}
\mathrm{reg}_{\Psi_{micro}}(\boldsymbol{h}) &\leq \frac{C}{2m} \sum_{j=1}^m \Big(R_\alpha(h_j) - R_\alpha(\boldsymbol{h}_{\alpha_\Psi^*}^*)\Big) \\
&= \frac{C}{2m} \sum_{j=1}^m \mathrm{reg}_\alpha(h_j).
\end{aligned}$$

If we now take $h_j = h_{j,\alpha_\Psi^*}$, for all $j \in \mathcal{L}$, then by using Proposition 5 we obtain:

$$\mathrm{reg}_{\Psi_{micro}}(\boldsymbol{h}_{\alpha_\Psi^*}) \leq \frac{C}{m} \sum_{j=1}^m \mathbb{E}_{\boldsymbol{x}}[|\eta(\boldsymbol{x}) - \hat{\eta}(\boldsymbol{x})|].$$

By using the bound (18) from Theorem 3 we have:

$$\mathrm{reg}_{\Psi_{micro}}(\boldsymbol{h}) \leq \frac{C}{m}\sqrt{\frac{2}{\lambda}} \sum_{v \in V} |L_v| \sqrt{\mathbf{P}(z_{\mathrm{pa}(v)} = 1)\mathrm{reg}_{\ell_c}(f_v)}.$$

The theorem now follows from noticing that

$$\tau^* = \arg\max_\tau \Psi_{\mathrm{micro}}(\boldsymbol{h}_\tau) = \arg\min_\tau \mathrm{reg}_{\Psi_{micro}}(\boldsymbol{h}_\tau),$$

we have that $\mathrm{reg}_{\Psi_{micro}}(\boldsymbol{h}_{\tau^*}) \leq \mathrm{reg}_{\Psi_{micro}}(\boldsymbol{h}_{\alpha_\Psi^*})$. $\qquad\square$

E   Proof of the result from Section 4.5

This appendix shows the full proof of Proposition 4.

Proposition 4. *Given conditionally independent labels, $\boldsymbol{h}_{@k} \in \mathcal{H}_{@k}^m$ predicting k labels with highest $\eta_j'(\boldsymbol{x})$, $j \in \mathcal{L}$, defined in (27), has zero regret in terms of the precision@k loss.*

Proof. To proof the proposition it suffices to show that for conditionally independent labels the order of labels induced by the marginal probabilities $\eta_j(\boldsymbol{x})$ is the same as the order induced by the values of $\eta_j'(\boldsymbol{x})$ obtained by the pick-one-label heuristic (27):

$$\eta_j'(\boldsymbol{x}) = \mathbf{P}'(y_j = 1 \,|\, \boldsymbol{x}) = \sum_{\boldsymbol{y} \in \mathcal{Y}} \frac{y_j}{\sum_{j'=1}^m y_{j'}} \mathbf{P}(\boldsymbol{y} \,|\, \boldsymbol{x}).$$

In other words, for any two labels $i, j \in \{1, \ldots, m\}$, $i \neq j$, $\eta_i(\boldsymbol{x}) \geq \eta_j(\boldsymbol{x}) \Leftrightarrow \eta_i'(\boldsymbol{x}) \geq \eta_j'(\boldsymbol{x})$.

Let $\eta_i(\boldsymbol{x}) \geq \eta_j(\boldsymbol{x})$. The summation over all $\boldsymbol{y}$ in (27) can be written in the following way:

$$\eta_j'(\boldsymbol{x}) = \sum_{\boldsymbol{y} \in \mathcal{Y}} y_j N(\boldsymbol{y}) \mathbf{P}(\boldsymbol{y}|\boldsymbol{x}) ,$$

where $N(\boldsymbol{y}) = (\sum_{i=1}^m y_i)^{-1}$ is a value that depends only on the number of positive labels in $\boldsymbol{y}$. In this summation we consider four subsets of $\mathcal{Y}$, creating a partition of this set:

$$\mathcal{S}_{i,j}^{u,w} = \{\boldsymbol{y} \in \mathcal{Y} : y_i = u \wedge y_j = w\}, \quad u, w \in \{0, 1\}.$$

The subset $\mathcal{S}_{i,j}^{0,0}$ does not play any role because $y_i = y_j = 0$ and therefore do not contribute to the final sum. Then (27) can be written in the following way for the i-th and j-th label:

$$\eta_i'(\boldsymbol{x}) \quad = \quad \sum_{\boldsymbol{y}:\mathcal{S}_{i,j}^{1,0}} N(\boldsymbol{y})\mathbf{P}(\boldsymbol{y}|\boldsymbol{x}) + \sum_{\boldsymbol{y} \in \mathcal{S}_{i,j}^{1,1}} N(\boldsymbol{y})\mathbf{P}(\boldsymbol{y}|\boldsymbol{x}) \tag{36}$$

$$\eta_j'(\boldsymbol{x}) \quad = \quad \sum_{\boldsymbol{y}:\mathcal{S}_{i,j}^{0,1}} N(\boldsymbol{y})\mathbf{P}(\boldsymbol{y}|\boldsymbol{x}) + \sum_{\boldsymbol{y} \in \mathcal{S}_{i,j}^{1,1}} N(\boldsymbol{y})\mathbf{P}(\boldsymbol{y}|\boldsymbol{x}) \tag{37}$$

The contribution of elements from $\mathcal{S}_{i,j}^{1,1}$ is equal for both $\eta_i'(\boldsymbol{x})$ and $\eta_j'(\boldsymbol{x})$. It is so because the value of $N(\boldsymbol{y})\mathbf{P}(\boldsymbol{y}|\boldsymbol{x})$ is the same for all $\boldsymbol{y} \in \mathcal{S}_{i,j}^{1,1}$: the conditional joint probabilities $\mathbf{P}(\boldsymbol{y}|\boldsymbol{x})$ are fixed and they are multiplied by the same factors $N(\boldsymbol{y})$.

Consider now the contributions of $\mathcal{S}_{i,j}^{1,0}$ and $\mathcal{S}_{i,j}^{0,1}$ to the relevant sums. By the definition of $\mathcal{Y}$, $\mathcal{S}_{i,j}^{1,0}$, and $\mathcal{S}_{i,j}^{0,1}$, there exists bijection $b_{i,j} : \mathcal{S}_{i,j}^{1,0} \to \mathcal{S}_{i,j}^{0,1}$, such that for each $\boldsymbol{y}' \in \mathcal{S}_{i,j}^{1,0}$ there exists $\boldsymbol{y}'' \in \mathcal{S}_{i,j}^{0,1}$ equal to $\boldsymbol{y}'$ except on the i-th and the j-th position.

Notice that because of the conditional independence assumption the joint probabilities of elements in $\mathcal{S}_{i,j}^{1,0}$ and $\mathcal{S}_{i,j}^{0,1}$ are related to each other. Let $\boldsymbol{y}'' = b_{i,j}(\boldsymbol{y}')$, where $\boldsymbol{y}' \in \mathcal{S}_{i,j}^{1,0}$ and $\boldsymbol{y}'' \in \mathcal{S}_{i,j}^{0,1}$. The joint probabilities are:

$$\mathbf{P}(\boldsymbol{y}'|\boldsymbol{x}) = \eta_i(\boldsymbol{x})(1 - \eta_j(\boldsymbol{x})) \prod_{l \in \mathcal{L}\backslash\{i,j\}} \eta_l(\boldsymbol{x})^{y_l}(1 - \eta_l(\boldsymbol{x}))^{1-y_l}$$

and

$$\mathbf{P}(\boldsymbol{y}''|\boldsymbol{x}) = (1 - \eta_i(\boldsymbol{x}))\eta_j(\boldsymbol{x}) \prod_{l \in \mathcal{L} \setminus \{i,j\}} \eta_l(\boldsymbol{x})^{y_l}(1 - \eta_l(\boldsymbol{x}))^{1-y_l}.$$

One can easily notice the relation between these probabilities:

$$\mathbf{P}(\boldsymbol{y}'|\boldsymbol{x}) = \eta_i(\boldsymbol{x})(1 - \eta_j(\boldsymbol{x}))q_{i,j} \quad \text{and} \quad \mathbf{P}(\boldsymbol{y}''|\boldsymbol{x}) = (1 - \eta_i(\boldsymbol{x}))\eta_j(\boldsymbol{x})q_{i,j},$$

where $q_{i,j} = \prod_{l \in \mathcal{L} \setminus \{i,j\}} \eta_l(\boldsymbol{x})^{y_l}(1 - \eta_l(\boldsymbol{x}))^{1-y_l} \geq 0$. Consider now the difference of these two probabilities:

$$\begin{aligned}
\mathbf{P}(\boldsymbol{y}'|\boldsymbol{x}) - \mathbf{P}(\boldsymbol{y}''|\boldsymbol{x}) &= \eta_i(\boldsymbol{x})(1 - \eta_j(\boldsymbol{x}))q_{i,j} - (1 - \eta_i(\boldsymbol{x}))\eta_j(\boldsymbol{x})q_{i,j} \\
&= q_{i,j}(\eta_i(\boldsymbol{x})(1 - \eta_j(\boldsymbol{x})) - (1 - \eta_i(\boldsymbol{x}))\eta_j(\boldsymbol{x})) \\
&= q_{i,j}(\eta_i(\boldsymbol{x}) - \eta_j(\boldsymbol{x})).
\end{aligned}$$

From the above we see that $\eta_i(\boldsymbol{x}) \geq \eta_j(\boldsymbol{x}) \Rightarrow \mathbf{P}(\boldsymbol{y}'|\boldsymbol{x}) \geq \mathbf{P}(\boldsymbol{y}''|\boldsymbol{x})$. Due to the properties of the bijection $b_{i,j}$, the number of positive labels in $\boldsymbol{y}'$ and $\boldsymbol{y}''$ is the same and $N(\boldsymbol{y}') = N(\boldsymbol{y}'')$, therefore we also get $\eta_i(\boldsymbol{x}) \geq \eta_j(\boldsymbol{x}) \Rightarrow \sum_{\boldsymbol{y}:\mathcal{S}_{i,j}^{1,0}} N(\boldsymbol{y})\mathbf{P}(\boldsymbol{y}|\boldsymbol{x}) \geq \sum_{\boldsymbol{y}:\mathcal{S}_{i,j}^{0,1}} N(\boldsymbol{y})\mathbf{P}(\boldsymbol{y}|\boldsymbol{x})$, which by (36) and (37) gives us finally $\eta_i(\boldsymbol{x}) \geq \eta_j(\boldsymbol{x}) \Rightarrow \eta_i'(\boldsymbol{x}) \geq \eta_j'(\boldsymbol{x})$.

The implication in the other direction, that is, $\eta_i(\boldsymbol{x}) \geq \eta_j(\boldsymbol{x}) \Leftarrow \mathbf{P}(\boldsymbol{y}'|\boldsymbol{x}) \geq \mathbf{P}(\boldsymbol{y}''|\boldsymbol{x})$ holds obviously for $q_{i,j} > 0$. For $q_{i,j} = 0$, we can notice, however, that $\mathbf{P}(\boldsymbol{y}'|\boldsymbol{x})$ and $\mathbf{P}(\boldsymbol{y}''|\boldsymbol{x})$ do not contribute to the appropriate sums as they are zero, and therefore we can follow a similar reasoning as above, concluding that $\eta_i(\boldsymbol{x}) \geq \eta_j(\boldsymbol{x}) \Leftarrow \eta_i'(\boldsymbol{x}) \geq \eta_j'(\boldsymbol{x})$.

Thus for conditionally independent labels, the order of labels induced by marginal probabilities $\eta_j(\boldsymbol{x})$ is equal to the order induced by $\eta_j'(\boldsymbol{x})$. As the precision@k is optimized by k labels with the highest marginal probabilities, we have that prediction consisted of k labels with highest $\eta_j'(\boldsymbol{x})$ has zero regret for precision@k. □

F The proof of the result from Section 5

Theorem 8 concerns two properties, the properness and the efficency, of an OPLT algorithm. We first prove that the OPLT algorithm satisfies each of the properties in two separate lemmas. The final proof of the theorem is then straight-forward.

Lemma 4. OPLT *is a proper* OPLT *algorithm.*

Proof. We need to show that for any $\mathcal{S}$ and t the two of the following hold. Firstly, that the set L_{T_t} of leaves of tree T_t built by OPLT correspond to $\mathcal{L}_t$, the set of all labels observed in S_t. Secondly, that the set H_t of classifiers trained by OPLT is exactly the same as $H = \text{IPLT.TRAIN}(T_t, A_{\text{online}}, \mathcal{S}_t)$, that is, the set of node classifiers trained incrementally by Algorithm 5 on $\mathcal{D} = \mathcal{S}_t$ and tree T_t given as input parameter. We will prove it by induction with the base case for $\mathcal{S}_0$ and the induction step for $\mathcal{S}_t$, $t \geq 1$, with the assumption that the statement holds for $\mathcal{S}_{t-1}$.

For the base case of $\mathcal{S}_0$, tree T_0 is initialized with the root node r_T with no label assigned and set H_0 of node classifiers with a single classifier assigned to the root. As there are no observations, this classifier receives no updates. Now, notice that IPLT.TRAIN, run on T_0 and $\mathcal{S}_0$, returns the same set of classifiers H that contains solely the initialized root node classifier without any updates

(assuming that initialization procedure is always the same). There are no labels in any sequence of 0 observations and also T_0 has no label assigned.

The induction step is more involved as we need to take into account the internal loop which extends the tree with new labels. Let us consider two cases. In the first one, observation $(\boldsymbol{x}_t, \mathcal{L}_{\boldsymbol{x}_t})$ does not contain any new label. This means that that the tree T_{t-1} will not change, that is, $T_{t-1} = T_t$. Moreover, node classifiers from H_{t-1} will get the same updates for $(\boldsymbol{x}_t, \mathcal{L}_{\boldsymbol{x}_t})$ as classifiers in IPLT.TRAIN, therefore $H_t = \text{IPLT.TRAIN}(T_t, A_{\text{online}}, \mathcal{S}_t)$. It also holds that $l_j \in L_{T_t}$ iff $j \in \mathcal{L}_t$, since $\mathcal{L}_{t-1} = \mathcal{L}_t$. In the second case, observation $(\boldsymbol{x}_t, \mathcal{L}_{\boldsymbol{x}_t})$ has $m' = |\mathcal{L}_{\boldsymbol{x}_t} \setminus \mathcal{L}_{t-1}|$ new labels. Let us make the following assumption for the UPDATETREE procedure, which we later prove that it indeed holds. Namely, we assume that the set $H_{t'}$ of classifiers after calling the UPDATETREE procedure is the same as the one being returned by IPLT.TRAIN$(T_t, A_{\text{online}}, \mathcal{S}_{t-1})$, where T_t is the extended tree. Moreover, leaves of T_t correspond to all observed labels seen so far. If this is the case, the rest of the induction step is the same as in the first case. All updates to classifiers in $H_{t'}$ for $(\boldsymbol{x}_t, \mathcal{L}_{\boldsymbol{x}_t})$ are the same as in IPLT.TRAIN. Therefore $H_t = \text{IPLT.TRAIN}(T_t, A_{\text{online}}, \mathcal{S}_t)$.

Now, we need to show that the assumption for the UPDATETREE procedure holds. To this end, we also use induction, this time on the number m' of new labels. For the base case, we take $m' = 1$. The induction step is proved for $m' > 1$ with the assumption that the statement holds for $m' - 1$.

For $m' = 1$ we need consider two scenarios. In the first scenario, the new label is the first label in the sequence. This label will be then assigned to the root node r_T. So, the structure of the tree does not change, that is, $T_{t-1} = T_t$. Furthermore, the set of classifiers also does not change, since the root classifier has already been initialized. It might be negatively updated by previous observations. Therefore, we have $H_{t'} = \text{IPLT.TRAIN}(T_t, A_{\text{online}}, \mathcal{S}_{t-1})$. Furthermore, all observed labels are appropriately assigned to the leaves of T_t. In the second scenario, set $\mathcal{L}_{t-1}$ is not empty. We need to consider in this scenario the three variants of tree extension illustrated in Figure 3.

In the first variant, tree T_{t-1} is extended by one leaf node only without any additional ones. ADDNODE creates a new leaf node v'' with the new label assigned to the tree. After this operation, the tree contains all labels from $\mathcal{S}_t$. The new leaf v'' is added as a child of the selected node v. This new node is initialized as $\hat{\eta}(v'') = \text{INVERSECLASSIFIER}(\hat{\theta}(v))$. Recall that INVERSECLASSIFIER creates a wrapper that inverts the behavior of the base classifier. It predicts $1 - \hat{\eta}$, where $\hat{\eta}$ is the prediction of the base classifier, and flips the updates, that is, positive updates become negative and negative updates become positive. From the definition of the auxiliary classifier, we know that $\hat{\theta}(v)$ has been trained on all positives updates of $\hat{\eta}(v)$. So, $\hat{\eta}(v'')$ is initialized with a state as if it was updated negatively each time $\hat{\eta}(v)$ was updated positively in sequence S_{t-1}. Notice that in S_{t-1} there is no observation labeled with the new label. Therefore $\hat{\eta}(v'')$ is the same as if it was created and updated using IPLT.TRAIN. There are no other operations on T_{t-1}, so we have that $H_{t'} = \text{IPLT.TRAIN}(T_t, A_{\text{online}}, \mathcal{S}_{t-1})$.

In the second variant, tree T_{t-1} is extended by internal node v' and leaf node v''. The internal node v' is added in INSERTNODE. It becomes a parent of all child nodes of the selected node v and the only child of this node. Thus, all leaves of the subtree of v do not change. Since v' is the root of this subtree, its classifier $\hat{\eta}(v')$ should be initialized as a copy of the auxiliary classifier $\hat{\theta}(v)$, which has accumulated all updates from and only from observations with labels assigned to the leaves of this subtree. The addition of the leaf node v'' can be analyzed as in the first variant. Since nothing else has changed in the tree and in the node classifiers, we have that $H_{t'} = \text{IPLT.TRAIN}(T_t, A_{\text{online}}, \mathcal{S}_{t-1})$. Moreover, the tree contains the new label, so the statement holds.

The third variant is similar to the second one. Tree T_{t-1} is extended by two leaf nodes v' and

v'' being children of the selected node v. Insertion of leaf v' is similar to the insertion of node v' in the second variant, with the difference that v does not have any children and its label has to be reassigned to v'. The new classifier in v' is initialized as a copy of the auxiliary classifier $\hat{\theta}(v)$, which contains all updates from and only from observations with the label assigned previously to v. Insertion of v'' is exactly the same as in the second variant. From the above, we conclude that $H_{t'} = \text{IPLT.TRAIN}(T_t, A_{\text{online}}, \mathcal{S}_{t-1})$ and that T_t contains all labels from T_{t-1} and the new label. In this way we prove the base case.

The induction step is similar to the second scenario of the base case. The only difference is that we do not extent tree T_{t-1}, but an intermediate tree with $m' - 1$ new labels already added. Because of the induction hypothesis, the rest of the analysis of the three variants of tree extension is exactly the same. This ends the proof that the assumption for the inner loop holds. At the same time, it finalizes the entire proof. □

Lemma 5. OPLT *is an efficient* OPLT *algorithm.*

Proof. The OPLT maintains one additional classifier per each node in comparison to IPLT. Hence, for a single observation there is at most one update more for each positive node. Furthermore, the time and space cost of the complete tree building policy is constant per a single label, if implemented with an array list. In this case, insertion of any new node can be made in amortized constant time, and the space required by the array list is linear in the number of nodes. Concluding the above, the time and space complexity of OPLT is in constant factor of C_t and C_s, the time and space complexity of IPLT respectively. This proves that OPLT is an efficient OPLT algorithm. □

Theorem 8. OPLT *is an proper and efficient* OPLT *algorithm.*

Proof. The theorem directly follows from Lemma 4 and Lemma 5. □

G   Synthetic data

All synthetic models use linear models parametrized by a weight vector $\boldsymbol{w}$ of size d. The values of the vector are sampled uniformly from a d-dimensional sphere of radius 1. Each observation $\boldsymbol{x}$ is a vector sampled from a d-dimensional disc of the same radius.

To create the multi-class data, we associate a weight vector $\boldsymbol{w}_j$ with each label $j \in \{1, \ldots, m\}$. This model assigns probabilities to labels at point $\boldsymbol{x}$ using softmax,

$$\eta_j(\boldsymbol{x}) = \frac{\exp(\boldsymbol{w}_j^\top \boldsymbol{x})}{\sum_{j'=1}^m \exp(\boldsymbol{w}_{j'}^\top \boldsymbol{x})},$$

and draws the positive label according to this probability distribution.

The multi-label data with conditionally independent labels are created similarly to the multi-class data. The difference lays is normalization as the marginal probabilities do not have to sum up to 1. To get a probability of the j-th label, we use the logistic transformation:

$$\eta_j(\boldsymbol{x}) = \frac{\exp(\boldsymbol{w}_j^\top \boldsymbol{x})}{1 + \exp(\boldsymbol{w}_j^\top \boldsymbol{x})}.$$

Then, we assign a label to an observation by:

$$y_j = [\![r < \eta_j(\boldsymbol{x})]\!],$$

where the random value r is sampled uniformly and independently from range $[0, 1]$, for each instance $\boldsymbol{x}$ and label $j \in \{1, \ldots, m\}$.

Generation of the multi-label data with conditionally dependent labels is more involved. We follow the mixing matrix model previously used to a similar purpose in [Dembczyński et al., 2012]. This model is based on m latent scoring functions generated by $\boldsymbol{W} = (\boldsymbol{w}_1, \ldots, \boldsymbol{w}_m)$. The $m \times m$ mixing matrix $\boldsymbol{M}$ introduces dependencies between noise $\boldsymbol{\epsilon}$, which stands for the source of randomness in the model. The models $\boldsymbol{w}_j$ are sampled from a sphere of radius 1, as in previous cases. The values in the mixing matrix $\boldsymbol{M}$ are sampled uniformly and independently from $[-1, 1]$. The random noise vector $\boldsymbol{\epsilon}$ is sampled from $N(0, 0.25)$. The label vector $\boldsymbol{y}$ is then obtained by element-wise evaluation of the following expression:

$$\boldsymbol{y} = [\![\boldsymbol{M}(\boldsymbol{W}^\top \boldsymbol{x} + \boldsymbol{\epsilon}) > 0]\!]$$

Notice that if $\boldsymbol{M}$ was an identity matrix the model would generate independent labels.

In the experiments, we used the following parameters of the synthetic models: $d = 3$, $n = 100000$ instances (with a $1:1$ split to training and test subsets), and $m = 32$ labels.

H   Hyperparamters

In Tables 16, 17, 18, and 19, we report values of hyperparameters used in all experiments. For the state-of-the-art algorithms, used in Section 7.5, we took values recommended in the original articles or default values from the provided implementations. For PLTs we tune the following parameters: c, η, *AdaGrad's* ϵ, λ_2, and *epochs*. The setting of the other parameters depends on a given experiment and is discussed in the main text. To replicate our experimental results we added corresponding scripts to the NAPKINXC repository.[14] Those scripts contain exact values of hyperparameters used.

hyperparameter	desription	values
t	number of trees	$\{50\}$
c	SVM weight co-efficient	$\{1.0\}$
l	number of label-probability pairs to retrain in a leaf	$\{100\}$
m	maximum allowed instances in a lead node	$\{10\}$
γ	γ parameter in tail label classifier (PFASTREXML only)	$\{30\}$
α	trade-off parameter between PFASTXML and tail classifier scores (PFASTREXML only)	$\{0.8\}$
A	parameter of the propensity model (PFASTREXML only)	$\{0.5, 0.55, 0.6\}$
B	parameter of the propensity model (PFASTREXML only)	$\{0.4, 1.5, 2.6\}$

Table 16: FASTXML and PFASTREXML hyperparamters.

---

[14]https://github.com/mwydmuch/napkinXC/experiments

hyperparameter	desription	values
λ_1	L1 regularization weight	$\{0.01, 0.1, 1\}$
c	cost of each sample	$\{1\}$
τ	degree of asynchronization	$\{0.1, 1, 10\}$
m	maximum number of iterations allowed	$\{30\}$

Table 17: PPDSPARSE hyperparamters.

hyperparameter	desription	values
c	LIBLINEAR cost co-efficient, inverse regularization	$\{1\}$
ϵ	LIBLINEAR tolerance of termination criterion	$\{0.01\}$
Δ	threshold value for pruning linear classifiers weights	$\{0.01\}$

Table 18: DISMEC hyperparamters.

hyperparameter	desription	values
ensemble	number of trees in ensemble	$\{1, 3\}$
k-means ϵ	tolerance of termination criterion of the k-means clustering used for the tree building procedure	$\{0.0001\}$
max leaves	maximum degree of pre-leaf nodes	$\{25, 100, 400\}$
c	LIBLINEAR cost co-efficient, inverse regularization strength (PARABEL, NXC only)	$\{1, 8, 12, 16, 32\}$
ϵ	LIBLINEAR tolerance of termination criterion (PARABEL, NXC only)	$\{0.1\}$
Δ	threshold value for pruning weights (PARABEL, NXC only)	$\{0.1, 0.2, 0.3, 0.5\}$
max iter	maximum iterations of LIBLINEAR (PARABEL only)	$\{20\}$
arity	arity of tree nodes, k for k-means clustering (XT, NXC only)	$\{2, 16, 64\}$
η	learning rate for SGD or Adagrad (XT, NXC only)	$\{0.02, 0.2, 0.5, 1\}$
epochs	number of passes over dataset when training with incremental algorithm (XT, NXC only)	$\{1, 3, 10\}$
AdaGrad's ϵ	determines initial learning rate (NXC only)	$\{0.01, 0.001\}$
λ_2	L2 regularization weight (XT only)	$\{0.001, 0.002, 0.003\}$
dim	size of hidden representation (XT only)	$\{500\}$

Table 19: Hyperparamters of different PLTs implementations: PARABEL, EXTREMETEXT (XT) and NAPKINXC PLT, OPLT and HSM (NXC).

I   Weight pruning

In all the experiments, we used a threshold of 0.1 for weight pruning. We present results for higher values of threshold and analyze their impact on the predictive and computational performance of PLTs. Table 20 reports results for logistic and squared hinge loss. We observe that for logistic loss

a more aggressive pruning can be beneficial. Precision@k decreases only slightly, while testing time can be reduced almost by two, and the model size even by 4. For squared hinge loss, precision@k drops more substantially, but the model size can be even reduced by a factor of 10. Let us also recall that weight pruning has also been investigated by Prabhu et al. [2018], with similar outcomes to those presented here.

	0.1	0.3	0.5	0.1	0.3	0.5
	$p@1$ [%]			$p@5$ [%]		
WikiLSHTC-325K	**61.96±0.03**	61.95±0.03	61.82±0.03	**30.19±0.02**	30.18±0.02	30.11±0.02
WikipediaLarge-500K	**66.20±0.05**	65.95±0.11	65.52±0.07	**36.83±0.01**	36.65±0.04	36.40±0.02
Amazon-670K	**43.54±0.01**	43.23±0.02	42.67±0.02	**35.15±0.03**	34.81±0.03	34.16±0.02
Amazon-3M	**46.09±0.02**	45.94±0.01	45.57±0.01	**40.98±0.01**	40.82±0.01	40.35±0.01
	T/N_{test} [ms]			M_{size} [GB]		
WikiLSHTC-325K	1.77±0.11	1.21±0.09	**1.02±0.04**	2.73±0.00	1.38±0.00	**0.89±0.00**
WikipediaLarge-500K	6.67±0.23	4.71±0.15	**4.15±0.03**	8.89±0.00	2.90±0.00	**1.55±0.00**
Amazon-670K	4.13±0.28	2.53±0.06	**2.20±0.11**	2.26±0.00	0.77±0.00	**0.42±0.00**
Amazon-3M	3.26±0.08	2.54±0.11	**2.03±0.09**	20.84±0.00	8.54±0.00	**4.61±0.00**

(a) Results for logistic loss.

	0.1	0.2	0.3	0.1	0.2	0.3
	$p@1$ [%]			$p@5$ [%]		
WikiLSHTC-325K	**62.78±0.03**	60.77±0.06	56.83±0.13	**30.25±0.02**	29.12±0.02	27.05±0.05
WikipediaLarge-500K	**66.77±0.08**	63.88±0.00	59.62±0.13	**36.94±0.02**	34.95±0.00	32.25±0.05
Amazon-670K	**43.31±0.03**	40.59±0.02	35.67±0.06	**34.31±0.03**	31.14±0.04	26.49±0.04
Amazon-3M	**46.23±0.01**	44.74±0.00	39.87±0.02	**41.41±0.01**	39.67±0.00	35.16±0.02
	T/N_{test} [ms]			M_{size} [GB]		
WikiLSHTC-325K	0.86±0.06	0.55±0.02	**0.45±0.01**	0.97±0.00	0.24±0.00	**0.10±0.00**
WikipediaLarge-500K	2.86±0.07	**1.99±0.00**	2.05±0.07	1.78±0.00	0.39±0.00	**0.17±0.00**
Amazon-670K	1.32±0.08	**1.01±0.02**	1.17±0.02	0.63±0.00	0.18±0.00	**0.10±0.00**
Amazon-3M	1.96±0.05	1.09±0.00	**0.95±0.02**	9.86±0.00	2.31±0.00	**0.89±0.00**

(b) Results for squared hinge loss.

Table 20: Precision@k for $k = 1$, 5, average prediction times, and model sizes with different thresholds of weight pruning for different losses.

J   Tree depth impact for the squared hinge loss

We present additional results concerning different tree shapes, namely the tree depth, for the squared hinge loss.

Arity	2	16	64	2	16	64
	$p@1$ [%]			T/N_{test} [ms]		
WikiLSHTC-325K	62.78±0.03	64.17±0.05	**64.61±0.04**	**0.86±0.06**	0.90±0.07	1.42±0.05
WikipediaLarge-500K	66.77±0.08	**68.16±0.10**	68.02±0.01	**2.86±0.07**	4.41±0.12	5.55±0.00
Amazon-670K	43.31±0.03	43.88±0.05	**44.03±0.05**	**1.32±0.08**	1.73±0.15	2.68±0.17
Amazon-3M	46.23±0.01	46.98±0.01	**47.33±0.00**	**1.96±0.05**	2.39±0.09	2.56±0.00
	T_{train} [h]			M_{size} [GB]		
WikiLSHTC-325K	**1.60±0.06**	2.18±0.07	3.85±0.17	0.97±0.00	0.90±0.00	**0.88±0.00**
WikipediaLarge-500K	**9.48±0.33**	15.91±0.55	28.68±0.74	1.78±0.00	1.52±0.00	**1.49±0.00**
Amazon-670K	**0.40±0.01**	0.64±0.02	1.57±0.04	0.63±0.00	0.55±0.00	**0.52±0.00**
Amazon-3M	**5.44±0.13**	9.82±0.23	20.82±0.00	9.86±0.00	9.36±0.00	**9.24±0.00**

(a) Results for arity equal to 2, 16 or 64 and pre-leaf node degree equal to 100.

Pre-leaf degree	25	100	400	25	100	400
	$p@1$ [%]			T/N_{test} [ms]		
WikiLSHTC-325K	61.96±0.03	62.78±0.03	**63.19±0.03**	**0.51±0.03**	0.86±0.06	1.78±0.03
WikipediaLarge-500K	66.01±0.10	66.77±0.08	**66.90±0.06**	**2.29±0.03**	2.86±0.07	6.14±0.11
Amazon-670K	42.93±0.02	**43.31±0.03**	43.25±0.04	**1.12±0.06**	1.32±0.08	2.43±0.08
Amazon-3M	45.84±0.02	46.23±0.01	**46.72±0.01**	**1.27±0.10**	1.96±0.05	5.61±0.23
	T_{train} [h]			M_{size} [GB]		
WikiLSHTC-325K	**1.54±0.03**	1.60±0.06	2.28±0.10	1.20±0.00	0.97±0.00	**0.84±0.00**
WikipediaLarge-500K	**7.41±0.14**	9.48±0.33	19.32±0.31	2.23±0.00	1.78±0.00	**1.49±0.00**
Amazon-670K	**0.39±0.01**	0.40±0.01	0.68±0.02	0.80±0.00	0.63±0.00	**0.51±0.00**
Amazon-3M	**4.80±0.29**	5.44±0.13	12.45±0.74	11.80±0.00	9.86±0.00	**8.60±0.00**

(b) Results arity equal to 2 and pre-leaf node degree equal to 25, 100, or 400.

Table 21: Precision@k1, average prediction time per example, training time and model size for k-means trees if different depths with squared hinge loss.

References

S. Agarwal. Surrogate regret bounds for bipartite ranking via strongly proper losses. *Journal of Machine Learning Research*, 15:1653–1674, 2014.

R. Agrawal, A. Gupta, Y. Prabhu, and M. Varma. Multi-label learning with millions of labels: Recommending advertiser bid phrases for web pages. In *Proceedings of the 22nd International Conference on World Wide Web*, page 13–24, New York, NY, USA, 2013. Association for Computing Machinery.

R. Babbar and B. Schölkopf. Dismec: Distributed sparse machines for extreme multi-label classification. In *Proceedings of the Tenth ACM International Conference on Web Search and Data Mining*, page 721–729, New York, NY, USA, 2017. Association for Computing Machinery.

S. Bengio, J. Weston, and D. Grangier. Label embedding trees for large multi-class tasks. In *Advances in Neural Information Processing Systems 23*, pages 163–171. Curran Associates, Inc., 2010.

A. Beygelzimer, J. Langford, Y. Lifshits, G. Sorkin, and A. Strehl. Conditional probability tree estimation analysis and algorithms. In *Proceedings of the Twenty-Fifth Conference on Uncertainty in Artificial Intelligence*, page 51–58, Arlington, Virginia, USA, 2009a. AUAI Press.

A. Beygelzimer, J. Langford, and P. Ravikumar. Error-correcting tournaments. In *Proceedings of the 20th International Conference on Algorithmic Learning Theory*, page 247–262, Berlin, Heidelberg, 2009b. Springer-Verlag.

A. Beygelzimer, H. Daumé, J. Langford, and P. Mineiro. Learning reductions that really work. *Proceedings of the IEEE*, 104:136–147, 2016.

K. Bhatia, K. Dahiya, H. Jain, A. Mittal, Y. Prabhu, and M. Varma. The extreme classification repository: Multi-label datasets and code, 2016. URL `http://manikvarma.org/downloads/XC/XMLRepository.html`.

R. Busa-Fekete, B. Szörényi, K. Dembczynski, and E. Hüllermeier. Online f-measure optimization. In *Advances in Neural Information Processing Systems 28*, pages 595–603. Curran Associates, Inc., 2015.

R. Busa-Fekete, K. Dembczynski, A. Golovnev, K. Jasinska, M. Kuznetsov, M. Sviridenko, and C. Xu. On the computational complexity of the probabilistic label tree algorithms. *CoRR*, abs/1906.00294, 2019.

P. Celis, P.-A. Larson, and J. I. Munro. Robin hood hashing. In *Proceedings of the 26th Annual Symposium on Foundations of Computer Science*, page 281–288, USA, 1985. IEEE Computer Society.

C. De Boom, S. Van Canneyt, T. Demeester, and B. Dhoedt. Representation learning for very short texts using weighted word embedding aggregation. *Pattern Recognition Letters*, 80:150–156, 2016.

O. Dekel and O. Shamir. Multiclass-multilabel classification with more classes than examples. In *Proceedings of the Thirteenth International Conference on Artificial Intelligence and Statistics*, pages 137–144, Chia Laguna Resort, Sardinia, Italy, 2010. PMLR.

K. Dembczyński, W. Cheng, and E. Hüllermeier. Bayes optimal multilabel classification via probabilistic classifier chains. In *Proceedings of the 27th International Conference on International Conference on Machine Learning*, page 279–286, Madison, WI, USA, 2010. Omnipress.

K. Dembczyński, W. Kotłowski, and E. Hüllermeier. Consistent multilabel ranking through univariate loss minimization. In *Proceedings of the 29th International Coference on International Conference on Machine Learning*, page 1347–1354, Madison, WI, USA, 2012. Omnipress.

K. Dembczyński, W. Kotłowski, W. Waegeman, R. Busa-Fekete, and E. Hüllermeier. Consistency of probabilistic classifier trees. In *ECML PKDD 2016 : machine learning and knowledge discovery in databases*, pages 511–526. Springer, 2016.

J. Deng, S. Satheesh, A. C. Berg, and F. Li. Fast and balanced: Efficient label tree learning for large scale object recognition. In *Advances in Neural Information Processing Systems 24*, pages 567–575. Curran Associates, Inc., 2011.

J. Duchi and Y. Singer. Efficient online and batch learning using forward backward splitting. *Journal of Machine Learning Research*, 10:2899–2934, 2009.

J. Duchi, E. Hazan, and Y. Singer. Adaptive subgradient methods for online learning and stochastic optimization. *Journal of Machine Learning Research*, 12:2121–2159, 2011.

R.-E. Fan, K.-W. Chang, C.-J. Hsieh, X.-R. Wang, and C.-J. Lin. Liblinear: A library for large linear classification. *Journal of Machine Learning Research*, 9:1871–1874, 2008.

J. Fox. *Applied regression analysis, linear models, and related methods*. Sage, 1997.

E. Grave, A. Joulin, M. Cissé, D. G. Facebook AI Research, and H. Jégou. Efficient softmax approximation for gpus. In *Proceedings of the 34th International Conference on Machine Learning - volume 70*, page 1302–1310. JMLR.org, 2017.

S. Hochreiter and J. Schmidhuber. Long short-term memory. *Neural Computation*, 9:1735–1780, 1997.

H. Jain, Y. Prabhu, and M. Varma. Extreme multi-label loss functions for recommendation, tagging, ranking & other missing label applications. In *Proceedings of the 22nd ACM SIGKDD International Conference on Knowledge Discovery and Data Mining*, page 935–944, New York, NY, USA, 2016. Association for Computing Machinery.

K. Jasinska. Efficient exact batch prediction for label trees. In *Extreme Multilabel Classification for Social Media at The Web Conference*, 2018.

K. Jasinska, K. Dembczynski, R. Busa-Fekete, K. Pfannschmidt, T. Klerx, and E. Hullermeier. Extreme f-measure maximization using sparse probability estimates. In *Proceedings of The 33rd International Conference on Machine Learning*, pages 1435–1444, New York, USA, 2016. PMLR.

K. Jasinska-Kobus, M. Wydmuch, D. Thiruvenkatachari, and K. Dembczyński. Online probabilistic label trees. *CoRR*, abs/2007.04451, 2020.

Y. Jernite, A. Choromanska, and D. Sontag. Simultaneous learning of trees and representations for extreme classification and density estimation. In *Proceedings of the 34th International Conference on Machine Learning - volume 70*, page 1665–1674. JMLR.org, 2017.

A. Joulin, E. Grave, P. Bojanowski, and T. Mikolov. Bag of tricks for efficient text classification. In *Proceedings of the 15th Conference of the European Chapter of the Association for Computational Linguistics: volume 2, Short Papers*, pages 427–431, Valencia, Spain, 2017. Association for Computational Linguistics.

S. Khandagale, H. Xiao, and R. Babbar. Bonsai - diverse and shallow trees for extreme multi-label classification. *CoRR*, abs/1904.08249, 2019.

W. Kotłowski and K. Dembczyński. Surrogate regret bounds for generalized classification performance metrics. *Machine Learning*, 10:549–572, 2017.

W. Kotlowski and K. Dembczyński. Surrogate regret bounds for generalized classification performance metrics. In *Asian Conference on Machine Learning*, pages 301–316, Hong Kong, 2016. PMLR.

O. O. Koyejo, N. Natarajan, P. K. Ravikumar, and I. S. Dhillon. Consistent multilabel classification. In *Advances in Neural Information Processing Systems 28*, pages 3321–3329. Curran Associates, Inc., 2015.

M. Kurzynski. On the multistage bayes classifier. *Pattern Recognition*, 21:355–365, 1988.

J. Langford, A. Strehl, and L. Li. Vowpal wabbit, 2007. URL `http://hunch.net/~vw/`.

C.-L. Li and H.-T. Lin. Condensed filter tree for cost-sensitive multi-label classification. In *Proceedings of the 31st International Conference on Machine Learning*, pages 423–431, Bejing, China, 2014. PMLR.

J. Liu, W.-C. Chang, Y. Wu, and Y. Yang. Deep learning for extreme multi-label text classification. In *Proceedings of the 40th International ACM SIGIR Conference on Research and Development in Information Retrieval*, page 115–124, New York, NY, USA, 2017. Association for Computing Machinery.

A. K. Menon, A. S. Rawat, S. Reddi, and S. Kumar. Multilabel reductions: what is my loss optimising? In *Advances in Neural Information Processing Systems 32*, pages 10600–10611. Curran Associates, Inc., 2019.

T. Mikolov, I. Sutskever, K. Chen, G. S. Corrado, and J. Dean. Distributed representations of words and phrases and their compositionality. In *Advances in Neural Information Processing Systems 26*, pages 3111–3119. Curran Associates, Inc., 2013.

F. Morin and Y. Bengio. Hierarchical probabilistic neural network language model. In *Proceedings of the Tenth International Workshop on Artificial Intelligence and Statistics*, pages 246–252. Society for Artificial Intelligence and Statistics, 2005.

J. Pennington, R. Socher, and C. Manning. Glove: Global vectors for word representation. In *Proceedings of the 2014 Conference on Empirical Methods in Natural Language Processing (EMNLP)*, pages 1532–1543, Doha, Qatar, 2014. Association for Computational Linguistics.

Y. Prabhu and M. Varma. Fastxml: A fast, accurate and stable tree-classifier for extreme multi-label learning. In *Proceedings of the 20th ACM SIGKDD International Conference on Knowledge Discovery and Data Mining*, page 263–272, New York, NY, USA, 2014. Association for Computing Machinery.

Y. Prabhu, A. Kag, S. Harsola, R. Agrawal, and M. Varma. Parabel: Partitioned label trees for extreme classification with application to dynamic search advertising. In *Proceedings of the 2018 World Wide Web Conference*, page 993–1002, Republic and Canton of Geneva, CHE, 2018. International World Wide Web Conferences Steering Committee.

S. Puthiya Parambath, N. Usunier, and Y. Grandvalet. Optimizing f-measures by cost-sensitive classification. In *Advances in Neural Information Processing Systems 27*, pages 2123–2131. Curran Associates, Inc., 2014.

S. Russell and P. Norvig. *Artificial Intelligence: A Modern Approach*. Prentice Hall Press, Upper Saddle River, New Jersey, USA, 2009.

Y. Tagami. Annexml: Approximate nearest neighbor search for extreme multi-label classification. In *Proceedings of the 23rd ACM SIGKDD International Conference on Knowledge Discovery and Data Mining*, page 455–464, New York, NY, USA, 2017. Association for Computing Machinery.

G. Tsoumakas, I. Katakis, and I. Vlahavas. Effective and efficient multilabel classification in domains with large number of labels. In *Proceedings of ECML/PKDD 2008 Workshop on Mining Multidimensional Data (MMD'08)*, 2008.

K. Weinberger, A. Dasgupta, J. Langford, A. Smola, and J. Attenberg. Feature hashing for large scale multitask learning. In *Proceedings of the 26th Annual International Conference on Machine Learning*, page 1113–1120, New York, NY, USA, 2009. Association for Computing Machinery.

J. Weston, A. Makadia, and H. Yee. Label partitioning for sublinear ranking. In *Proceedings of the 30th International Conference on Machine Learning*, pages 181–189, Atlanta, Georgia, USA, 2013. PMLR.

M. Wydmuch, K. Jasinska, M. Kuznetsov, R. Busa-Fekete, and K. Dembczynski. A no-regret generalization of hierarchical softmax to extreme multi-label classification. In *Advances in Neural Information Processing Systems 31*, pages 6355–6366. Curran Associates, Inc., 2018.

I. E. Yen, X. Huang, W. Dai, P. Ravikumar, I. Dhillon, and E. Xing. Ppdsparse: A parallel primal-dual sparse method for extreme classification. In *Proceedings of the 23rd ACM SIGKDD International Conference on Knowledge Discovery and Data Mining*, page 545–553. Association for Computing Machinery, 2017.

I. E.-H. Yen, X. Huang, P. Ravikumar, K. Zhong, and I. Dhillon. Pd-sparse : A primal and dual sparse approach to extreme multiclass and multilabel classification. In *Proceedings of The 33rd International Conference on Machine Learning*, pages 3069–3077, New York, New York, USA, 2016. PMLR.

R. You, Z. Zhang, Z. Wang, S. Dai, H. Mamitsuka, and S. Zhu. Attentionxml: Label tree-based attention-aware deep model for high-performance extreme multi-label text classification. In *Advances in Neural Information Processing Systems 32*, pages 5820–5830. Curran Associates, Inc., 2019.

J. Zhuo, Z. Xu, W. Dai, H. Zhu, H. Li, J. Xu, and K. Gai. Learning optimal tree models under beam search. In *Proceedings of the 37th International Conference on Machine Learning*, Vienna, Austria, 2020. PMLR.